INFORMATION TO USERS

This manuscript has been reproduced from the microfilm master. UMI films the text directly from the original or copy submitted. Thus, some thesis and dissertation copies are in typewriter face, while others may be from any type of computer printer.

The quality of this reproduction is dependent upon the quality of the copy submitted. Broken or indistinct print, colored or poor quality illustrations and photographs, print bleedthrough, substandard margins, and improper alignment can adversely affect reproduction.

In the unlikely event that the author did not send UMI a complete manuscript and there are missing pages, these will be noted. Also, if unauthorized copyright material had to be removed, a note will indicate the deletion.

Oversize materials (e.g., maps, drawings, charts) are reproduced by sectioning the original, beginning at the upper left-hand corner and continuing from left to right in equal sections with small overlaps. Each original is also photographed in one exposure and is included in reduced form at the back of the book.

Photographs included in the original manuscript have been reproduced xerographically in this copy. Higher quality 6" x 9" black and white photographic prints are available for any photographs or illustrations appearing in this copy for an additional charge. Contact UMI directly to order.

UMI

A Bell & Howell Information Company
300 North Zeeb Road, Ann Arbor MI 48106-1346 USA
313/761-4700 800/521-0600

A Study of Drag Reduction and Convective Heat Transfer Reduction in Turbulent Flow Through Pipes

by

Arun Sood

A Thesis Submitted to the
Faculty of Engineering
in Partial Fulfilment of the Requirements
for the Degree of

DOCTOR OF PHILOSOPHY

Major Subject: Chemical Engineering

APPROVED:

[redacted]

Dr. Edward Rhodes, Supervisor

[redacted]

Dr. A.M. Al Taweel

[redacted]

Dr. Feridun Hamdullahpur

[redacted]

Dr. John C. O'C. Young, St. Mary's University

[redacted]

Dr. Rajinder Pal, University of Waterloo, External Examiner

TECHNICAL UNIVERSITY OF NOVA SCOTIA

Halifax, Nova Scotia

1997

National Library of Canada
Acquisitions and Bibliographic Services
395 Wellington Street
Ottawa ON K1A 0N4
Canada

Bibliothèque nationale du Canada
Acquisitions et services bibliographiques
395, rue Wellington
Ottawa ON K1A 0N4
Canada

Your file Votre référence

Our file Notre référence

The author has granted a non-exclusive licence allowing the National Library of Canada to reproduce, loan, distribute or sell copies of this thesis in microform, paper or electronic formats.

L'auteur a accordé une licence non exclusive permettant à la Bibliothèque nationale du Canada de reproduire, prêter, distribuer ou vendre des copies de cette thèse sous la forme de microfiche/film, de reproduction sur papier ou sur format électronique.

The author retains ownership of the copyright in this thesis. Neither the thesis nor substantial extracts from it may be printed or otherwise reproduced without the author's permission.

L'auteur conserve la propriété du droit d'auteur qui protège cette thèse. Ni la thèse ni des extraits substantiels de celle-ci ne doivent être imprimés ou autrement reproduits sans son autorisation.

0-612-31534-7

Canada

TECHNICAL UNIVERSITY OF NOVA SCOTIA LIBRARY

"AUTHORITY TO DISTRIBUTE MANUSCRIPT THESIS"

TITLE:

A Study of Drag Reduction and Convective Heat Transfer Reduction in Turbulent Flow Through Pipes

The above library may make available or authorize another library to make available individual photo/microfilm copies of this thesis without restrictions.

Full Name of the Author: Arun Sood

Signature of the Author: [redacted]

Date: Sept 4, 1997

For Dear Mom and Dad

TABLE OF CONTENTS

10. APPENDICES

LIST OF TABLES

LIST OF FIGURES

NOMENCLATURE

C_A = concentration of surfactant molecules, [moles/ m^3]

C_p = specific heat of the fluid, [J/ kg/ °C]

$d_1\ d_2, d_3\ .\ d.\ D$ = pipe diameter, [m]

DR = drag reduction

f, f_1, f_2 = fanning's friction factor

F_A = molar flow rate of surfactant molecules, [moles/ s]

h = convective heat transfer coefficient, [W/ m^2/ °C]

HTR = heat transfer reduction

j_H = heat transfer j-factor

k = conductivity of fluid, [W/ m/ °C]

k_R = rate constant, [/ s]

K = Prandtl's mixing length constant

l = Prandtl's mixing length, [m]

l_E = length of energy dissipating eddies, [m]

L = length of the tube, [m]

N_{De} = Deborah number

N_{pr} = Prandtl's number

N_{re} = Reynolds number

N_{St} = Stanton number

q_w = heat flux at the wall, [W/ m^2]

$\left(\overline{q^2}\right)^{\frac{1}{2}}$ = average intensity of turbulence, [m/ s]

R,r = pipe radius, [m]

r_A = rate of reaction, [moles/ m^3]

s = velocity shift, [m/ s]

t = temperature, [°C]

$\bar{t}$ = average fluid temperature, [°C]

t_R = recovery time, [sec]

T_R = characteristic time, [sec]

u = fluid velocity, [m/ s]

u_* = shear velocity, [m/ s]

$\bar{u}$ = average bulk velocity, [m/ s]

$\overline{u'^2}, \overline{v'^2}, \overline{w'^2}$ = average square velocity fluctuation in x, y, z direction, [(m/ s)^2]

V = volume of the reactor, [m^3]

y = distance from the wall, [m]

Greek

α = molecular diffusivity, [m^2/ s]

β = drag reduction ratio

ε = eddy diffusivity, [m^2/ s]

λ = size of energy dissipating eddy

μ = viscosity, [kg/ m s]

ν = kinematic viscosity, [m^2/ s]

ρ = density, [kg/ m^3]

τ = shear stress, [N/ m^2]

Ω = frequency of energy dissipating eddies, [1/ s]

ΔL = length of pipe, [m]

ΔP = pressure drop, [N/ m^2]

Subscripts

b = bulk fluid

c = centerline

H = heat

l_s = laminar sublayer

N = Newtonian

M = momentum

p = drag reducing fluid

s = pure solvent

sh = shearing device

t = turbulent

w = at the wall

ACKNOWLEDGMENTS

I would like to take this opportunity to thank Dr. Edward Rhodes for his wisdom and steady guidance throughout the course of this project. I wish to extend my gratitude to him for his valuable suggestions and generous support over the years.

I would like to thank Dr. John Young, Dr. A.M. Al Taweel and Dr. Feridun Hamdullahpur for serving on my guiding committee and for always making time for me in their busy schedules. Dr. A.M. Al Taweel is also gratefully acknowledged for allowing me to set up experiments in his laboratory and making me feel at home.

Mr. Ray Dube helped in maintaining the experimental setup.

Financial support was provided by the Department of Chemical Engineering (Technical University of Nova Scotia) and the Technical University of Nova Scotia.

Finally, I wish to thank my wife, Sumita and my parents for their support and encouragement.

ABSTRACT

Addition of a small quantity of certain long chain polymers or micelle forming surfactant additives to a fluid will cause the frictional drag and convective heat transfer to be reduced in turbulent pipe flow. Reynolds number has been proven to be inadequate for characterizing the flow of such drag reducing solutions in different diameter pipes.

The reduction in drag and convective heat transfer occurs due to dampening of the velocity fluctuations in the turbulent boundary layer. Velocity fluctuations close to the wall are dependent upon shear stress, and are independent of the pipe diameter. Consequently, reduction in drag and heat transfer, calculated at a constant shear stress, should also be independent of the pipe diameter. The above hypothesis was successfully tested on polymer-oil and surfactant-water systems.

Dampening of velocity fluctuations results in thickening of the laminar sublayer and can also be equated to a reduction in Prandtl's mixing length. Velocity-shear stress data generated by flow experiments in a laboratory scale pipe along with viscosity measurements enable determination of the modified mixing length constant and the thickness of the laminar sublayer for a given drag reducing fluid, which can be subsequently used for predicting flow and heat transfer in any diameter pipe. The above methodology was successfully used for predicting drag reduction scale-up for surfactant-water and polymer-oil systems and heat transfer reduction for surfactant-water and polymer-water systems. The Model predictions were compared with other models available in published literature.

The use of drag reducing surfactant additives in heating or cooling systems causes an unwanted reduction in convective heat transfer in heat exchangers. This adverse effect can be overcome by intentionally breaking the heat transfer reducing surfactant micelles at the inlet to the heat exchanger. The micelles would recover further downstream and regain their drag reducing properties. A preliminary experimental investigation was conducted to study micellar break-up and recovery in a pipe. It was observed that the recovery length of micelles for a given bulk velocity was constant and was independent of pressure drop across the shearing device. A methodology, which assumes the test pipe to be a plug flow reactor, has been presented for calculating the recovery time of micelles.

1. INTRODUCTION

It is well known that the addition of small amounts (measured in parts per million) of certain high molecular weight polymeric additives to a liquid can reduce the friction loss in turbulent pipe flow, and therefore pumping power by as much as 80% below that exhibited by the solvent alone at that flow rate. Over the last few decades, considerable research in the field of fluid dynamics has centered around this fascinating phenomenon, also known as "Drag Reduction". The phenomenon was discovered by Toms (1948) during flow experiments with solutions of poly(methylmethacrylate) in monochlorobenzene.

Reduction in drag for turbulent pipe flow is also accompanied by a corresponding reduction in convective heat transfer (Heat Transfer Reduction), which on relative terms, is usually greater than the reduction in drag (Matthys, 1991). Heat transfer reduction due to these additives is advantageous in applications where convective heat losses to the surroundings have to be minimized in pipeline transfer of fluids (Burger et al., 1982). At the same time, these additives become a problem in heat exchangers where additional heat transfer area would be required to overcome the heat transfer reduction.

Synthetic polymers having a linear long-chain unbranched structure and molecular weight over a million have been found to be effective drag reducers. An extremely simplified, but universally accepted, hypothesis to explain the mechanism of drag reduction represents polymer molecules as springs which absorb energy from turbulent eddies. This leads to a reduction in energy dissipation and hence a reduction in drag is achieved. Over the years, researchers have identified certain surfactant solutions having the ability to reduce drag with almost the same efficiency as polymers (Shenoy, 1984). These solutions

form aggregates of surfactant molecules (known as micelles) at higher concentrations. These micelles are capable of absorbing energy from turbulent eddies in the same way as the polymer molecules do.

Polymeric drag reducing additives have found limited implementation on an industrial scale because polymer molecules undergo shear induced degradation. But in recent years the prospect of using surfactants for large scale heating and cooling systems has revived research interest in this area. Heating and cooling systems in large buildings provided an ideal opportunity to apply the concept of drag and heat transfer reduction. Of the total power consumption in large heating or cooling systems, 10% to 15% may be spent on driving the circulating pumps. A saving of 50% of this energy would be substantial in terms of the money saved (Gasljevic and Matthys, 1993). In addition, surfactant aggregates have an advantage over polymers in closed circulation systems as they have high resistance to shear induced degradation. If at all, these aggregates are broken up by high shear, however, they are grouped further downstream and recover their drag reducing ability (Young, 1996). This property of surfactant solutions allows for introduction of artificial roughness at the inlet of the heat exchangers to break-up the surfactant aggregates and enhance heat transfer. The molecules form the aggregates again further downstream and drag reducing characteristics are restored.

Despite the large volume of work done in this area, a theoretical expression relating the characteristics of these solutions to basic rheological properties has not yet been obtained. Attempts to predict flow and heat transfer in large industrial scale pipes from experimental data obtained in small laboratory scale pipes have met with very limited success. All existing models in the literature (discussed in Chapter 5) have been able to predict scale-up over a diameter ratio of 1.5-2.0, but have failed miserably when tested on field scale data.

The objective of this study was to identify a scale-up criteria which was independent of the diameter of the pipe and to use this criteria to develop a scale-up model which would enable prediction of drag and heat transfer reduction in large industrial pipes from results obtained in laboratory size pipes. Keeping in view the current emphasis in research on the use of drag reducing surfactant additives in closed circulation heating and cooling systems and the adverse effect of these additives on heat exchanger performance, a study was also carried out to understand the mechanism of micelle break-up and the factors which would control their subsequent recovery.

A brief overview of research conducted in the field of drag and heat transfer reduction over the last 50 years is presented in the next few sections. Though extensive literature is available, the focus of this review is on the topics which have not been tackled satisfactorily to date. The following discussion provides a background and helps us in defining the scope of the current work.

1.1 Present State of Knowledge

A number of review articles have been published over the years documenting the progress made in the areas of drag and heat transfer reduction, namely, by Hoyt (1972), Virk (1975), Berman (1978), Sellin, et al. (1982), Cho and Hartnett (1982), Kulicke et al. (1989) and Matthys (1991).

Since discovery of the phenomenon of drag reduction by Toms (1948), a number of drag reducing additives have been identified by researchers. Though synthetic polymers, biopolymers, surfactants, suspended fibres and solid particles have proved to be effective drag reducers, synthetic polymers and surfactants have been the focus of research.

1.1.1 Polymers and Surfactants

Drag reducing polymers have a linear, unbranched, long-chain structure with a molecular weight typically ranging from 10^5 to 10^8 (Virk, 1975). The polymer molecules are viscoelastic in nature and absorb energy from turbulent velocity fluctuations to reduce drag. If the additive molecules break, the drag reducing effect vanishes. Our experience with Poly(ethylene oxide) (Sood, 1993) and numerous studies available in published literature have indicated that shear induced degradation inevitably occurs in polymers after a certain amount of time in flow. Polymeric additives were used by ARCO Oil Company in the Trans Alaska Pipeline for transporting crude oil (Burger et al., 1982) in the early 1980s, but the polymer was continuously replenished at each pumping station to offset the loss due to degradation. However, polymers have been found to be the most efficient drag reducing additives. In most cases, only 200 parts per million, or even less is sufficient to obtain the maximum drag reduction effect (Matthys, 1991).

Surfactants, or surface-active agents have a lower molecular weight compared to the polymers. Their molecules form aggregates (containing roughly 50-100 molecules) known as micelles, which are viscoelastic in nature and interact with turbulence in the same way as the large molecules of polymers do. Surfactant molecule aggregates have much more resistance to mechanical degradation as compared to polymers, but degradation does occur at higher values of shear. Whereas polymer molecules permanently lose the power to reduce drag once the molecules are broken, surfactant solutions recover the drag reducing ability when the shear is below a critical level. This can be illustrated clearly from Figure 1.1 which shows the temperature profile for a surfactant solution (Ethoquad O12) which undergoes constant flux heating along the length of a pipe (our data). The micelles are broken up by a high shear induced by a wire mesh plug at the entrance to the pipe. Initially, the difference between average fluid bulk temperature and wall temperature is only 4 °C, indicating a high heat transfer coefficient. Further

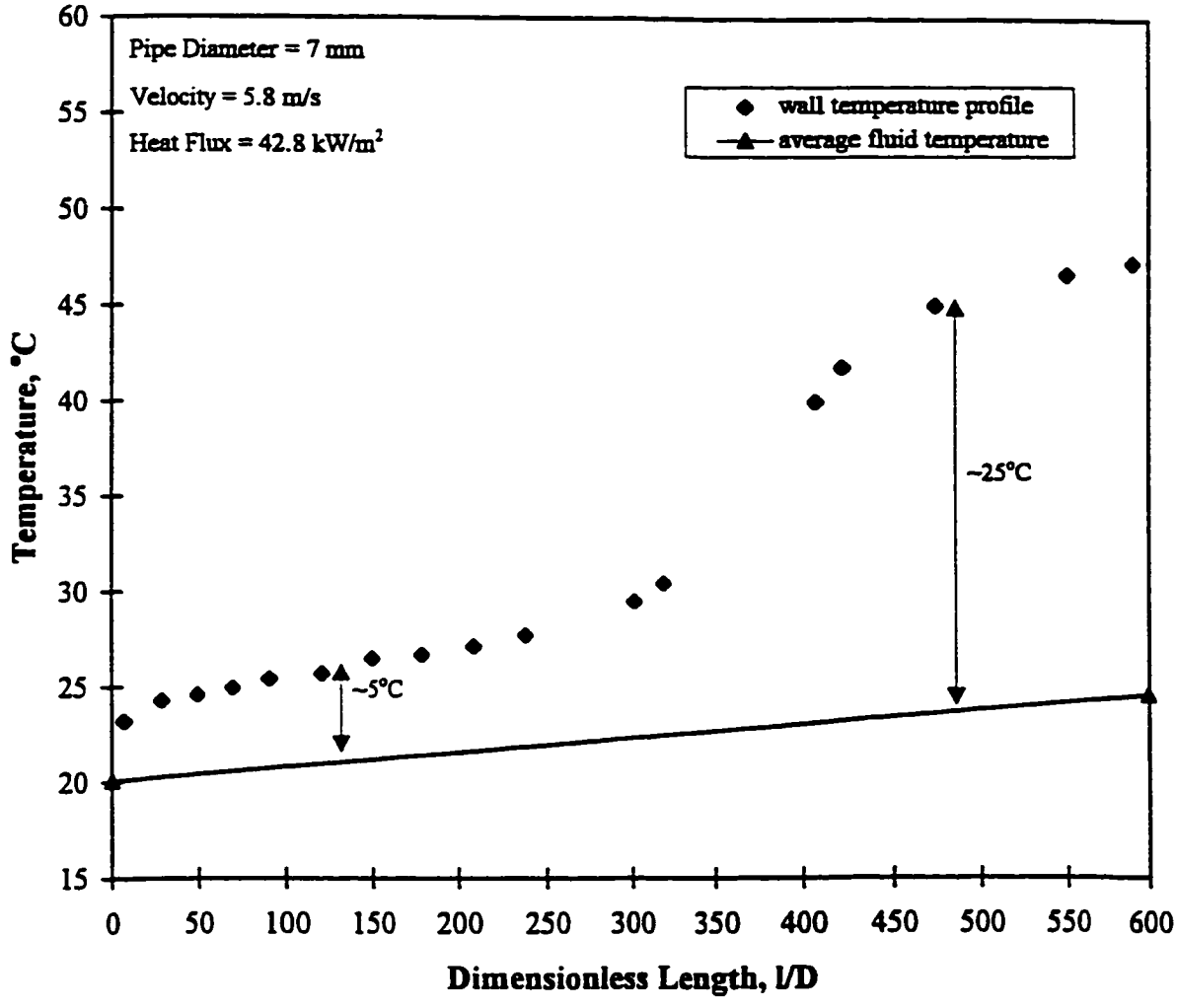

Figure 1.1 Temperature profile along length of the tube showing micellar break-up and recovery (1400 ppm Ethoquad O12 solution)

downstream, the surfactant molecules regroup to form the micelles again leading to a temperature difference of about 25 °C, indicating a very low heat transfer coefficient (or heat transfer reduction).

Since Ethoquad O12 was used for all our experiments, a brief but relevant introduction to surfactants and their micelle forming characteristics are discussed in Chapter 2.

1.1.2 Applications of Drag Reducing Additives

The application of drag reduction that generated a large amount of interest was in the Trans Alaska Pipeline (Burger et al., 1982). Drag reducing polymer CONOCO CDR was injected into the pipeline (20 ppm concentration) at pumping stations located every 100 km over a distance of 1300 km. Due to the drag reduction effect, two pumping stations were not required and the heat transfer reduction effect enabled maintenance of crude oil temperature at about 50 °C for the entire length of the pipeline with substantially less heating.

Fire fighting, Oil well operations and sewage disposal are examples of other successful applications of drag reducing additives. These and other examples of applications are listed in Table 1.1.

Use of polymeric additives in closed loop heating systems was attempted by Rochefort et al. (1989) with limited success as polymer concentration had to be continually replenished due to ongoing degradation. In the past few years surfactants have

Table 1.1. Applications of Drag Reduction and Heat Transfer Reduction

Engineering Application	Reference
Oil well operations	Savins, 1995
Crude oil movement by pipelines	Burger et al., 1982
Fire fighting	Fabula, 1971
Agriculture	Singh et al., 1989
Sewage and storm water disposal	Sellin, et al. 1982
Long distance heat transport	Sellin, et al. 1982
Transport of solid particle suspensions	Golda, 1986
Increasing speed of boats & submarines	Hoyt, 1972
Biomedical applications	Green et al., 1980
District heating & cooling systems	Steiff et al., 1989

been used successfully in large scale heating and cooling systems. Steiff et al. (1989b) have reported the use of surfactant additives in a district heating system, where 70% reduction in drag was achieved in the main transport line (2.4 km long, 0.45m dia.). The use of surfactant additives has also been successfully incorporated in a library cooling system by Young (1996).

Laboratory scale tests on drag and heat transfer characteristics of cationic surfactant additives in closed loop systems have been reported by Day (1991), Usui and Saeki (1993) and Gasljevic (1995). Gasljevic and Matthys (1991) conducted a feasibility study on the use of surfactant additives to reduce pumping power requirements in building

heating systems and reported that operating costs for the pump could be slashed by almost 50%.

All researchers have reported on problems encountered in the heat exchangers due to the presence of these additives. Gasljevic (1995) conducted tests on heat transfer in different types of heat exchangers and recommended the use of inserts for heat transfer enhancement. But so far, no study has been reported on factors which control the break-up and regrouping of surfactant molecules.

We were able to conduct experiments to study micelle break-up and their subsequent recovery in a long tube (length to diameter ratio = 600) maintained under constant flux heating. Micelles were broken up at the entrance of the tube using different combinations of wire mesh screens. Changing wall temperature profile along the length of the tube gave a clear indication of micelle break-up at the entrance and their regrouping further downstream (Figure 1.1). Effect of pressure drop across the screens and fluid velocity on micelle recovery were studied.

A detailed discussion of this work is presented in Chapter 7.

1.1.3 Theories on Mechanism of Drag Reduction

Many theoretical explanations were put forward over the years in an attempt to explain the mechanism of drag reduction. A brief outline is presented here including the hypothesis proposed by Lumley (1973) which has been universally accepted.

Toms (1948) suggested the possibility of the flow containing a shear thinning wall layer having an extremely low viscosity which resulted in lower friction coefficients for

drag reducing solutions. The presence of a shear thinning wall layer was discounted by the viscosity measurements on Poly(ethylene oxide) and Guar Gum (Hoyt, 1972), which are not shear thinning and are in fact shown to be Newtonian by conventional viscometric methods in the concentrations needed for optimum drag reduction.

El'Perin et al. (1967) proposed the existence of an adsorbed layer of additive molecules at the pipe wall during flow which could lower viscosity, dampen turbulence and prevent any initiation of vortices at the wall. Later work by Little (1969), with rotating disks of various materials, showed that the surface composition of the disk does not change the observed drag reduction in polymer solutions.

Gadd (1965) and later Walsh (1967) proposed that the cause of drag reduction was the decreased production of turbulence. According to this theory, the additive molecules slightly alter the energy balance of the turbulent fluctuations close to the wall. Additive molecules, which have a very high extensional viscosity, stretch out and absorb energy from turbulent shear stresses. This process leads to viscous dissipation to destroy disturbances which would have had sufficient kinetic energy to grow into large scale disturbances downstream, resulting in lower Reynolds stresses and hence lower friction.

Lumley (1973) agreed with the above theory but proposed that this was not the only phenomenon taking place. If decreased production of turbulence in the wall region was alone responsible for the drag reduction effect, then turbulence damping in free flows could not be explained. He proposed that viscoelastic polymer molecules absorb energy from the velocity fluctuations, which give rise to turbulence, and also interact with the small energy dissipating eddies and make them conservative. As a result, still smaller eddies must be produced for viscous dissipation to take place which means a decrease in friction. In other words, the drag reducing additives act at both ends of the energy spectrum, i.e., they affect the rate at which energy is fed to turbulence and also the rate at

which the energy is dissipated.

The above hypothesis has been accepted as the most plausible explanation of the phenomenon of drag reduction. Decreased production of turbulence in the boundary layer for wall bounded flows leads to a thickening of the laminar sublayer which accounts for the decreased convective heat transfer coefficient.

The above concept of interaction of drag reducing additives with turbulent shearing stresses and the subsequent thickening of the laminar sublayer has been used in Chapter 5 and Chapter 6 to develop a scale-up model for drag and heat transfer reduction.

1.1.4 Complexities Involved in Pipeline Scale-up

For Newtonian fluids, a Reynolds number is sufficient to characterize flow through different diameter pipes. In other words, maintaining the same Reynolds number flow in different diameter pipes would yield the same friction factor for a given Newtonian fluid. The above is not true for drag reducing fluids. The degree of drag reduction is dependent on the diameter of the pipe even for the same Reynolds number and fluid. This so called the "diameter effect" is explained schematically in Figure 1.2 where the friction factor is shown as a function of Reynolds number in two different diameter pipes (diameter D2> diameter D1) for a drag reducing solution and a Newtonian fluid. As can be seen from the figure, a single curve (Prandtl-Karman law) is able to represent flow of the Newtonian fluid in pipes of any diameter. For the drag reducing fluid, Prandtl-Karman law represents the flow at lower Reynolds number where the drag reduction effect has not yet come in to play. At higher Reynolds numbers, the viscoelastic additive molecules are able to absorb energy from the velocity fluctuations and reduce drag. At this point, the friction factor curve for the drag reducing fluid pulls away from the Prandtl-Karman law, showing lower

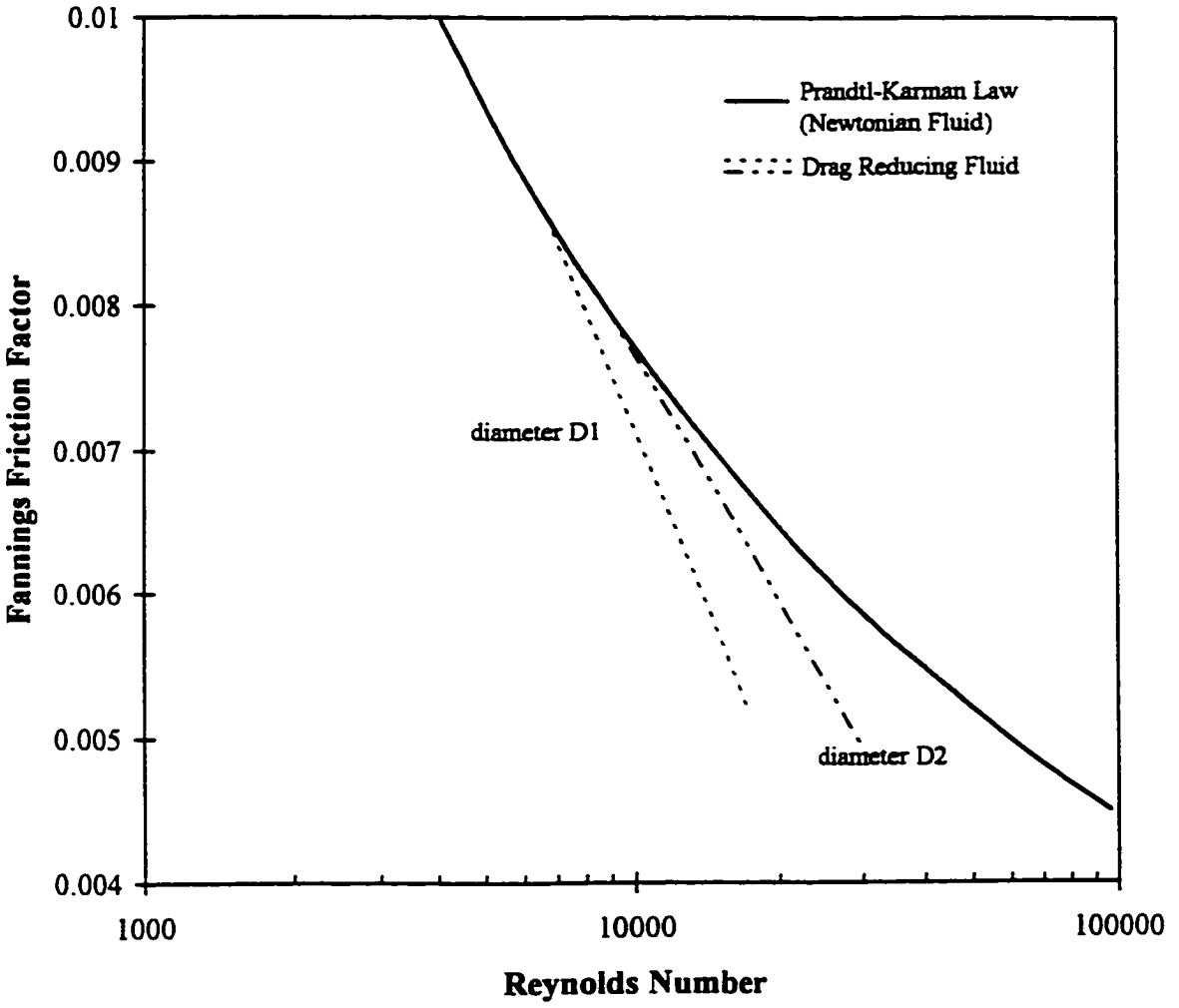

Figure 1.2 Schematic diagram explaining diameter effect for drag reducing solutions (Diameter D2>Diameter D1)

friction factors. The friction factors obtained for the drag reducing solution in smaller diameter D1 are lower than those obtained in diameter D2 for the same Reynolds number. Also, the drag reduction effect is seen earlier in diameter D1.

The problem of diameter effect has been a major stumbling block in the industrial implementation of drag reducing fluids. A point in case is the use of drag reducing additives by ARCO Oil company in the Trans Alaska Pipeline (Burger et al., 1982). Due to the inability to scale-up results from laboratory size pipes, tests had to be carried out in the Trans Alaska pipeline (1.2m diameter) itself.

A complete and detailed description of the interaction of additive molecules with the turbulent boundary layer is extremely complex for very dilute solutions. Hence to be able to predict drag and heat transfer reduction in big industrial pipes, results obtained in small laboratory size pipes have to be scaled up using a characteristic of the flow which is invariant with pipe diameter. Scale-up models are available in the literature (Astarita et al., 1969, Darby and Chang, 1984, Yoon and Ghajar, 1988 and Darby and Pivsa-art, 1991) which have used the interaction of energy dissipating eddies with molecular relaxation time as the invariant property. Since molecular relaxation times are nearly impossible to measure for dilute solutions, these models have taken the form of empirical correlations. Another approach has been based on Virk's (1975) three-layered velocity profile model which uses a hypothetical velocity shift in the buffer layer as the diameter invariant characteristic. Scale-up models along these lines have been proposed by Granville (1978), Matthys and Sabersky (1982) and Sellin and Ollis (1983).

All these models have proved unsuccessful in predicting pipeline scale-up of drag reducing flows. They seem to work satisfactorily when scaling up over a narrow diameter range (1:1.5 to 2), but give predictions for large industrial scale pipes which are off by 40-50%.

Since scale-up attempts for drag reduction have been largely unsuccessful, few attempts have been made to scale-up heat transfer reduction. Matthys and Sabersky (1982) proposed a model, based on Virks' hypothesis (1975), which was not tested at the time due to unavailability of heat transfer data. Yoon and Ghajar (1988) proposed a scale-up model based on the molecular characteristics, which was successful for predicting their heat transfer results for polyacrylamide solutions, but was not tested for universal applicability.

It is clear from the above discussion that there is lack of a theoretical model which can predict drag and heat transfer reduction using measurable fluids properties.

We were able to demonstrate (Sood, 1993) that wall shear stress could be used as a criteria for comparing drag and heat transfer results in different diameter pipes for Poly (ethylene oxide) solutions. It has also been shown that turbulent velocity fluctuations in the wall region can be quantified by the shear stress at the wall (Tritton, 1988). The above two facts encouraged us to investigate the possibility of using wall shear stress as a pipeline scale-up criteria instead of molecular characteristics or velocity shift, both of which are hypothetical parameters (as discussed above).

In Chapter 4, wall shear stress has been successfully used as the criteria for comparing results in different diameter pipes for surfactant-water, polymer-water and polymer-oil drag reducing systems. The same criteria has been used to develop models for scale-up of drag and heat transfer reduction in Chapter 5 and Chapter 6. These models use measurable rheological properties and flow results to predict scale-up.

1.1.5 Role of Concentration

Polymer or surfactant additives in solution can decrease the wall friction below that corresponding to its Newtonian solvent, but only down to a certain point. The solution is then said to have reached the asymptotic drag reducing conditions (Virk, 1971). Under these conditions, a further increase in additive concentration does not lead to an additional further decrease in friction coefficient. Figure 1.3 is a plot of average bulk velocity against wall shear stress for Ethoquad O12 solutions in water. It can be seen that the velocity tends towards an asymptotic value for the 600 ppm solution and a further increase in concentration to 1400 ppm does not result in any appreciable increase in velocity.

Virk (1971) proposed a correlation for calculating the maximum drag reduction asymptote, which is given by

$$\sqrt{\frac{1}{f}} = 19.0\log_{10}\left(N_{re}\sqrt{f}\right) - 32.4 \qquad (1.1)$$

or,

$$f = 0.58N_{re}^{-0.58} \qquad (1.2)$$

Very recently, Zakin (1996) has indicated that for certain non-polymeric systems, reduction in drag lower than Virk's Asymptote has been achieved. They have proposed a new equation for the drag reduction asymptote:

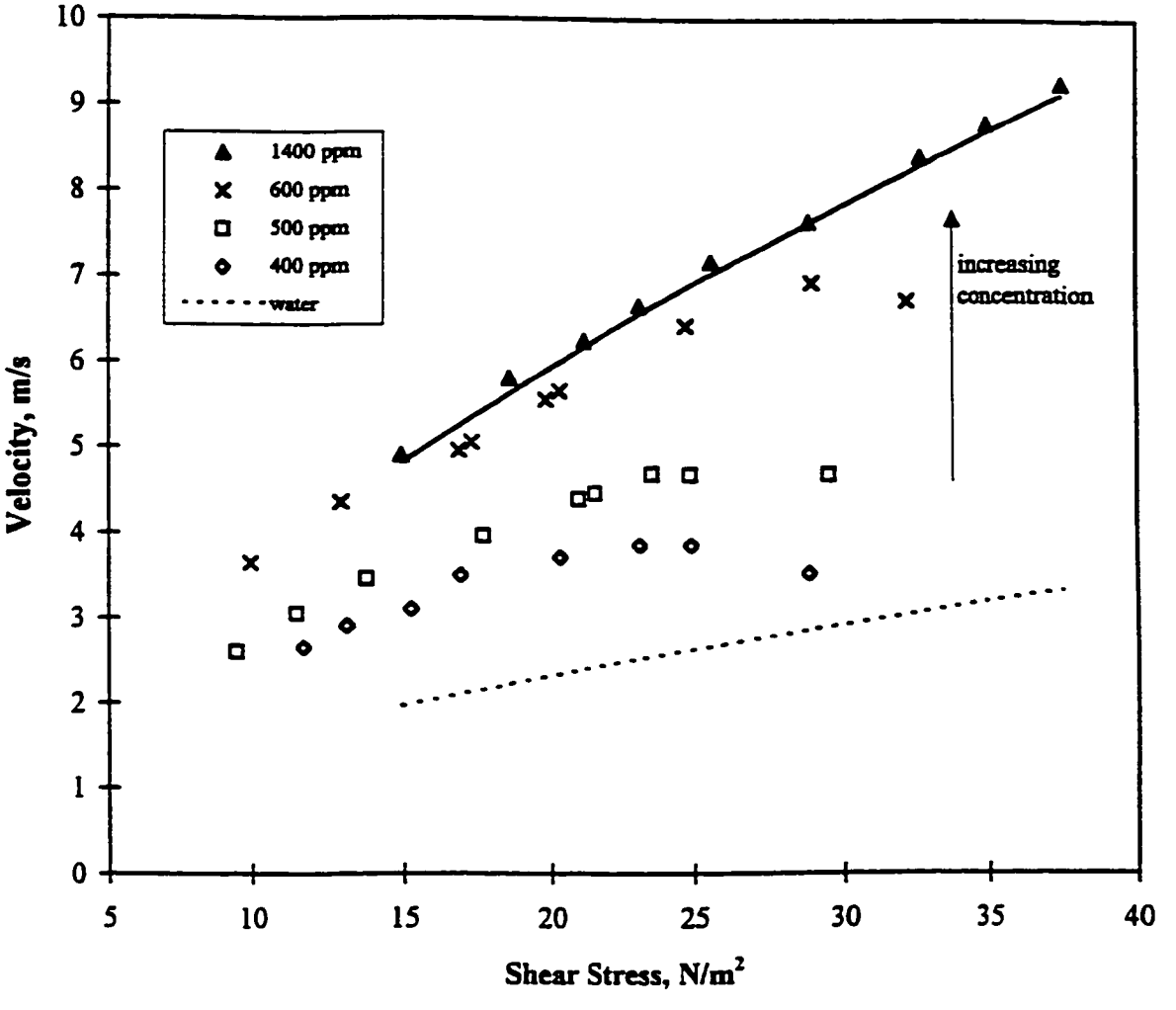

Figure 1.3 Effect of concentration on drag reduction in the 7 mm diameter pipe (Ethoquad O12 solutions)

$$f = 0.32 N_{re}^{-0.55} \tag{1.3}$$

Dependence of heat transfer reduction on concentration is similar to that of drag reduction. A correlation for the maximum heat transfer reduction has been proposed by Cho and Hartnett (1982):

$$j_H = 0.03 N_{re}^{-0.45} \tag{1.4}$$

where,

$$j_H = N_{St} N_{\mathrm{Pr}}^{2/3} \tag{1.5}$$

Though the above equations represent drag and heat transfer reduction reasonably well in the asymptotic regime, they are of little practical use since the concentrations of drag reducing additives needed for commercial viability are much lower. They lie in the range where drag and heat transfer reduction are still a function of concentration (non-asymptotic).

The scale-up model presented in Chapter 5 and Chapter 6 use a modified Prandtl's mixing length constant to account for the dependency of drag and heat transfer reduction on concentration.

1.1.6 Onset Phenomenon

It has been known for a long time that for the drag reduction effect to become apparent, a critical value of shear stress at the wall has to be exceeded (Gadd, 1966 and Virk, 1975). This critical value of shear stress is independent of the pipe diameter. Similar observations were made in regard to heat transfer reduction (Cho and Hartnett, 1982).

Steiff et al. (1989a) have reported that the break down of surfactant micelles and subsequent loss of drag reducing characteristics at very high flowrates is also dependent on the wall shear stress. According to their observations, for a given concentration, degeneration of micelles would occur at a particular value of shear stress, which is independent of the pipe diameter. A similar trend can be observed in Figure 1.4 for 400 ppm, 500 ppm and 600 ppm Ethoquad O12 solutions for runs in 7mm and 10.2mm diameter tubes in our experimental set-up.

The observations reported above provide support to the hypothesis presented in our earlier work (Sood, 1993), where based on our experimental results, we proposed the use of wall shear stress as a correlating parameter not only for the onset phenomena but for all drag reduction and heat transfer reduction results in different diameter pipes.

A detailed discussion on the role of shear stress in correlating drag and heat transfer reduction results and also in quantifying turbulence in the near wall region is presented in Chapter 4.

1.2 Focus of Current Study

This work was undertaken to establish a theoretical basis and correlating

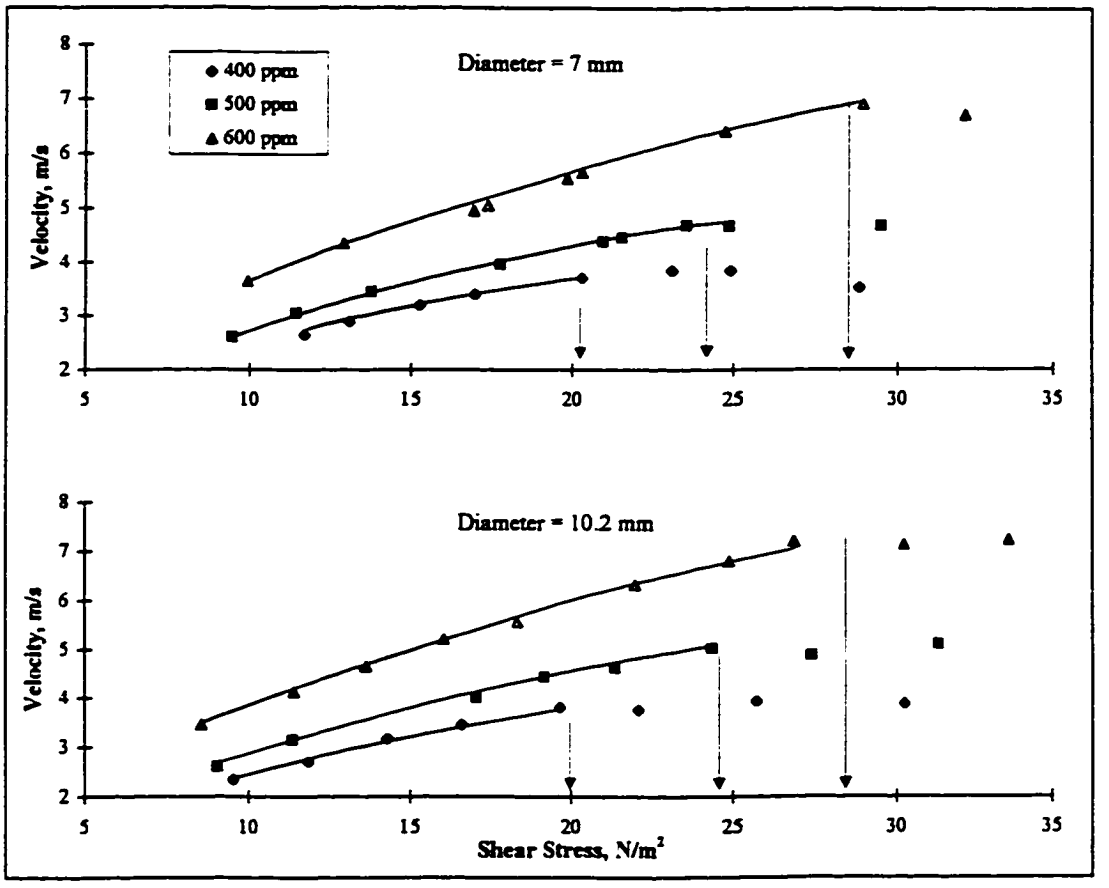

Figure 1.4 Evidence for the existence of critical shear stress

parameter for drag reduction and heat transfer reduction in pipeline flow and to use this parameter along with the basic understanding of various aspects of turbulence to develop a scale-up model for predicting flow and heat transfer in industrial scale pipes for these fluids.

As mentioned in the previous section, the problems associated with the application of drag reducing fluids on an industrial scale are numerous and in many cases, there is a lack of basic understanding. Though many aspects of turbulence are well understood and described, the procedures of predicting friction and heat transfer in turbulent flow, to this date, are empirical to a certain extent even for Newtonian fluids. As well, it is extremely difficult to directly measure viscoelasticity of dilute polymeric or surfactant solutions. Hence our approach to developing a scale-up method will be the use of flow and heat transfer results obtained in small laboratory scale pipes for predicting results in bigger industrial size pipes.

Finally, a study was also carried out to understand micellar break-up under high shear and the factors which control their subsequent regrouping. Understanding this phenomenon is important if we are to minimize the heat transfer problems in heat exchangers while using drag reducing additives.

The experimental part of this study is a continuation of the work already presented as a Master of Applied Science thesis, with new additions to the experimental set-up and improvements to some old techniques. These are discussed in Chapter 3. To avoid repetition, detailed calibrations and error analysis for the experimental techniques employed and calculation procedure have not been discussed here as they have already been presented elsewhere (Sood, 1993). The results obtained in this study, theoretical background and scale-up modeling are presented in Chapters 4, 5, 6 and 7. Each chapter is self-contained with sections on literature review, theoretical background, specific

experimental measurements etc., pertaining to the particular problem discussed.

2. SURFACTANTS AS DRAG REDUCING ADDITIVES

Drag reduction effect has been observed in solutions containing only a few parts per million of soluble high molecular weight polymers in both aqueous and organic solvents. In fact, any polymeric material with a linear, long chain and unbranched structure and high molecular weight can be an effective drag reducer. Although effective at very low concentrations, the use of these additives is seriously limited due to their susceptibility to permanent mechanical degradation under high shear stresses such as those encountered in pumps and highly turbulent flow through pipes.

In recent times, surface active agents or surfactants have replaced polymers as the major class of drag reducing agents as they have comparatively a very high resistance to mechanical degradation. The surfactant molecules associate to form particles, which are called micelles, under certain conditions which are characteristic of each solvent-solute system. Micellar structures (an aggregation of 50-100 surfactant molecules) can be of a variety of shapes, but cylindrical micelles have been found to reduce drag in turbulent pipe flow. Although these additives only reduce drag at much higher concentrations relative to the polymeric materials, they exhibit a much higher resistance to mechanical degradation and an extraordinary ability to fully recover their drag reducing ability after the mechanical stress has been removed. This ability has made surfactants the main focus of recent studies of additives for district heating and cooling systems, where the micelles have to be broken down in the heat exchangers to facilitate heat transfer, but recover further downstream to take advantage of the drag and heat transfer reducing properties when being transported through pipes (Young, 1996).

2.1 Physical Chemistry of Surfactant Systems

Though a detailed study of the surfactant chemistry is beyond the scope of this work, a brief and relevant discussion of the micelle forming characteristics of surfactant solution is presented here.

Surfactant molecules (e.g. Ethoquad O12, C_9H_{19}=C_9H_{17}-$N(CH_3)(C_2H_4OH)_2Cl$} are amphiphilic in nature, which means that the molecule consists of two parts, one of which is highly soluble (-$N(CH_3)(C_2H_4OH)_2Cl$) in the medium concerned and the other which is insoluble (C_9H_{19}=C_9H_{17}-). In the case of aqueous systems, surfactant molecules consist of a hydrophilic group (head group) which is attached to a hydrophobic hydrocarbon group (tail).

A micelle is an aggregation of individual surfactant molecules in solution in such a way that they present a hydrophillic surface (or interface) to the solvent and the hydrophobic core is of hydrocarbon environment. The formation of micelles depends upon the balance of the intermolecular forces between the solute and the solvent and Van der Waals forces (Everett, 1988). Micelles contain about 50-100 individual molecules and their formation is thermodynamically favored, once a certain concentration has been reached. This concentration is called the Critical Micellar Concentration (CMC). The solubility of the surfactant increases drastically once CMC has been reached. This is because the micellar form is highly soluble while the solubility of the monomer is limited.

In addition of concentration of molecules, micelle formation is also dependent upon temperature, i.e., with an increase in temperature, the concentration required for achieving micelle formation also increases. The temperature at which the CMC is achieved for a given surfactant solution is called its Krafft point (Figure 2.1). At any temperature below the Krafft point temperature, the surfactant is unable to form micelles because its

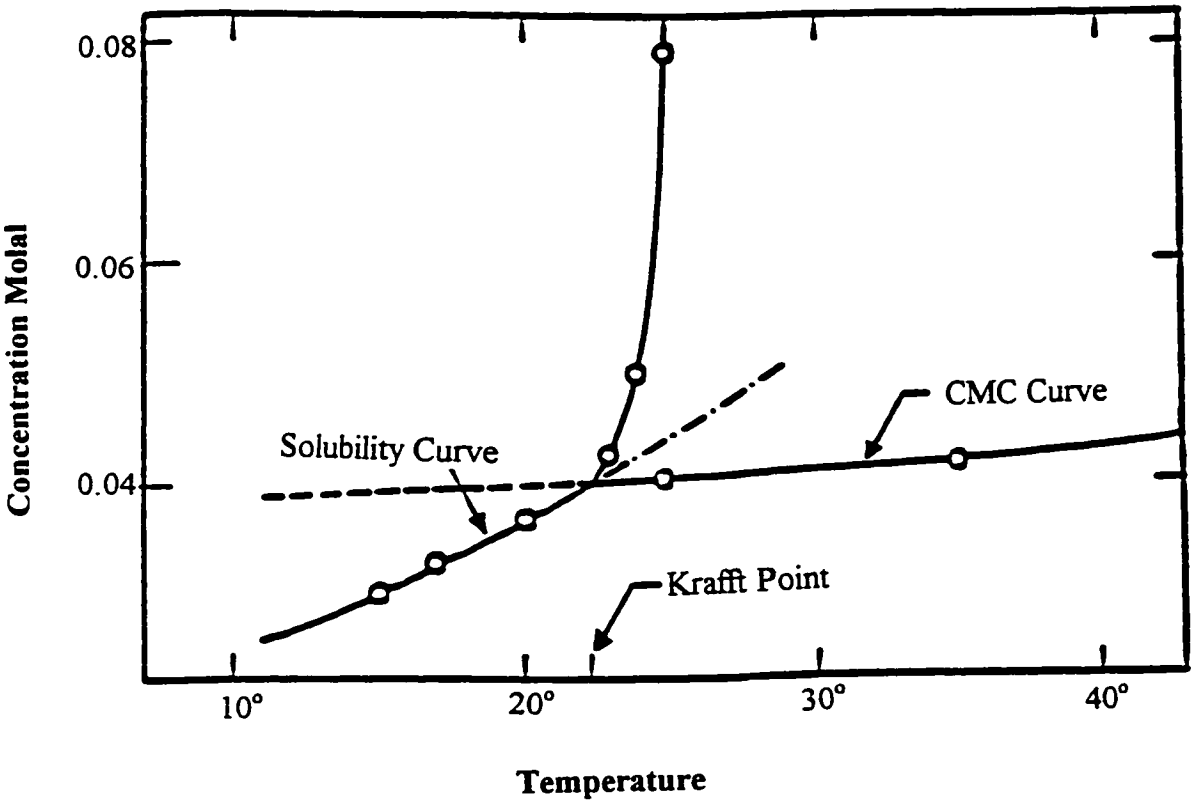

Figure 2.1 Typical solubility and CMC curves for drag reducing surfactant solutions (Shinoda et. al, 1963)

solubility is lower than the CMC. At temperatures above the Krafft point, micelles are formed if the surfactant concentration exceeds the CMC value.

Micelle formation can be enabled at a lower concentration than CMC by introducing a substance to the system that helps promote micelle formation. In the case of ionic surfactants, an oppositely charged ion, referred to as a counter ion, can reduce the repulsion between the charged surfactant head groups and therefore allow the surfactant molecules to approach each other more easily to form micellar aggregations (Day, 1991). Counterions play an important role in determining the shape of the micelle. In addition, the counterion also affects the micelle's viscoelasticity and its ability to cause drag reduction.

2.2 Micelle Structure and Drag Reduction

When a surfactant is added to a solvent, the concentration of the monomer increases until the critical micellar concentration is reached. At this point the surfactant forms the micelles. At relatively low concentrations of surfactant, the micelles are essentially spherical structures. With a further increase in monomer concentration, the micelle concentration remains constant but they grow in size and form cylindrical or rod shaped micelles. At much higher surfactant concentrations of 20% to 30% by weight, the arrangement of surfactant molecules into bilayers become favorable and another liquid crystalline phase known as the lamellar micelles forms. Figure 2.2 schematically shows: a) spherical b) cylindrical (rod like) and c) lamellar micelle structures.

It has been shown by tests carried out on various cationic surfactant additives (Hoffman et al., 1985) that the concentration range over which rod shaped micelles begin to form also coincides with the onset of viscoelasticity. At these concentrations, the

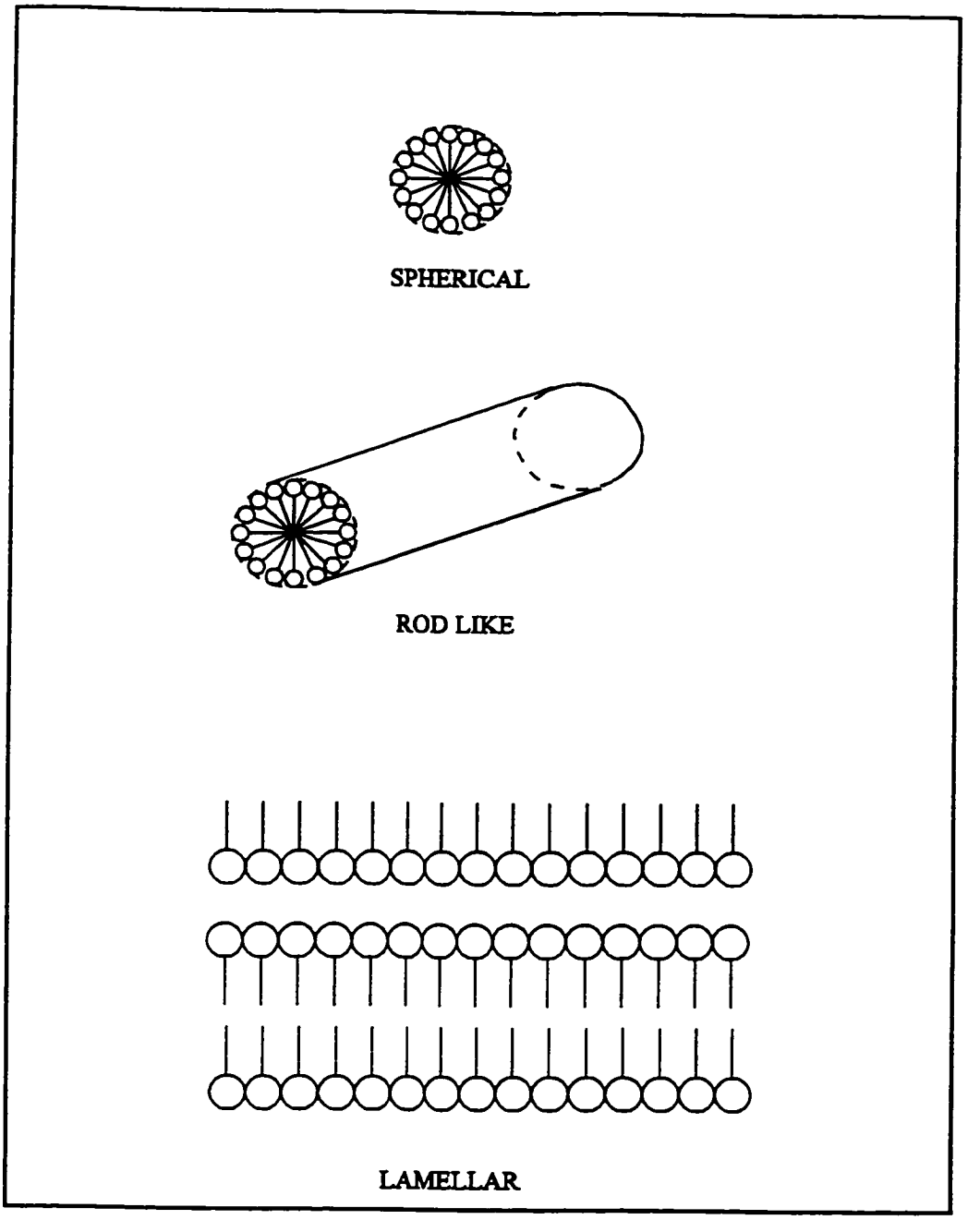

Figure 2.2 Possible structures for micellar aggregations (Everett, 1988)

surfactant solutions begin to exhibit drag reduction and heat transfer reduction phenomena under turbulent flow conditions.

2.3 Preparation And Addition of Drag Reducing Additive

In principle, any viscoelastic surfactant solution would show drag reduction, but cationic surfactants are recognized in the literature (Gasljevic, 1995) as the most suitable for aqueous solutions. Most cationic surfactants are quaternary ammonium salts with the addition of a counterion (an anion).

The choice of a surfactant as a drag reducing agent for practical application is governed by the operating temperature range. Several surfactant additives have been developed by Hoechst AG of Germany for high temperature applications in district heating systems which are listed in Table 2.1.

The surfactant used in our experiments was Ethoquad O12, which is manufactured by Akzo Nobel Chemicals Inc., Illinois. It was chosen for the reason that it is commonly used in North America and data are available in published literature for comparison and reproducibility of flow and heat transfer experiments. It also provides full drag reduction in the temperature range of 2 °C to 30 °C, making it convenient to carry out all the tests at ambient temperatures (18-23 °C). Details of the chemicals used in our experiments are listed in Table 2.2:

The following procedure was employed while preparing a concentrated surfactant solution:

1. A solution of Sodium Hydroxide in water was prepared on a hot plate/ Stirrer combination.
2. The appropriate amount of counterion (Methyl Salicylic acid) was weighed and slowly transferred into a beaker containing the hot stirring Sodium Hydroxide solution to form an equimolar mixture of acid and Sodium Hydroxide.

3. The mixture was left to stir at the elevated temperature till all of Methyl Salicylic Acid dissolved and a clear solution was formed.

4. At this stage, the commercial Ethoquad O12 concentrate in an isopropanol solution was weighed and added to the gently stirring mixture. The stirring was continued till the surfactant dissolved in the counterion/ Sodium Hydroxide mixture.

Flow and heat transfer experiments were carried out in our experimental set-up using 400 ppm, 500 ppm, 600 ppm, 1200 ppm and 1400 ppm surfactant solutions in tap water. The desired concentration solution for an experimental run was prepared in the Solution Preparation Tank (experimental set-up details are discussed in Chapter 3) using the procedure given below:

1. The Solution Preparation Tank was filled up to the 200 litre mark with tap water.

2. The valves at the pump discharge line were adjusted to the recirculation mode, i.e., suction line of the pump was connected to the outlet of the Solution Preparation Tank and discharge line transferred the solution back to the tank (Figure 3.2, Chapter 3). The centrifugal pump was now turned on.

3. Previously weighed surfactant solution concentrate was slowly poured into the tank to bring up to the desired concentration.

4. The pump was run in the recirculation mode for half an hour to thoroughly homogenize the solution. The solution was now ready for an actual run in the flow loop (Figure 3.2, Chapter 3).

Table 2.1 Surfactants for High Temperature Applications

Name	Temperature Range
Habon:	50-100 °C
Obon:	60-120 °C
Dobon:	95-145 °C

Table 2.2 Chemicals used in Our Experiments

Chemical	Trade Name	Formula	Molecular Weight	Manufacturer	Supply Form
Surfactant	Ethoquad O12	$C_9H_{18}=C_9H_{17}$-$N(CH_3)(C_2H_4OH)_2Cl$	403	Akzo Nobel Chemicals Inc., USA	72% w/w solution in isopropanol
Counter ion	3-Methyl-salicylic acid	2-(OH)-3(CH_3)-C_6H_3-COO^-	152.15	Fluka Chemicals Corp., NY, USA	Powder

3. EXPERIMENTAL SET-UP AND TECHNIQUES

The main objectives of the experimental part of the research project were to enable friction and heat transfer measurements for a surfactant solution flowing through different diameter steel tubings. The experimental set-up was designed for flow and heat transfer experiments on dilute polymer solutions (Sood, 1993) keeping in view the constraints imposed by the susceptibility of the polymer solution to undergo shear induced degradation. Drag reducing surfactant solutions do not present this problem since they have a high resistance to mechanical degradation. If the surfactant molecule aggregates are indeed broken up, they have a tendency to regroup once the shearing force is removed. Hence the existing set-up was used for experiments with surfactant solutions after incorporating a few minor changes.

A detailed diagram of the experimental set-up is shown in Figure 3.1. The salient features of the experimental set-up are briefly described below (a detailed description of the set-up and experimental techniques follows later):

- The surfactant solution of desired concentration was prepared in the Solution Preparation Tank. The solution was transferred to the Pressure Tank using a centrifugal pump, which was also used to homogenize the surfactant solution in the Solution Preparation Tank before every run.

- Compressed air was used in the Pressure Tank to make the solution flow through the system at very steady flow rates over a wide range.

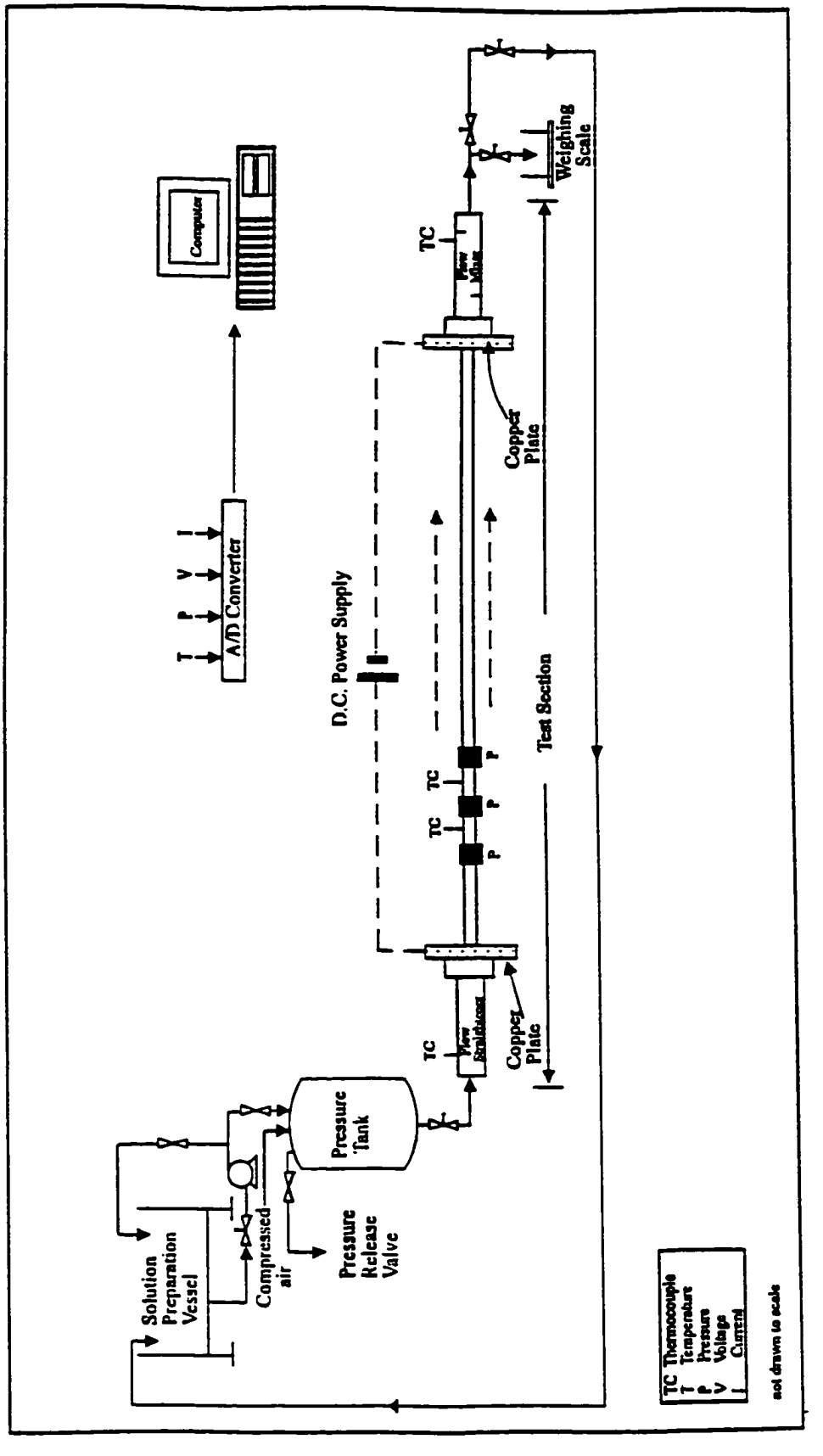

Figure 3.1 Detailed experimental set-up

- Flexible Polypropylene tubing was used everywhere (except for the test section which was made of SS 304 tubing), to avoid bends and fittings which cause unnecessary friction due to discontinuous surfaces.

- Instead of using an online flowmeter, the volumetric flow rates were measured by collecting samples over a period of time and measuring the volume. This is probably the most accurate way of measuring the flowrates for drag reducing fluids as they have been known to affect the calibrations of on-line flowmeters (Gasljevic, 1995).

- The data acquisition system selected for making measurements was directly connected up to a Personal IBM Compatible Computer which made it possible to simultaneously collect data at a large number of points. It could make measurements as a function of time and perform averaging of the data as the run progressed. The software also enabled graphical monitoring of measured data during the course of a run.

- A constant heat flux mode was employed to study the heat transfer characteristics of the surfactant solution. This was obtained by direct electrical heating of the stainless steel tubing. A Direct Current power supply was connected to two ends of the test section and the electrical resistance of the tube generated the heat flux. Care was taken to isolate the test section from rest of the flow loop.

- The entire test section was supported in such a way that it allowed for free thermal expansion of the tube at both ends. No clamps were used all along the tube length and the supports were designed so that the tube rested freely on them. The supports could slide on a square metal tube which was used as the base support.

3.1 Solution Preparation Tank (Figure 3.2)

The surfactant solution was prepared in a 1.15 m^3 high density polyethylene tank . The dimensions of the tank are shown in Figure 3.2. The tank was provided with a draining line at the bottom, which was connected to a centrifugal pump. The discharge line of the pump was connected to the Pressure Tank. Through a combination of valves, the discharge from the pump could also be directed back to the Solution Preparation Tank (recirculation mode).This arrangement was used prior to each experimental run to homogenize the surfactant solution.

3.2 Pressure Tank (Figure 3.2)

The prepared surfactant solution was gravity drained into an Stainless Steel SS 304 cylindrical pressure tank of 0.45 m^3 capacity with dished ends. As shown in Figure 3.2, the pressure tank was fitted with a plastic sight tube for monitoring the level of liquid inside the tank. Air at 150-346 kN/m^2 from an air compressor was used to push the solution from the bottom of the tank and through the flow loop. The tank has a pressure release valve which was set to go off at 484 kN/m^2 and a pressure gauge to monitor pressure inside the tank. According to design specifications supplied by the manufacturer, the tank has a maximum operating pressure limit of 830 kN/m^2 and a burst pressure of 1245 kN/m^2. The bottom of the tank was connected to the test tube using 12.7 mm OD flexible high pressure polypropylene tubing.

3.3 Flow Calming / Flow Mixing Chamber (Figure 3.3)

Just before the solution entered the test section, it passed through a flow calming section which was a plexiglass chamber of 75 mm inside diameter. Turbulent fluid flow in

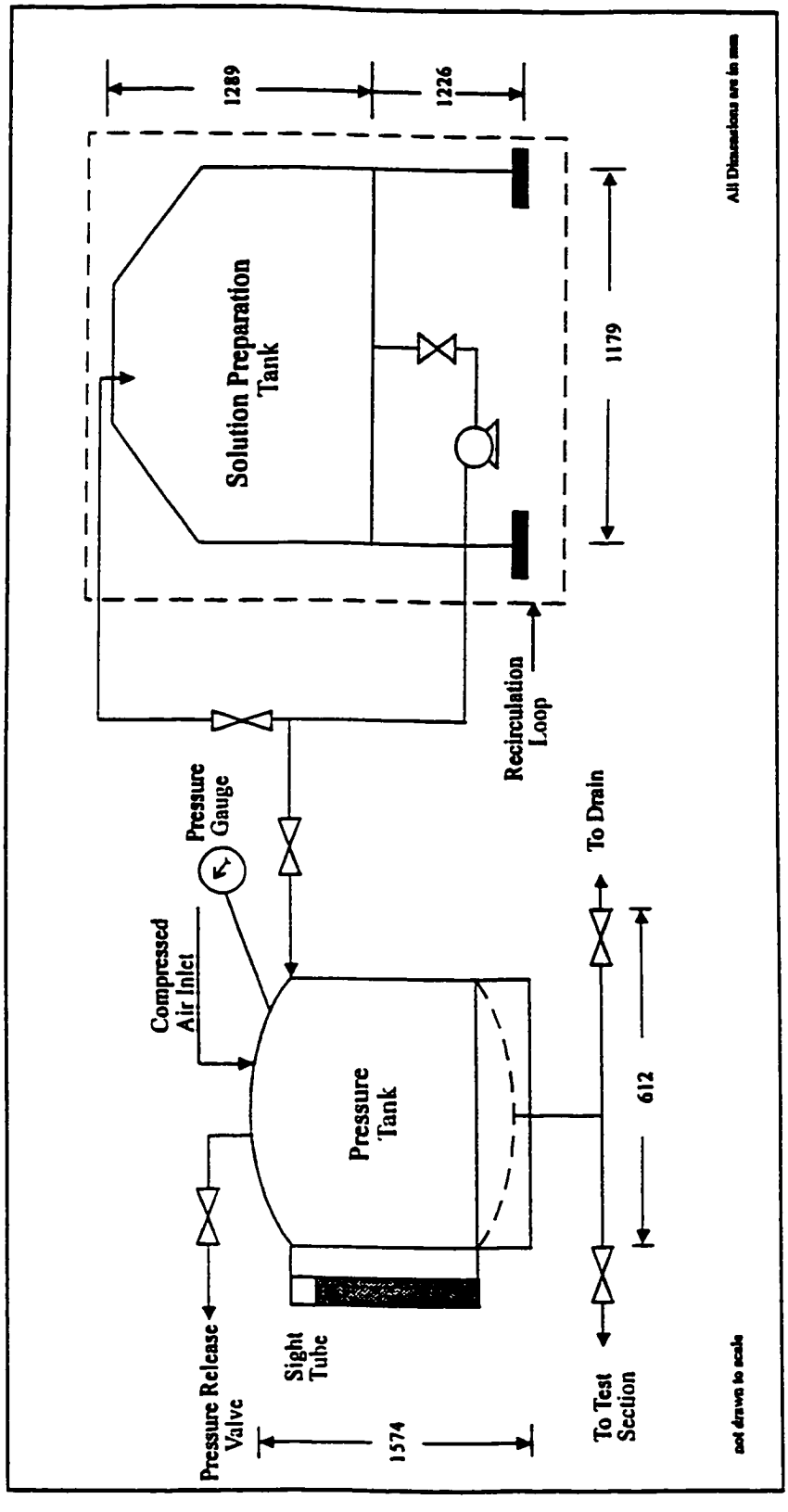

Figure 3.2 Layout of pressure tank and solution preparation tank showing the recirculation Loop

a circular pipe is characterized by a boundary layer flow and an inner core of bulk flow. In the bulk flow region, the velocity profile is flat and coherent eddy structures are present. Turbulent fluctuations are confined to the boundary later flow. The flow calming chamber, which is approximately 10 times in diameter more than the test section, ensured that uniform flow with a flat velocity profile entered the test section. Also, an increase in diameter from the vinyl tubing (2.00 cm) to flow calming chamber (8.9 cm) reduced the shear stress at the wall and hence less turbulent fluctuations resulted in the flow calming chamber. The inlet temperature of the liquid going to the test section was measured here by means of a thermocouple probe sitting in a glass capillary tube which projected into the chamber.

At the end of the test section a flow mixing chamber ensured that a well mixed outlet temperature was measured. The flow mixing chamber was a plexiglass chamber of same dimensions as the flow calming section with two half discs fitted inside to act as baffles. When the fluid flows past an obstruction, such as a flat plate, a high vorticity region is generated at the back of the plate due to flow separation and leads to the formation of wakes which increase the intensity of turbulence and provide effective mixing. Such an arrangement was necessary because constant flux heating at the walls results in non-uniform fluid temperatures across a given cross section as fluid next to the wall has a higher temperature than the fluid near the center of the tube.

3.4 Test Tube (Figure 3.4)

Two different diameter SS 304 tubings (9.53mm OD and 12.6mm OD) were used in the current study for making pressure drop and heat transfer measurements. Both the tubes had a wall thickness of 1.2 mm. Drag reducing polymer solutions reportedly (Cho and Harnett, 1982) have a thermal entrance length of about 500 diameter for high

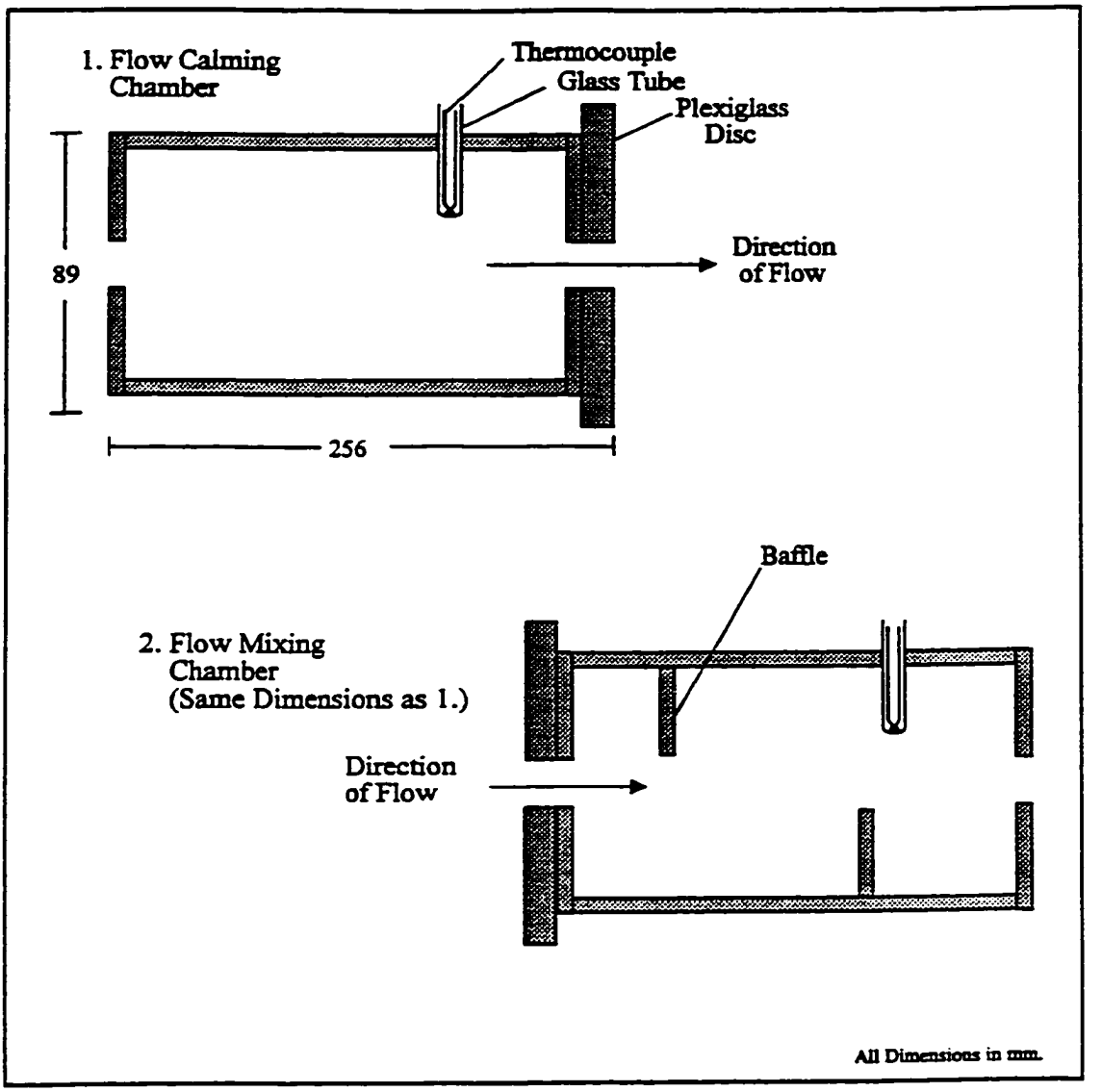

Figure 3.3 Flow calming and flow mixing sections

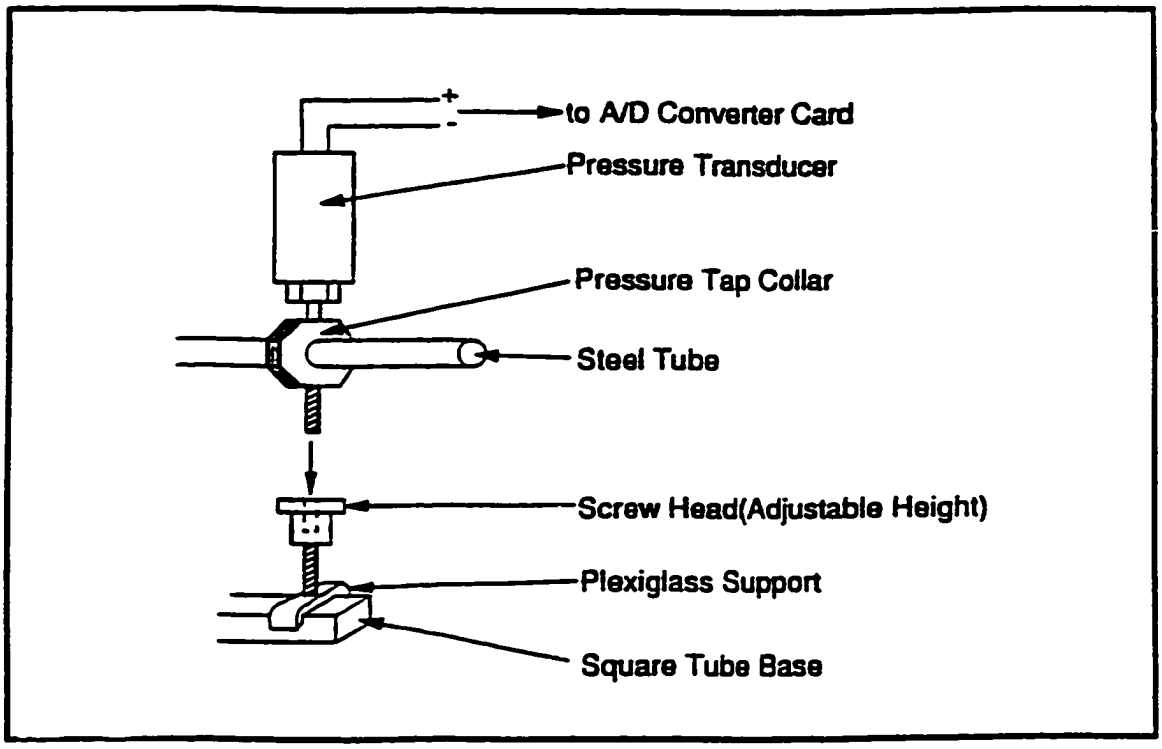

Figure 3.4 Arrangement of support for the test tubes

Reynolds number flow while surfactant solutions have a thermal entrance length of about 300 diameters (Gasljevic, 1995). Since both the tubes used in our experiments were approximately 600 diameter long, we were able to make heat transfer measurements in the fully developed region for surfactant solutions.

To ensure that the test tubes were in the horizontal plane when making experimental measurements, the supports used all along the length of the tubes had screw heads, which could be used to adjust the height of the tubes (as shown in Figure 3.4)

3.5 Pressure Measurements (Figure 3.5 and 3.6)

Pressure drop along the length of the tube was measured by ten pressure transducers (Barksdale CVD-2000, 0 to 120 psi range). The positions for the pressure tappings (Figure 3.5) were selected in such a way that they were closely spaced in the first half of the tube so that data could be gathered to study the development of the hydrodynamic entrance region. At each pressure tap location, two holes, 1.5 mm in diameter, were drilled diametrically opposite and a Teflon collar was placed over them (Figure 3.6). The Teflon collar has a sealed circular chamber overlapping the two holes which was also connected to the pressure transducer. This arrangement allowed the measurement of average pressure across the cross section where the pressure tap was located. Drilling of the holes resulted in the formation of burrs inside the tubes which were cleaned carefully to avoid any unintentional distortion of the flow and unreliable pressure readings.

In the later experiments, when studies on micellar break-up and recovery were carried out, another pressure tap location was drilled just past the inlet to the tube. This

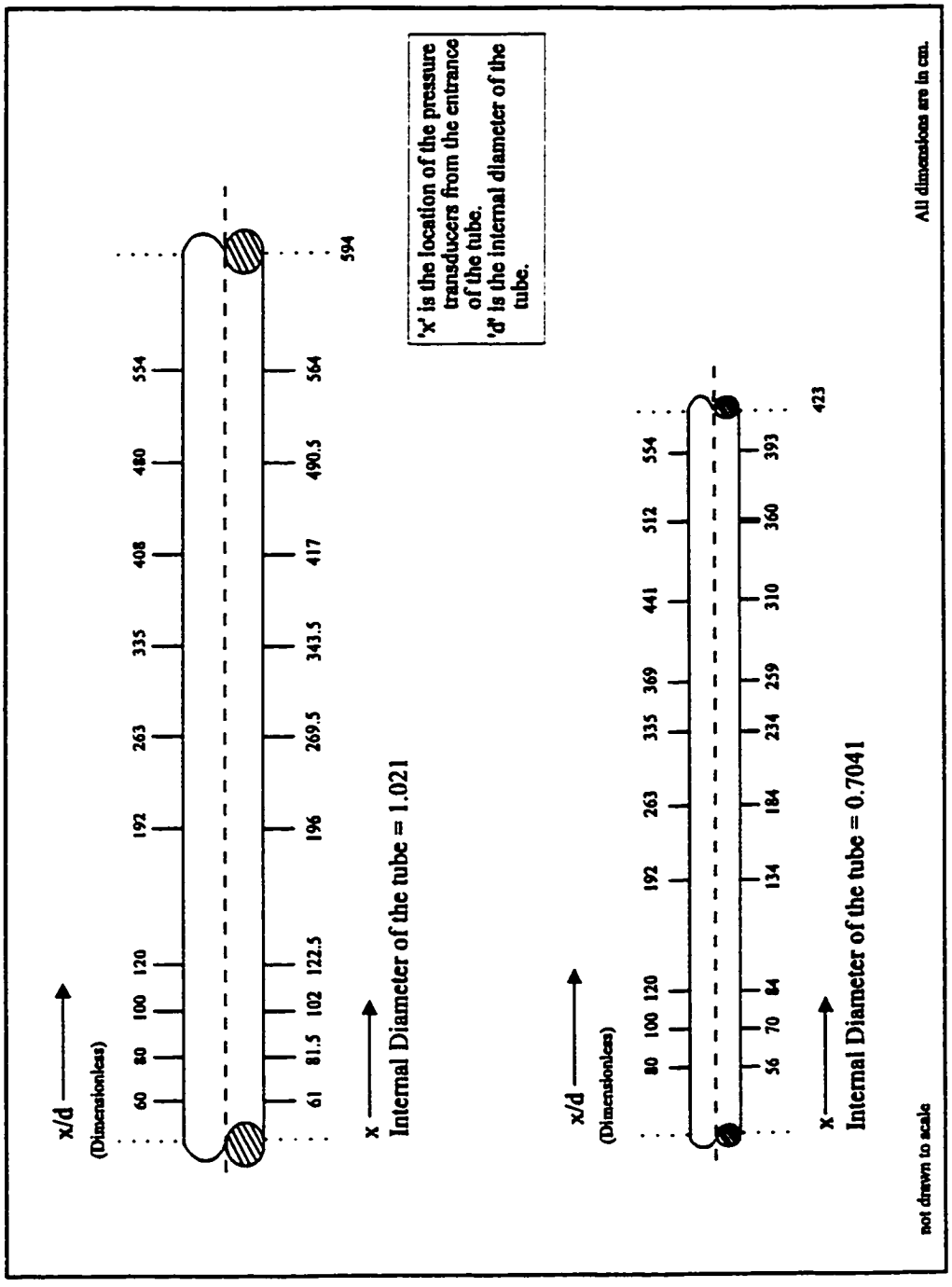

Figure 3.5 Location of pressure taps on the test tubes

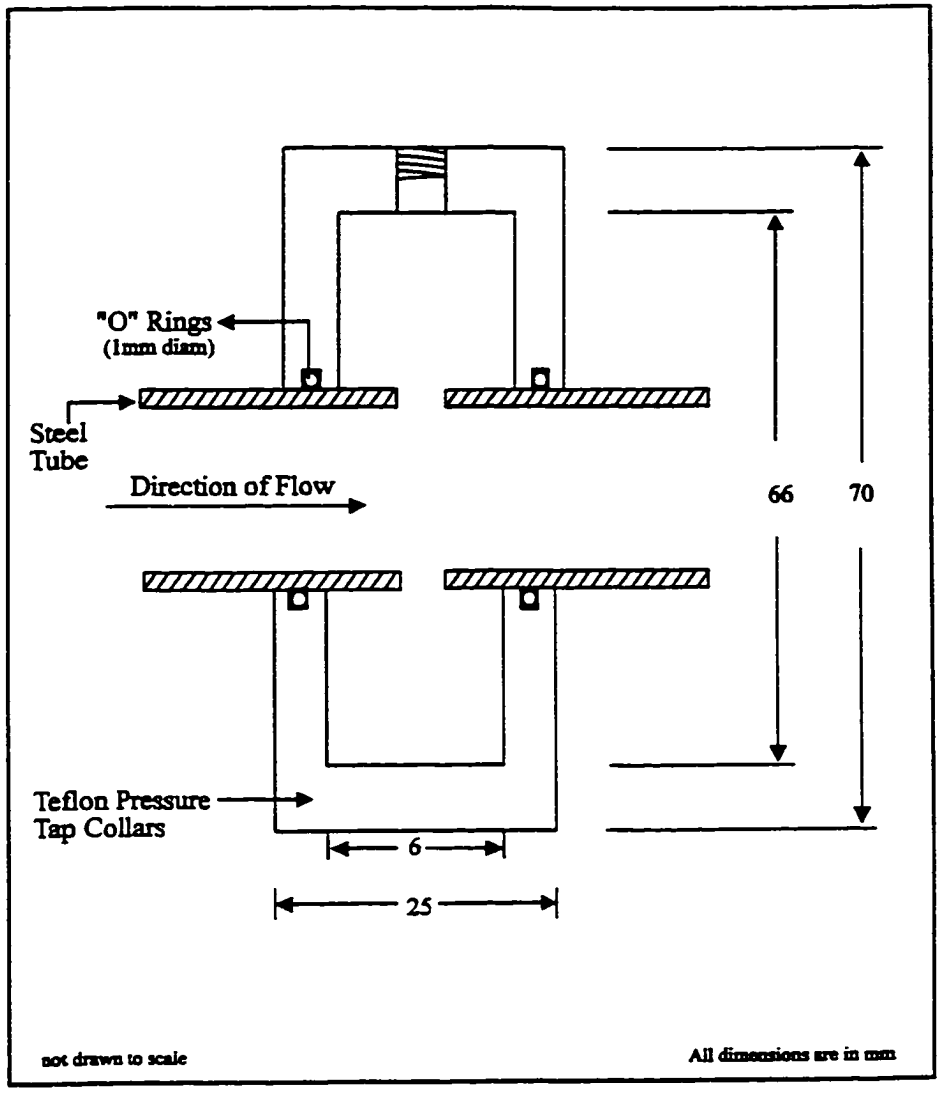

Figure 3.6 Inside view of a pressure tap

enabled pressure drop measurement across a wire mesh plug which was placed at the inlet of the tube.

3.6 Temperature Measurement (Figure 3.7)

For heat transfer measurement 'T'-type 30 gauge copper-constantan thermocouples were attached at 17 different axial locations on the surface of the tube.

- Bare thermocouple probes could not be attached directly to the tube surface as the DC current passing through the tube for constant flux heating would have distorted the readings. To overcome this problem, a Beryllium Oxide (BeO) disc, 6.35 mm in diameter and .76 mm thick was attached on the surface of the tube. The disc offers excellent thermal conductivity and electrical resistivity. Its normal use is in the cooling of power transistors. The following procedure for thermocouple installation was employed:
- A drop of heat sink compound was placed on the tube at the correct spot.
- The BeO disc was put on the spot over the drop of heat sink compound and a little more of the heat sink compound was put on it.
- Teflon tape was wrapped around the tube up to this spot.
- The thermocouple was placed in position, so that its tip was embedded in the heat sink compound on the BeO disc and wrapped with a further layer of Teflon tape to hold it in place.

3.7 Constant Flux Heating

Heating of the tube was done by DC power. A 13.5 kW DC welder which could work in constant current or constant voltage mode was used for this purpose. The

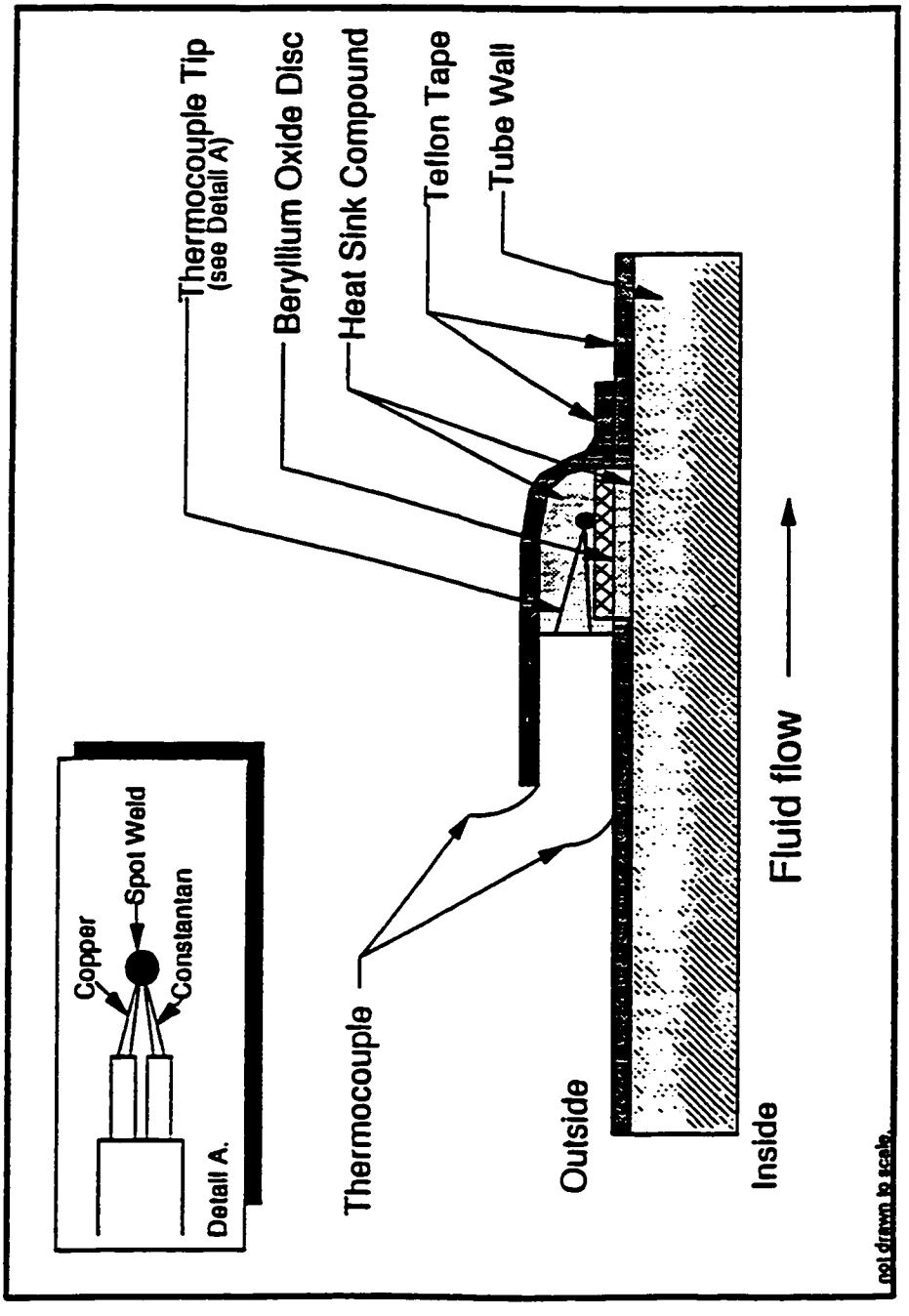

Figure 3.7 Thermocouple attachment technique

electrical resistance of the tube generated heat, which was transferred to the solution flowing through the tube.

For passing DC power through the test tube, Copper plates were soldered on to the tube at both ends and leads from the DC supply were clamped tightly to them (Figure 3.1).

The test section was electrically isolated from rest of the flow system by placing phenolic discs in between the copper plates and flow calming/ flow mixing chamber at the two ends of the tube. Phenolic is not only an electrical and thermal insulator but can also withstand operating temperatures of up to 150 °C, hence it was considered suitable for use in our experimental set up as runs were to be carried out in the temperature range of 15°C-60 °C.

The tube was wrapped with two layers of Teflon tape all along the length to insulate it against heat losses to the ambient. In addition, a rubber insulation, which is used for low temperatures, was used on top of the Teflon tape to ensure that heat losses were minimized.

3.8 Flow Measurement

Average bulk velocity of the solution flowing through the system was calculated by collecting a sample over a known period of time. The volume of the collected sample was measured and the velocity was calculated by dividing the flow rate by cross-sectional area of the tube.

3.9 Data Acquisition System

Relatively short runs at high flow rates made the manual collection of data at a large number of points impossible. Consequently, an on line data acquisition system was used which was directly connected to the computer, where with the help of a software data files were generated. The software also enabled on-line graphical monitoring of the run conditions which proved useful for keeping track of any abnormalities during the course of a run. Also, since we were interested in collecting data at steady state, the graphical display was used to determine when they had been reached and thus eliminated collection of data in the unsteady state.

The signals from 10 pressure transducers, 19 thermocouples and voltage and current output from the DC power supply were fed to two analog to digital conversion cards. With the help of a computer interface card, these signals were transmitted to the computer where the data acquisition software interpreted the signals and provided the output in engineering units. Data were collected at a frequency of 4 Hz. The software received 4 readings per second from each input device, calculated the average and wrote the final value to a file.

3.10 Experimental Run Procedure

The following sequence of operations was followed for every experimental run:

The Solution Preparation Tank was cleaned with water to remove any traces of the previous solution. A fresh surfactant solution of required concentration was prepared following the procedure described in the last chapter. The pressure tank was cleaned and the flow system was purged with water to ensure that no surfactant material from previous

run was remaining in the system. The flow calming and flow mixing chambers were drained to remove accumulated water. Before transferring the prepared solution into the Pressure Tank, uniform concentration was ensured by thoroughly mixing the solution using the recirculation mode of the centrifugal pump as described in section 3.1. The solution was then transferred to the Pressure Tank. The level of liquid in the Pressure Tank was monitored through the sight glass and when the tank was filled to the top, the pump was stopped and disconnected from the Pressure Tank. A line from the air compressor was connected to the pressure tank. The pressure regulator on the compressor was set to the desired pressure. The desired output from the DC power supply in the constant voltage mode was selected. The pressure tank was pressurized by opening the valve from the air compressor. The valves at the end of the test section were set to allow the solution to return to the Solution Preparation Tank during initial parts of the run. The Data Acquisition System was put online to graphically monitor the run conditions.

The valve at the bottom of the pressure tank was opened to let the solution flow through the system. The DC power supply was turned on to pass electric current through the wall tubes. A constant watch was kept on the graphical display to ensure that the pressure and temperature profiles had reached steady state values. At steady state conditions, transfer of data to the data files was initiated and by adjusting the valves, the flow at the outlet of the system was directed to the vessel used for measuring the mass flow rate for a set period of time (using a stop watch). The valves were then again switched to allow flow of the solution back to the Solution Preparation Tank. Transfer of data to the data files was stopped. The power supply was turned off and the valve at the bottom of the Pressure Tank was closed to complete one cycle of operation.

4. ROLE OF SHEAR STRESS IN TURBULENT DRAG REDUCTION

To understand the process by which polymeric or surfactant additives cause reduction in drag or convective heat transfer in turbulent flow through pipes, we have to look at the structure of turbulence close to the wall:

The description of a turbulent flow starts by dividing the velocity and pressure field into mean and fluctuating parts. The action of the velocity fluctuations produces a stress on the mean flow, which is frequently large compared to the viscous stress. A gradient of this stress, also known as the Reynolds stress, produces a net acceleration of the fluid in the same way as a gradient of the viscous stress.

The Reynolds stress works against the mean velocity gradient to remove energy from the mean flow, just as the viscous stress works against the velocity gradient. However, the energy removed by the latter process is directly dissipated, reappearing as heat, whereas the action of the Reynolds stress provides energy for the turbulence. This energy is ultimately dissipated by the action of viscosity on the turbulent fluctuations. Hence the loss of mean flow energy to turbulence is very large compared with the direct viscous dissipation. In other words, Reynolds stresses generated by the velocity fluctuations in the region next to the viscous sublayer virtually gives rise to friction in pipe flow.

The region next to the viscous sublayer in the turbulent boundary layer has been termed as the 'seat of turbulence' by Schlichting (1979). The velocity fluctuations in this region, also known as the buffer layer, grow into large eddies of the bulk flow further downstream. These eddies are called 'coherent structures', emphasising that the fluctuations in a turbulent flow are

not totally random. The fluctuation field involves distinctive patterns of motion in which similar, although not identical, patterns occur repeatedly.

4.1 Dampening of Velocity Fluctuations by Additive Molecules

The interaction of the drag reducing additive molecules with velocity fluctuations in the boundary layer flow has been described in detail by Lumley (1964, 1973). His hypothesis, which is widely accepted, assumes that these molecules alter the energy balance of turbulent velocity fluctuations. These fluctuations stretch out the coiled polymer molecules or the surfactant micelles, and since these molecules have a very high extensional viscosity, they tend to extract energy from these disturbances in the boundary layer while undergoing extension. Since a fraction of the energy associated with these disturbances is used up in stretching the additive molecules, the net effect is the dampening of the velocity fluctuations, resulting in lower Reynolds stresses and hence lower drag.

It has been found that the temperature gradient in a fluid being heated or cooled follows the same course as the velocity gradient. The temperature gradient is large at the wall and through the viscous sublayer, small in the turbulent core and rapidly changing in the buffer zone. The reason for the large temperature gradient through the viscous sublayer is that heat must flow through this layer by conduction, which results in a steep temperature gradient in most fluids because of the low thermal conductivity. Hence the viscous sublayer acts as a resistance to heat flow. The dampening of velocity fluctuations in the buffer layer effectively increases the thickness of the viscous sublayer and offers an additional resistance to heat transfer between the wall and the bulk of the fluid, which translates into the heat transfer reduction effect.

4.2 Velocity Fluctuations and Their Relation to Shear Stress

Intensity of turbulence, q, is defined in terms of the sum of the mean square velocity fluctuations, where,

$$\left(\overline{q^2}\right)^{\frac{1}{2}} = \left(\overline{u'^2} + \overline{v'^2} + \overline{w'^2}\right)^{\frac{1}{2}} \qquad 4.1)$$

As discussed above, it has been generally accepted and experimentally shown (Lumley, 1964 and Virk, 1975) that the interaction of the additive molecules with turbulent velocity fluctuations in the region next to the viscous sublayer of the boundary layer flow is responsible for the drag reduction effect. This region of the boundary layer is called the buffer layer.

Though the Reynolds number or the bulk velocity might be the same in different diameter pipes, the intensity of the turbulent fluctuations, q, is not the same in the buffer layer. At a given Reynolds number or bulk velocity, q decreases with an increase in the pipe diameter. Hence any model that aims to predict drag reduction scale up based on these parameters would not be successful in predicting the actual flow over a wide range of pipe diameters. A study of the available models in published literature (discussed in Chapter 5) has indicated that though most of them are able to predict the drag reduction results over a narrow range of diameters, they all fail poorly when predictions are extrapolated to fit actual field data for large scale commercial pipelines. A point in case (Burger et al., 1982) is the use of drag reducing additives by Arco Oil Company in its 1300 km long (120 cm dia) Trans Alaska Pipeline for crude oil transportation. Due to the inadequacy of available scale-up models to predict over a wide range of diameters, tests had to be carried out in a comparable diameter pipe (34 cm dia), even though results from 2.65 cm and 5.25 cm pipes were available.

In this study we propose the use shear stress as a basis for comparing the experimental results in different diameter pipes. This approach takes advantage of the experimentally proven fact that the velocity fluctuations next to the viscous sublayer in the turbulent boundary layer can be quantified by the shear stress at the wall and are independent of the pipe diameter. This will facilitate the development of an effective scale up model and methodology.

The same turbulence intensity field can, in principle, be produced by many different patterns of velocity fluctuations. It has been confirmed experimentally (Schlichting, 1979 and Tritton, 1988) that flow in the inner part of the turbulent boundary layer, where velocity fluctuations originate, can be characterised by shear stress at the wall, or the shear velocity, u_τ, which is defined as,

$$u_\tau = \left(\frac{\tau_w}{\rho}\right)^{\frac{1}{2}} \tag{4.2}$$

The velocity fluctuations in the inner part of the boundary layer have been shown to be a function of u_τ and totally independent of the diameter of the pipe (Tritton, 1988). Hence once u_τ is specified, structure of the inner boundary layer and the intensity of turbulence is also specified, irrespective of the diameter of the pipe. In other words, if the same value of shear stress at the wall is maintained, the time averaged intensity of the turbulent velocity fluctuations would also be the same in different diameter pipes even though the pattern of fluctuations at a given instant of time may be different.

From the above discussion it becomes clear that since it is the interaction of the drag reducing additive molecules with the turbulent velocity fluctuations (or the shear stress) that is

responsible for the drag reduction and heat transfer reduction effect, a constant value of shear stress at the wall in different diameter pipes should yield similar results for a given solution concentration. This prompted us to investigate the effect of shear stress at the wall on friction and heat transfer results for drag reducing flows in different diameter pipes.

4.3 Use of Shear Stress to Correlate Drag Reduction Results

The drag reducing additive used in our experiments was Ethoquad O12 manufactured by Akzo Chemicals (Table 2.2).

Prior to the tests using the drag reducing solutions, calibration runs were conducted using water. To validate the experimental apparatus and the overall experimental procedure, friction and heat transfer coefficients for fully developed flow were compared with well established correlations available in the literature (Kays and Crawford, 1980). As shown in Appendix 2, the friction results were correlated well by the Prandtl-Karman equation, while the heat transfer results were within ±13% of the predictions by the Seider-Tate equation.

Drag Reduction is defined as the ratio of the change in friction factor due to the presence of the drag reducing additive to the friction factor of the pure solvent. Or,

$$DR = \left(1 - \frac{f_p}{f_s}\right) x100 \tag{4.3}$$

where the friction factor, f, is defined as,

$$f = \frac{\tau_w}{\frac{1}{2}\rho \bar{u}^2} \tag{4.4}$$

and,

$$\tau_w = \frac{\Delta P}{\Delta L}\frac{D}{4} \tag{4.5}$$

Substituting equation (4.4) into equation (4.3) and rearranging the terms to satisfy the condition of a constant shear stress at the wall, i.e., $\tau_{w,p} = \tau_{w,s}$, equation (4.3) takes the form,

$$DR = \left(1 - \frac{\bar{u}_s^2}{\bar{u}_p^2}\right) x100 \tag{4.6}$$

or, for a constant bulk velocity, i.e., $\overline{u_p} = \overline{u_s}$,

$$DR_u = \left(1 - \frac{\tau_p}{\tau_s}\right) x100 \tag{4.7}$$

Using the definition of τ_w from equation (4.5) and substituting in equation (4.7) for a given D and ΔL,

$$DR_u = \left(1 - \frac{\Delta P_p}{\Delta P_s}\right) x100 \tag{4.8}$$

Equations (4.7) and (4.8) are the conventional ways of representing drag reduction which have been used in published literature so far.

Even during the early days of research in this area, it was recognised that a certain value of shear stress, which is independent of the pipe diameter, has to be exceeded for the drag reduction effect to manifest itself. But it appears that no attempts were made to investigate whether this diameter independent relationship between drag reduction and τ_w could be observed at higher values of shear stress. Several investigators (Savins, 1977, Whitsitt, 1969 and Sellin and Ollis, 1983) attempted to correlate DR results as a function of solvent shear velocity. They used equation (4.3) to calculate DR, but the friction factors were calculated at either a constant N_{re}, a constant bulk velocity or a constant mass flowrate. It appears from the literature that solvent shear velocity was chosen as the abscissa because of the known dependence of turbulent velocity fluctuations on τ_w (as discussed in the last section). But the fact that a constant N_{re} or a constant bulk velocity for the drag reducing solution and the pure solvent implies vastly different values of shear stress at the wall, was overlooked.

Figure 4.1 shows the dependence of bulk velocity on the shear stress for a 1400 ppm ethoquad solution in water (7 mm and 10.2 mm tube) and pure water (7 mm). It can be seen from this Figure that calculating drag reduction based on a constant velocity would mean that the drag reduction results have been calculated at different values of shear stress. This argument would still hold if a constant mass flowrate or N_{re} was chosen as a basis for calculating drag reduction. Further, the use of these as a basis for comparing results obtained from different diameter pipes again implies that the comparison is being made at different values of shear stress as the same velocity (or N_{re} or mass flow rate) would be obtained in a bigger diameter pipe at a lower shear stress (Figure 4.1).

It is clear from the above discussion that earlier attempts at correlating drag reduction results for solving the scale-up problem did not uphold the underlying assumption of the widely accepted theory (Lumley, 1964, 1973) on the mechanism of drag reduction. Though it was accepted that the additive molecules absorb energy from turbulent velocity fluctuations in the buffer layer and cause drag reduction, the sanctity of the fact that these velocity fluctuations are

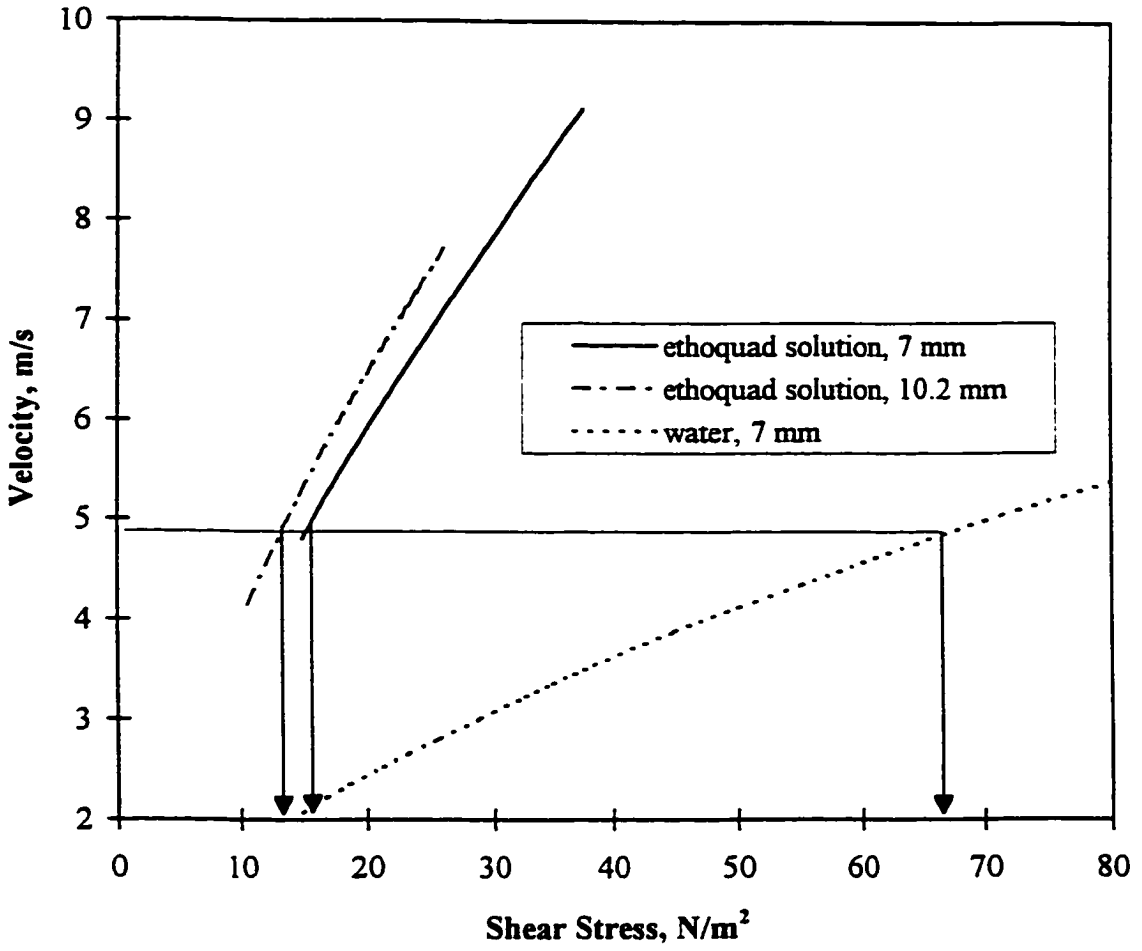

Figure 4.1 Dependence of bulk velocity on shear stress (1400 ppm Ethoquad O12 solution and water)

quantified by the shear stress at the wall and not by velocity (or N_{re} or flow rate) was violated in subsequent scale-up attempts.

As shown in the last section, a true measure of the dampening of turbulent velocity fluctuations by drag reducing additives, which is invariant with the pipe diameter and is dependent only on the concentration of the solution (or its viscoelasticity) could be obtained by using shear stress as a criteria for calculating drag reduction and comparing results in different diameter pipes. Hence equation (4.6) was used to compare drag reduction results obtained in our experimental set-up and several others obtained from the published literature (as listed in Table 4.1). These results and bulk velocity data are shown in Figures 4.2-4.9, as a function of shear stress.

As is clear from these Figures, drag reduction data can be correlated by a single curve for a given additive-solvent system if equation (4.6) is used for calculating drag reduction and the results are compared in different diameter pipes as a function of shear stress at the wall. The data have been selected from surfactant-water, polymer-water and polymer-crude oil systems to verify the universal applicability of this hypothesis. The amount of drag reduction obtained may vary depending upon the type and concentration of the additive, its viscoelasticity and susceptibility to mechanical degradation. But the dependence of drag reduction on shear stress is independent of the pipe diameter and the type of drag reducing system.

A comparison of the DR calculated using equation (4.6) and the conventional way of calculating DR (equation (4.7)) is presented in Figure 4.10, where DR has been expressed as a function of the solution shear stress for the 1400 ppm Ethoquad O12 solution. It can be seen from Figure 4.10 that the magnitude of DR is more when it is calculated at a constant shear stress.

Table 4.1: Drag Reducing Systems Investigated

Source	Drag Reducing System	Additive	Concentration	Pipe Diameter (mm)
Sood, 1993	polymer-water	Poly(ethylene oxide)	200 ppm	7, 10.2
Present Work	surfactant-water	Ethoquad O12	400 ppm*	7, 10.2
Present Work	surfactant-water	Ethoquad O12	500 ppm*	7, 10.2
Present Work	surfactant-water	Ethoquad O12	600 ppm*	7, 10.2
Present Work	surfactant-water	Ethoquad O12	1400 ppm	7 , 10.2
Gasljevic, 1995	surfactant-water	Ethoquad T13	2300 ppm	10, 20, 51.7
Savins, 1995	polymer-water	Hydroxyethyl cellulose	-	25.4, 33
Burger et al., 1982	polymer-crude oil	Conoco CDR (patented)	20 ppm	26.5, 52.5

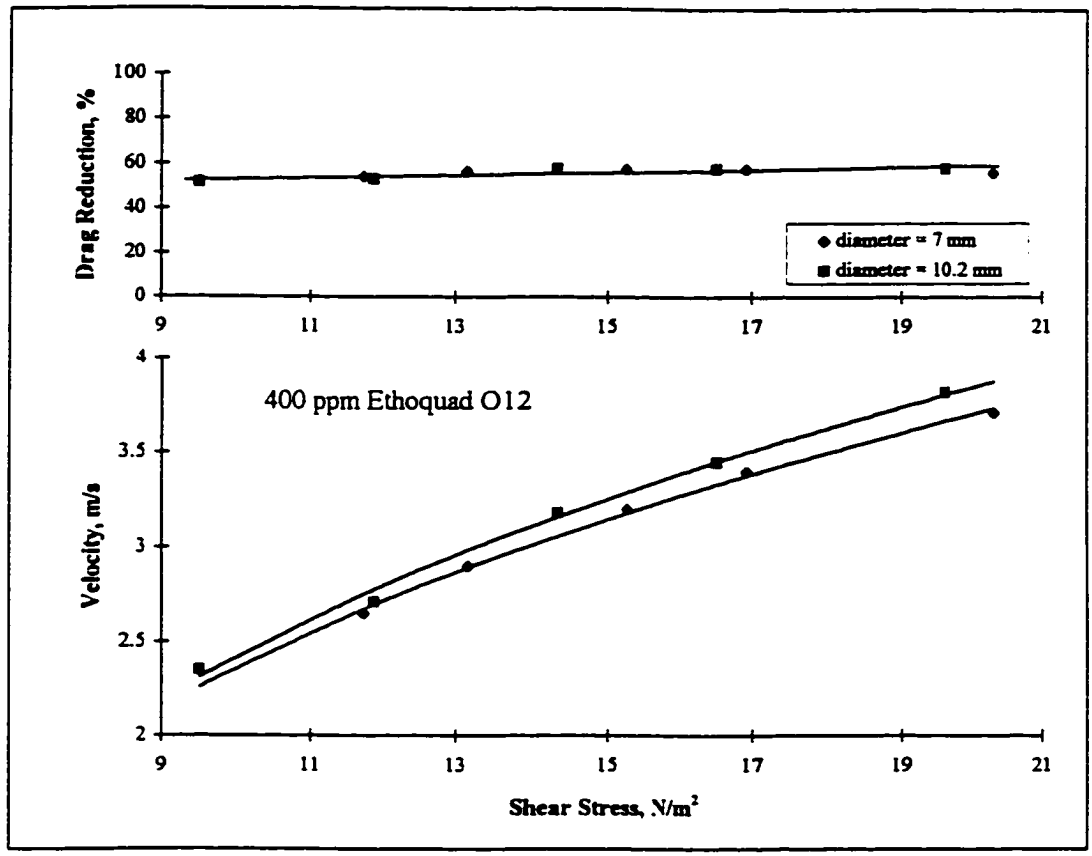

Figure 4.2 Bulk velocity data (7 mm and 10.2 mm diameter) and corresponding drag reduction (equation 4.6) for a surfactant-water system (our data, 400 ppm Ethoquad O12 solution)

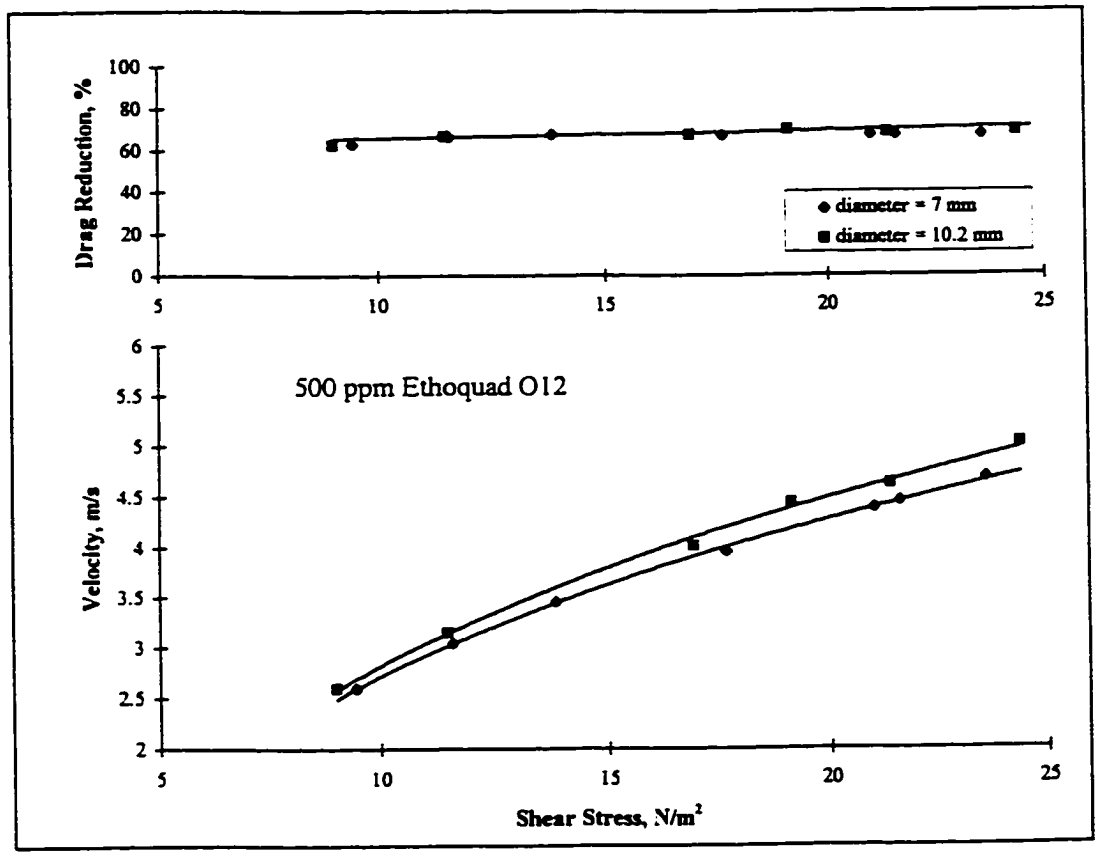

Figure 4.3 Bulk velocity data (7 mm and 10.2 mm diameter) and corresponding drag reduction (equation 4.6) for a surfactant-water system (our data, 500 ppm Ethoquad O12 solution)

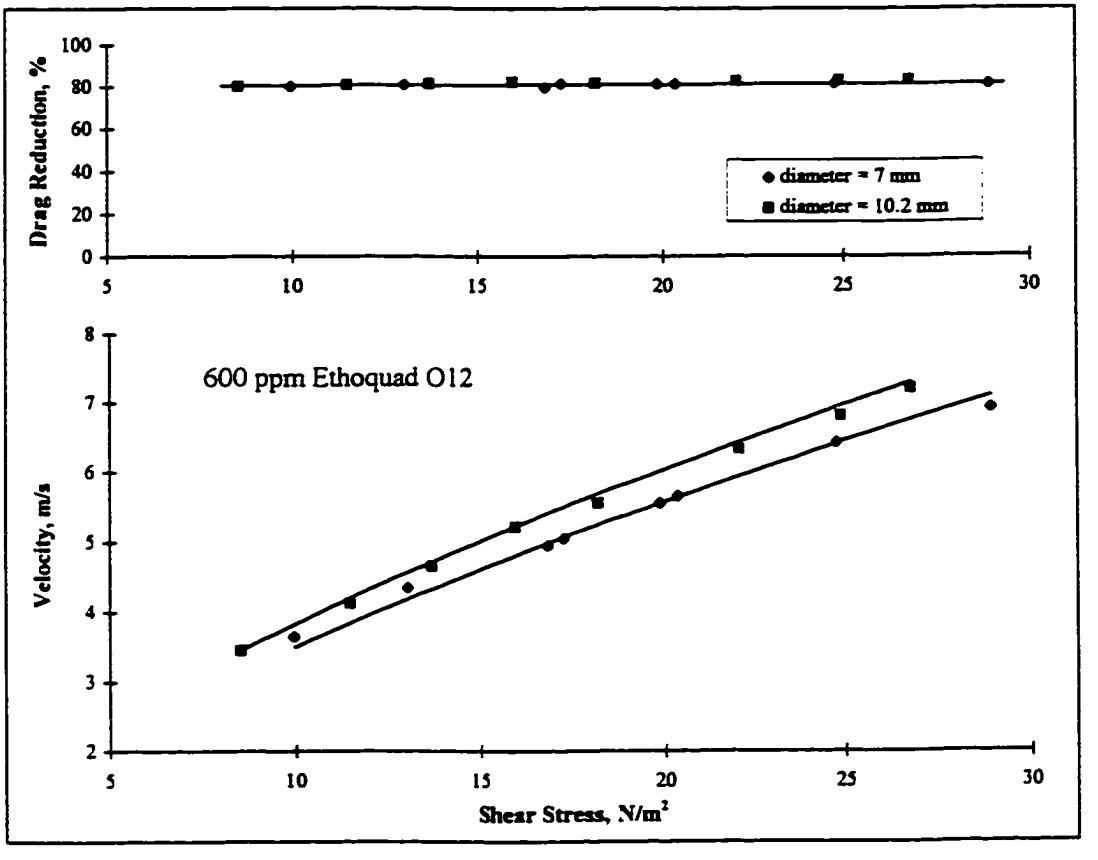

Figure 4.4 Bulk velocity data (7 mm and 10.2 mm diameter) and corresponding drag reduction (equation 4.6) for a surfactant-water system (our data, 600 ppm Ethoquad O12 solution)

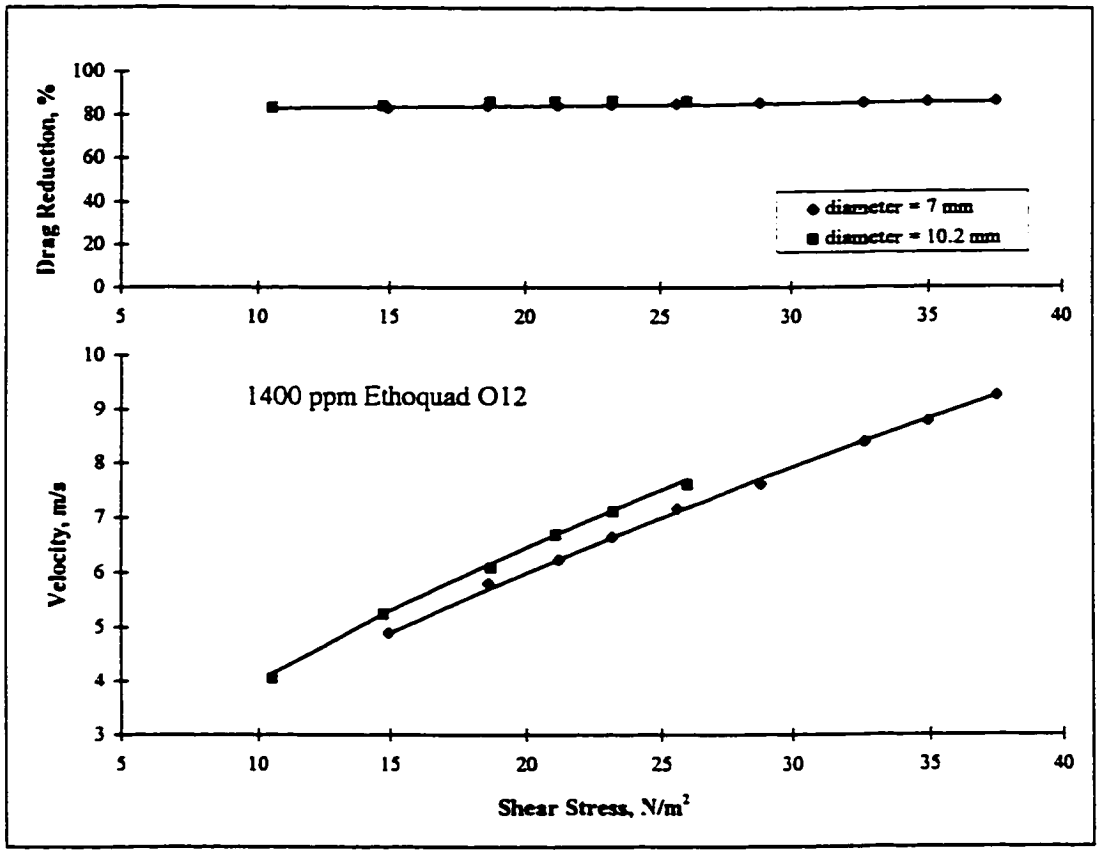

Figure 4.5 Bulk velocity data (7 mm and 10.2 mm diameter) and corresponding drag reduction (equation 4.6) for a surfactant-water system (our data, 1400 ppm Ethoquad O12 solution)

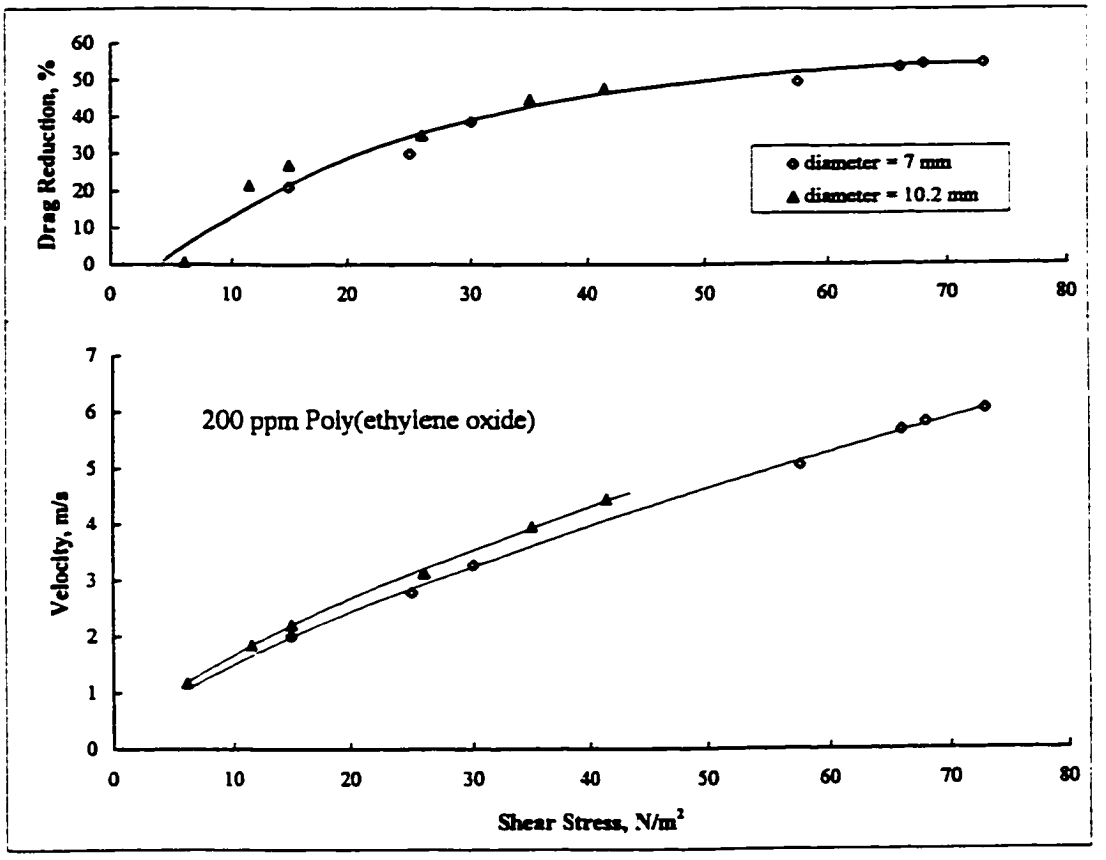

Figure 4.6 Bulk velocity data (7 mm and 10.2 mm diameter) and corresponding drag reduction (equation 4.6) for a polymer-water system (data of Sood, 1993, 200 ppm Poly(ethylene oxide) solution)

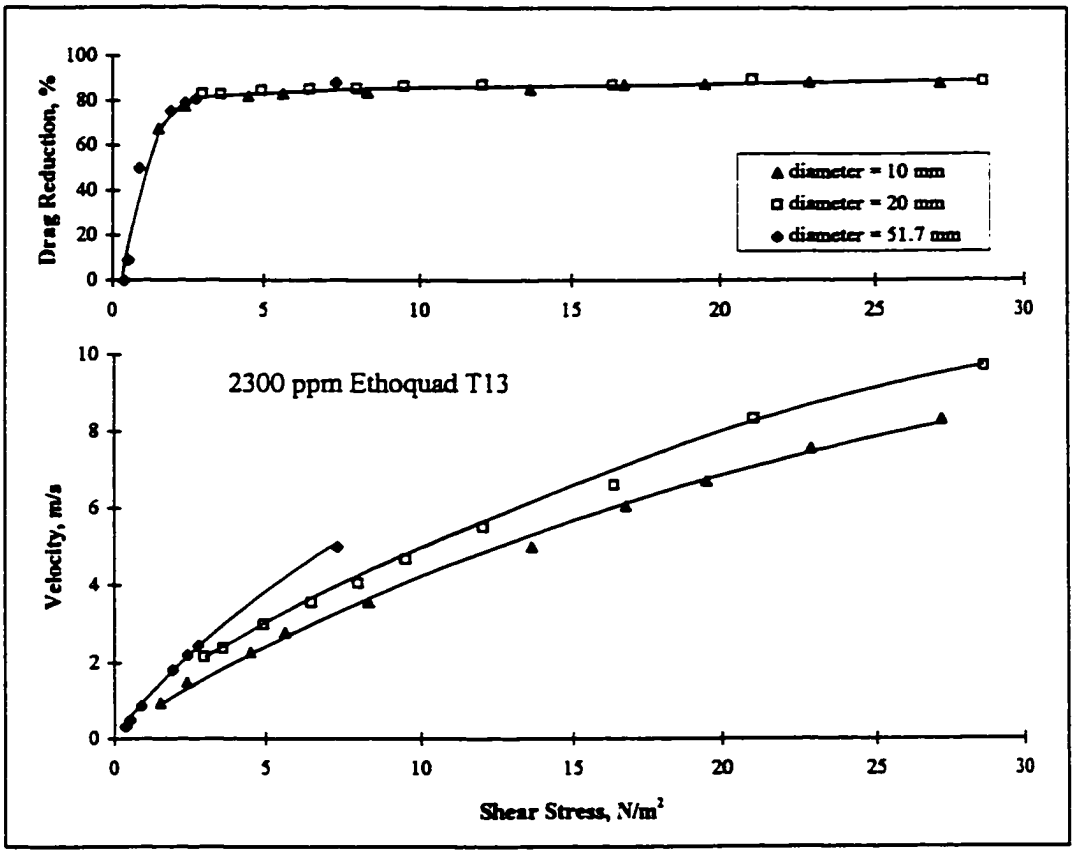

Figure 4.7 Bulk velocity data (10 mm, 20 mm and 51.7 mm diameter) and corresponding drag reduction (equation 4.6) for a surfactant-water system (data of Gasljevic, 1995, 2300 ppm Ethoquad T13 solution

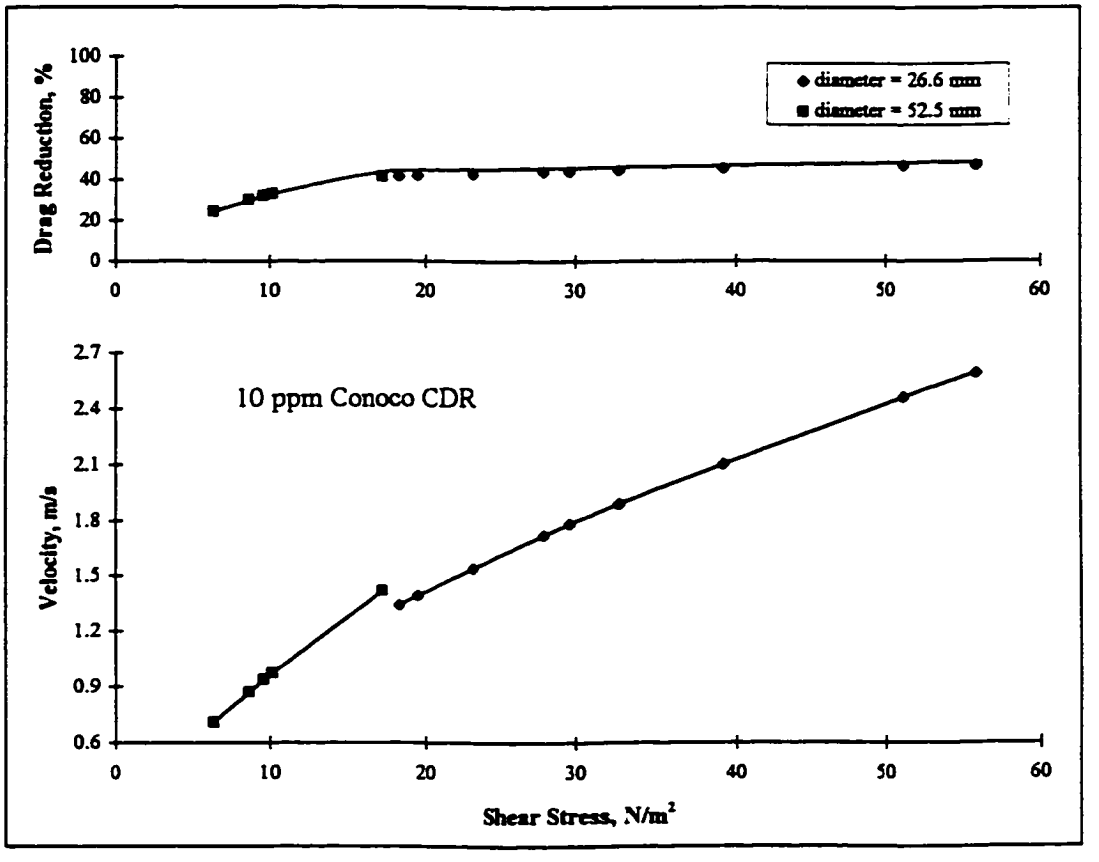

Figure 4.8 Bulk velocity data (26.6 mm, and 52.5 mm diameter) and corresponding drag reduction (equation 4.6) for a polymer-crude oil system (data of Burger et. al, 1982, 10 ppm Conoco CDR solution)

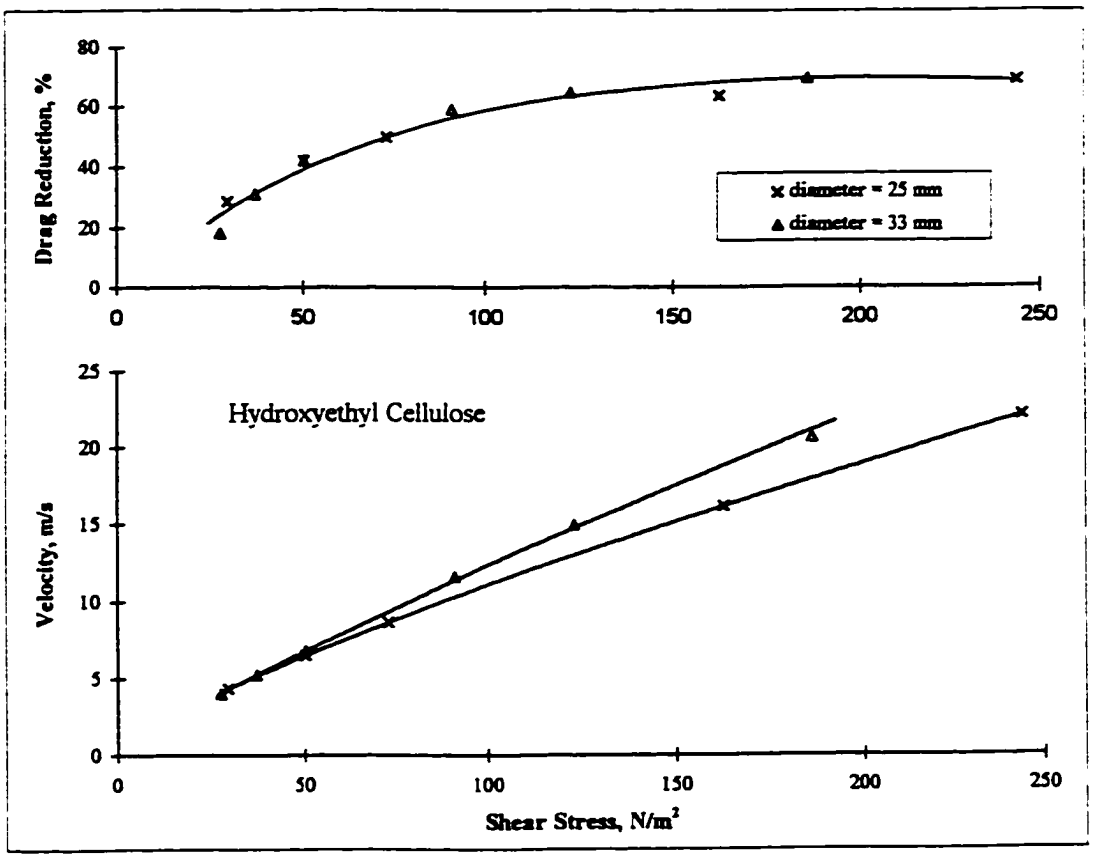

Figure 4.9 Bulk velocity data (25 mm, and 33 mm diameter) and corresponding drag reduction (equation 4.6) for a for a polymer-water system (data of Savins, 1995, Hydroxymethyl Cellulose solution)

4.4 Use of Shear Stress to Correlate Heat Transfer Reduction Results

The evidence that drag reduction can be correlated as a function of shear stress prompted us to investigate whether heat transfer reduction could be explained based on the same criteria. Figure 4.10 depicts the heat transfer coefficients obtained in our experimental set-up for a 1400 ppm Ethoquad O12 solution corresponding heat transfer reduction. Heat transfer reduction was calculated from the following equation,

$$HTR = \left(1 - \frac{h_p}{h_s}\right) x100 \tag{4.9}$$

h_p and h_s are the average heat transfer coefficients obtained from the fully developed temperature profiles, well away from the entrance and at the same shear stress at the wall.

As can be seen from Figure 4.10, heat transfer reduction results for the 7 mm and 10.2 mm diameter tubes seem to fall on to a single curve when expressed as a function of shear stress. This kind of behaviour is expected considering that heat transfer reduction is in fact caused by the effective thickening of the viscous sublayer by the dampening of the velocity fluctuations in the buffer layer. Since the dampening of the velocity fluctuations (or, drag reduction) is invariant with the pipe diameter and dependent only on the shear stress at the wall, the same should hold for the apparent thickening of the viscous sublayer (or, heat transfer reduction).

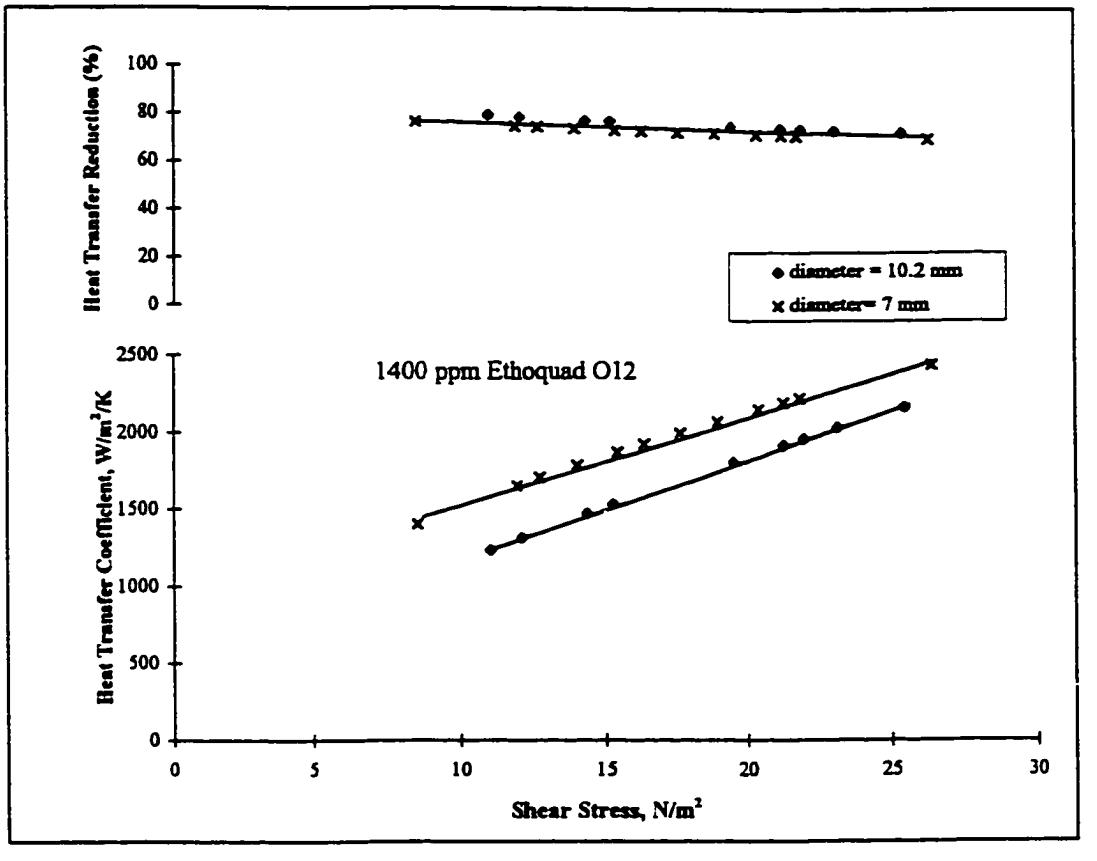

Figure 4.10 Heat transfer coefficients (7 mm and 10.2 mm diameter) and corresponding heat transfer reduction (equation 4.9) for a surfactant-water system (our data, 1400 ppm Ethoquad O12 solution)

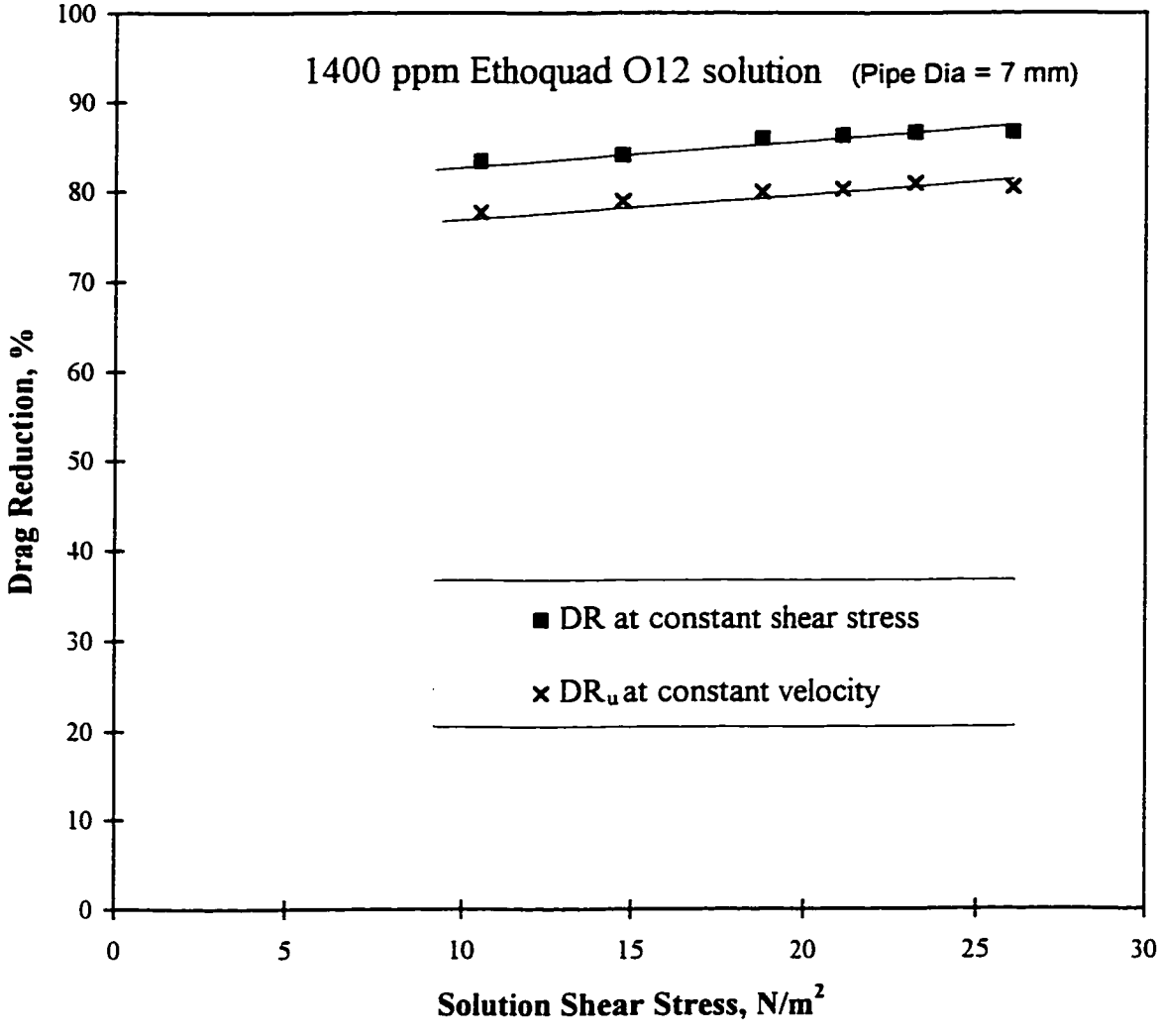

Figure 4.11 Comparison of Drag Reduction (DR) calculated at constant shear stress and at constant bulk velocity

4.5 Summary

We have presented an effective method for comparing drag reduction results in different diameter pipes. The impetus for calculating drag reduction based on a constant shear stress came from the dependence of turbulent velocity fluctuations on shear stress, which is invariant with the pipe diameter, indicating that the dampening of the velocity fluctuations (and hence drag reduction) due to interaction with drag reducing additives would also be independent of the pipe diameter.

Using equation (4.6), which calculates drag reduction at the same shear stress, we were able to show that results in different diameter pipes for a polymer-water, polymer-oil, surfactant-water system fall onto the same curve. This shows that drag reduction is a function of shear stress while it is independent of the diameter of the pipe. The important point to be noted here is that the "diameter effect" vanishes when drag reduction is calculated at a constant value of shear stress. As has been discussed in the previous sections, earlier investigators calculated drag reduction at a constant mass flow-rate (or velocity) or Reynolds number, which was like comparing apples and oranges because same flow-rate or Reynolds number for a drag reducing fluid and the pure solvent means vastly different values of shear stress at the wall.

Further, we have shown that heat transfer reduction results obtained in our experimental set-up appear to be independent of the pipe diameter when heat transfer reduction is calculated at a constant shear stress (equation (4.9)). The trend obtained appears to be encouraging but more data would be required to verify the hypothesis beyond doubt.

5. SCALE-UP MODEL FOR DRAG REDUCTION

Despite the general agreement that turbulent drag reduction (and hence heat transfer reduction) is a consequence of the interaction of the viscoelastic additive molecules with the turbulent boundary layer (Virk, 1975) direct experimental verification of these properties is very difficult because of the low concentrations of these solutions. Though a large volume of work has been done on this subject, a theoretical expression or correlation relating the turbulent friction and convective heat transfer loss characteristics of these solutions to readily measurable flow and rheological properties has not yet been obtained.

5.1 Previous Work

The flow of Newtonian fluids in circular pipes can be adequately correlated by the well known universal laws:

$$f = \frac{16}{N_{re}} \qquad \text{(laminar flow)} \qquad (5.1)$$

and

$$\left(\frac{2}{f}\right)^{\frac{1}{2}} = 2.5\ln\left(N_{re}\left(\frac{f}{8}\right)^{\frac{1}{2}}\right) + 2.0 \qquad \text{(turbulent flow)} \qquad (5.2)$$

Unlike Newtonian fluids, there is a rather strong influence of the pipe diameter on the friction law for drag reducing fluids. These solutions cannot be characterized by Reynolds number of the flow. In other words, maintaining the same Reynolds number in different diameter pipes would not yield the same friction factor due to the so called 'Diameter Effect'. Tackling the problem of the diameter effect assumes considerable importance and interest, knowing that a complete and detailed description of the interaction of additive molecules with the turbulent boundary layer is very complex. It requires information on the behavior of the additive molecules in a very dilute solution which, in practice, may not be available. Hence the ideal approach to develop a scale up model would be to be able to predict friction and heat transfer in large industrial scale pipes from data obtained with relatively small size pipes in laboratories. A number of attempts along these lines have been made over the years to model the diameter effect, which can be broadly classified into two groups: (1) Correlation models and (2) Velocity profile models.

5.1.1 Correlation Models

It was realized in the early stages of research in this area that Reynolds number was not sufficient to characterize drag reducing flows. The strong dependence on the pipe diameter indicated a need for the introduction, in addition to the Reynolds number, of a second dimensionless group. This group should contain the tube diameter in order to correlate the observed diameter effect.

Astarita (1969) proposed an interpretation of the drag reduction phenomenon based on the smallest frequency of the energy dissipating eddies, Ω and some characteristic time scale, T_R, of the fluid considered. This approach was based on the energy cascade model of turbulence. According to this model (Tritton, 1988), energy fed

into the turbulence is generated due to velocity fluctuations in the buffer layer and goes primarily into the larger eddies (Figure 5.1). From these, smaller eddies are generated and then still smaller ones. The process continues until the length scale is small enough for viscous action to be important and dissipation to occur. According to Astarita (1965), the size (λ) of the energy dissipating eddies is such that,

$$N_{re_\lambda} = \frac{u_\lambda \lambda}{\nu} = 1 \tag{5.3}$$

Astarita's interpretation tries to show that the turbulence in viscoelastic drag reduction is less dissipative. The elastic properties of the fluid make the energy dissipating eddies conservative and as a result much smaller eddies have to be generated for the viscous dissipation to occur. In other words, presence of drag reducing additives in a solution elongates the energy cascade and reduces the loss of energy due to viscous dissipation, hence resulting in lower friction.

The proper dimensionless group to be considered, following this line of thought was given by the product ΩT_R, or the Deborah number (N_{De}) of the flow. Following an order of the magnitude analysis, Ω was defined by the expression (Astarita, 1965 and Astarita et al., 1969):

$$\Omega = \frac{\bar{u}}{d} N_{re}^{0.5} \tag{5.4}$$

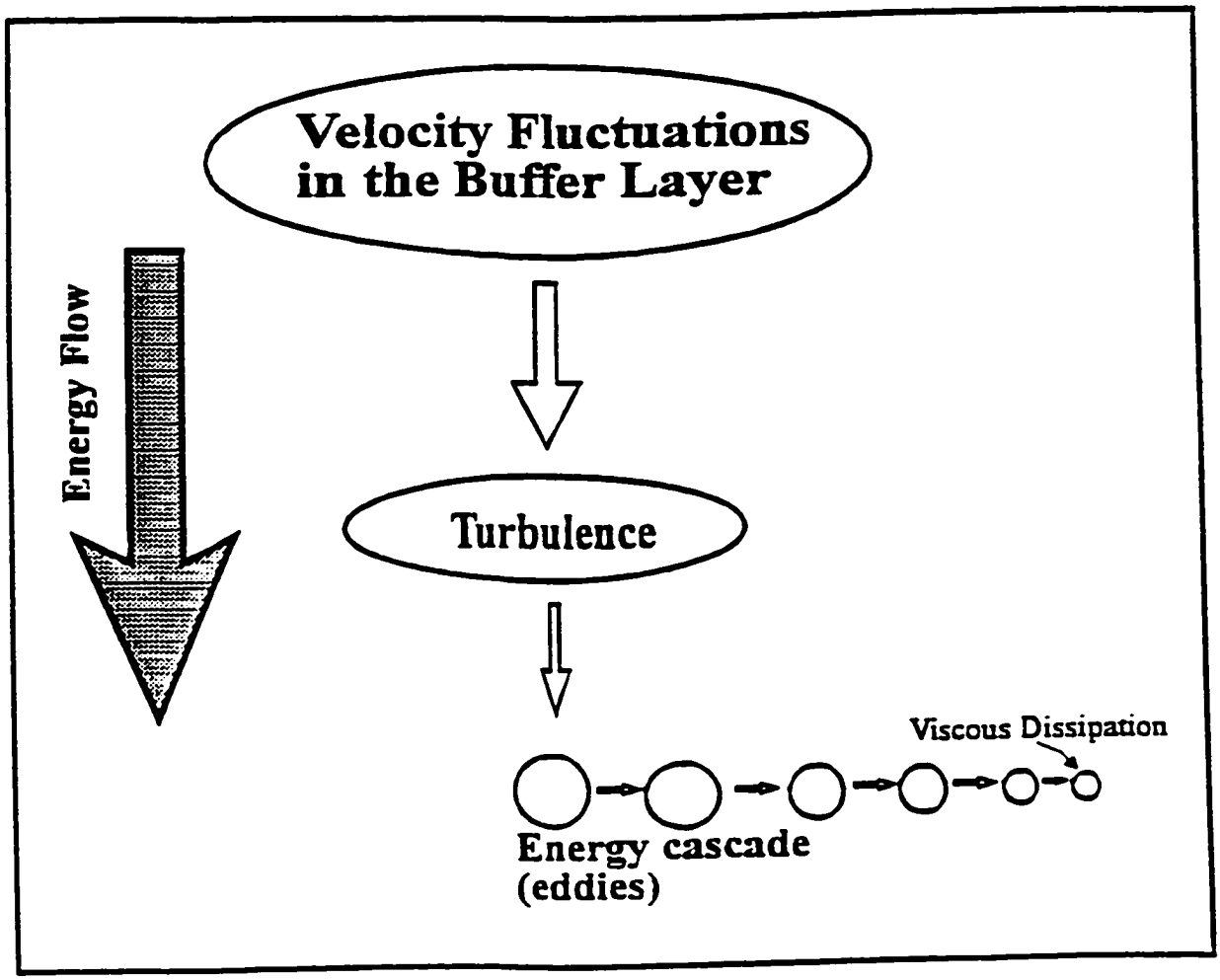

Figure 5.1 Energy cascade model for turbulence

The exponent 0.5 was changed to 0.75 by Seyer and Metzner (1967). Dimensional considerations suggested that the friction factor for a drag reducing solution, f_p , should now be a function of both Reynolds number and the Deborah number:

$$f = f\left(N_{re}, \Omega T_R\right) \tag{5.5}$$

Astarita defined drag reduction ratio, $\beta = (f_p \; f_s)$ and assumed that value of β is uniquely determined by the Deborah number of the flow, i.e.,

$$\beta = \beta\left(N_{De}\right) \tag{5.6}$$

For a given drag reducing fluid, the value of T_R is a constant and if different solutions need to be compared, its value should be known. Astarita et al. (1969) made a further simplifying assumption to get rid of the troublesome parameter T_R and used this modified model to fit experimental data from the test tubes of diameters 0.69, 1.10 and 2.05 cm, respectively. A similar approach was used by Yoon and Ghajar (1988) to predict the results in 1.11 and 1.88 cm diameter tubes.

Although Astarita et al. (1969) were able to determine that β was uniquely dependent on N_{De} and should be a monotonically decreasing function, they could not establish the exact relationship. Using the interaction of energy dissipating eddies with viscoelastic polymer molecules as a basis, Darby and Chang (1984) derived an expression for β, which was given as:

$$\beta = \frac{1}{\sqrt{1 + N_{De}^2}} \tag{5.7}$$

The form of the above generalized correlation equation involved an approximation which was estimated to be valid for tube diameters less than 0.5 cm, but it has been able to correlate data for diameters up to 5 cm (Darby and Pivsa-Art, 1991). The frequency of energy dissipating eddies for the polymer solution (Ω_p) was shown to be dependent on N_{re_p}, N_{re_s}, Ω_s and T_R. Ω_s was calculated from an expression similar to Astarita's characteristic frequency, but derived for $N_{re_\lambda} = 9$. T_R was calculated from fluid rheological parameters obtained from shear viscosity data. Darby and Pivsa-Art (1991) have presented an improved version of this model in which the fluid rheological parameters are obtained from flow measurements.

The concept of the interaction of small energy dissipating eddies with polymer solution viscoelasticity is helpful in explaining the mechanism of drag reduction. But in practice, T_R is not uniquely defined in terms of measurable rheological properties and secondly, reliable rheological measurements needed to evaluate T_R at the very low additive concentrations are extremely difficult to perform (Astarita et al., 1969). Matthys (1991) has also stated that dilute polymeric solutions do not exhibit readily measurable elasticity and better measurement techniques need to be developed before parameters based on the extensional viscosity (i.e. relaxation time and N_{De}) can be routinely used for modeling drag and heat transfer reduction.

5.1.2 Velocity Profile Models

For Newtonian fluids, the inner boundary layer in turbulent flow can be characterized by a two layer velocity profile model, i.e., a viscous sublayer and a logarithmic layer, where,

$$u^+ = y^+ \qquad \text{(viscous sublayer)} \qquad (5.8)$$

$$u^+ = 2.5 \ln y^+ + 5.5 \qquad \text{(logarithmic layer)} \qquad (5.9)$$

where,

$$y^+ = \frac{y u_\tau}{\nu} \; ; \; u^+ = \frac{u}{u_\tau} \qquad (5.10)$$

Virk et al.(1967) and Virk (1975) proposed a three layer velocity profile model for drag reducing solutions. The characteristic feature of this model is the appearance of a region (elastic sublayer) lying between the viscous sublayer and the logarithmic layer, in which the mean velocity increases above Newtonian by an amount s^+. The velocity profile for this region is given by:

$$u^+ = 2.5 \ln y^+ + 5.5 + s^+ \qquad (5.11)$$

According to Virk, the increase in velocity takes place due to the interaction of the viscoelastic additive molecules with the velocity fluctuations in the region next to the viscous sublayer. With increase in drag reduction, there is a progressive shrinkage of the Newtonian core, until at maximum drag reduction, the core vanishes. This implies a corresponding increase in the elastic sublayer extent, which advances outward from the wall, until at maximum drag reduction, it encompasses the entire cross-section of the flow.

Using the drag reduction data from a wide range of systems, Virk was able to determine the asymptotic regime in which the friction factor is independent of concentration or the type of additive. This regime is known as the Virk's asymptote:

$$f^{-1/2} = 8.26\ln\left(N_{re}f^{1/2}\right) - 32.4 \qquad (5.12)$$

The above equation was used by Virk (1975) to infer the ultimate velocity profile for the asymptotic region, which is given as:

$$u^{+} = 11.7\ln y^{+} - 17.0 \qquad (5.13)$$

From Figure 5.2, it can be observed that with an increase in drag reduction, the solution velocity profiles are shifted upwards. According to Virk (but not proven experimentally), the upward shift is parallel to the Newtonian law (equation (5.9)). The parallel upward shift, called the effective slip (s^{+}), increases with increasing concentration of the additive in solution. Finally, at maximum drag reduction conditions, the entire velocity profile for the logarithmic layer corresponds to equation (5.13).

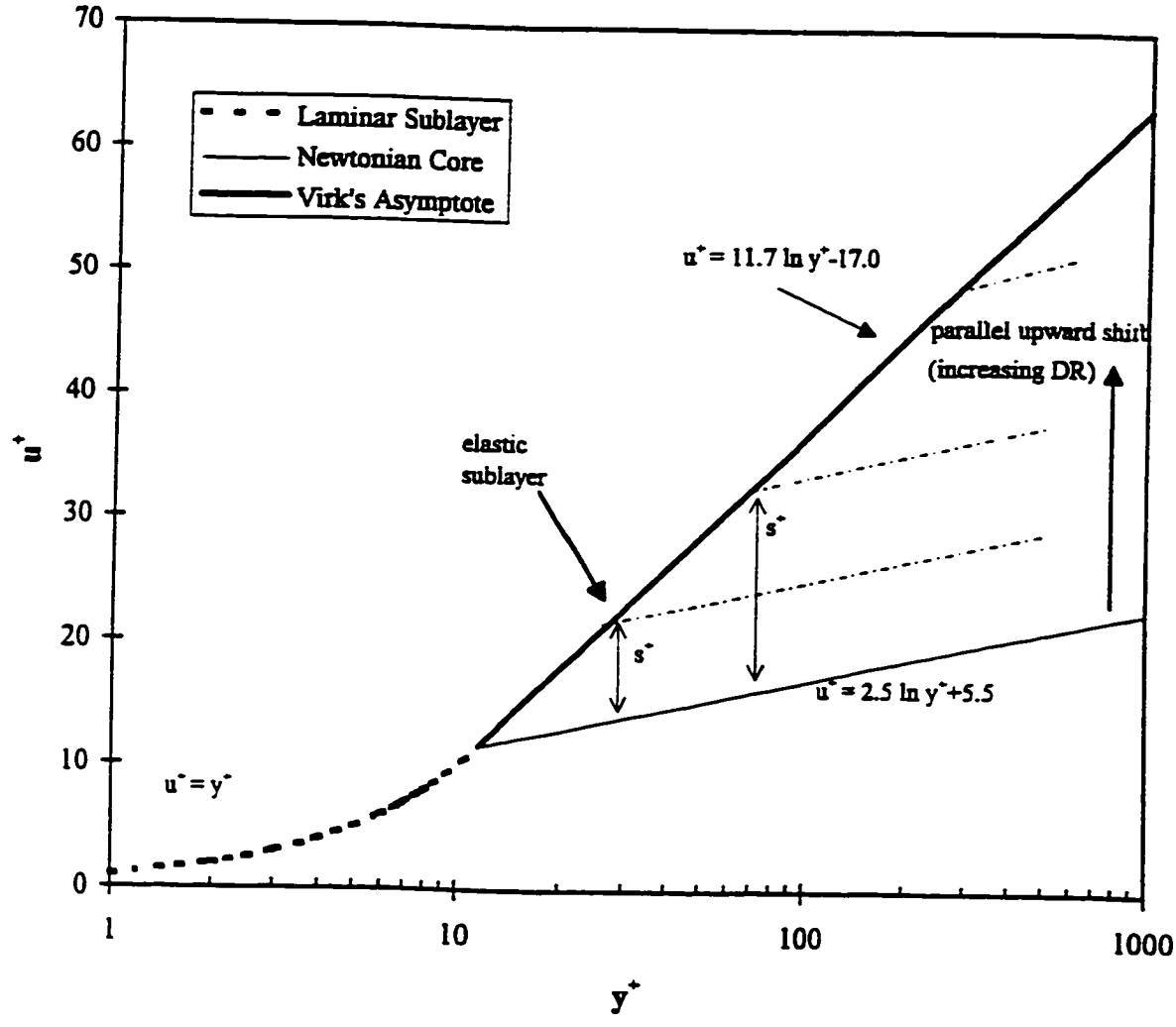

Figure 5.2 Virk's (1975) elastic sublayer model for drag reducing solutions

A scale-up method based on Virk's three layer velocity profile model was proposed by Granville (1978). The value of s^+ was hypothesized to be some function of the shear velocity u_τ and the drag reducing additive properties, i.e.

$$s^+ = f\left(\frac{u_\tau T_R}{\nu}\right) \tag{5.14}$$

The characteristic time T_R, is regarded as a fixed quantity for any particular drag reducing solution. As a consequence, s^+ is a function of u_τ only. Since,

$$u_\tau = \bar{u}\left(\frac{f}{2}\right)^{\frac{1}{2}} \tag{5.15}$$

therefore,

$$\frac{u_\tau T_R}{\nu} = \bar{u}\left(\frac{f}{2}\right)^{\frac{1}{2}}\frac{T_R}{\nu} = \frac{1}{\sqrt{2}}\left(\frac{T_R}{d}\right)\left(N_{re}\sqrt{f}\right) \tag{5.16}$$

for the same additive and a given value of (u_τ, T_R, ν),

$$\left(N_{re}f^{\frac{1}{2}}\right)_2 = \left(N_{re}f^{\frac{1}{2}}\right)_1\left(\frac{d_2}{d_1}\right) \tag{5.17}$$

From the known results in tube of diameter d_1, an expression in terms of (N_{re} $f^{1/2}$)and s^- can be obtained by integrating equation (5.11) across the tube cross-section, which can be used to calculate s^-. Since for a given additive and u_τ, s^- is assumed to be constant, the scaled value of $(N_{re}f^{1/2})_2$ and hence f_2 can be calculated from equation (5.17).

This approach eliminated the need for calculating the characteristic time T_R from the fluid rheological properties. Different graphical and computational procedures based on Granville's model were proposed by Sellin and Ollis (1983) and Matthys and Sabersky (1982).

Though the above model was relatively simple to use, it yielded satisfactory results for scale-up only in a narrow diameter range, say for predicting results in a 10mm diameter tube from results in a 5mm diameter tube. But when Sellin and Ollis (1983) attempted to scale-up results to predict flow in bigger tubes, the model gave predictions which were lower by about 40% or more. A similar trend can be observed in Figure 5.3 where we have compared the experimental results of Gasljevic (1995) with the predictions obtained from Matthys and Sabersky (1982) model.

A comprehensive review of the available literature as presented above has indicated the need for a scale-up model by which friction coefficients may be predicted for pipes of any size using test data obtained in a single laboratory scale pipe. Such a model should make use of simple flow and viscometric measurements to predict the interaction of additive molecules with the turbulent boundary and hence drag reduction. This would exclude the need for estimating the molecular characteristic time.

We have shown in Chapter 4 that shear stress at the wall can be used as a scale-up criteria for drag reducing solutions. Drag reduction was defined as:

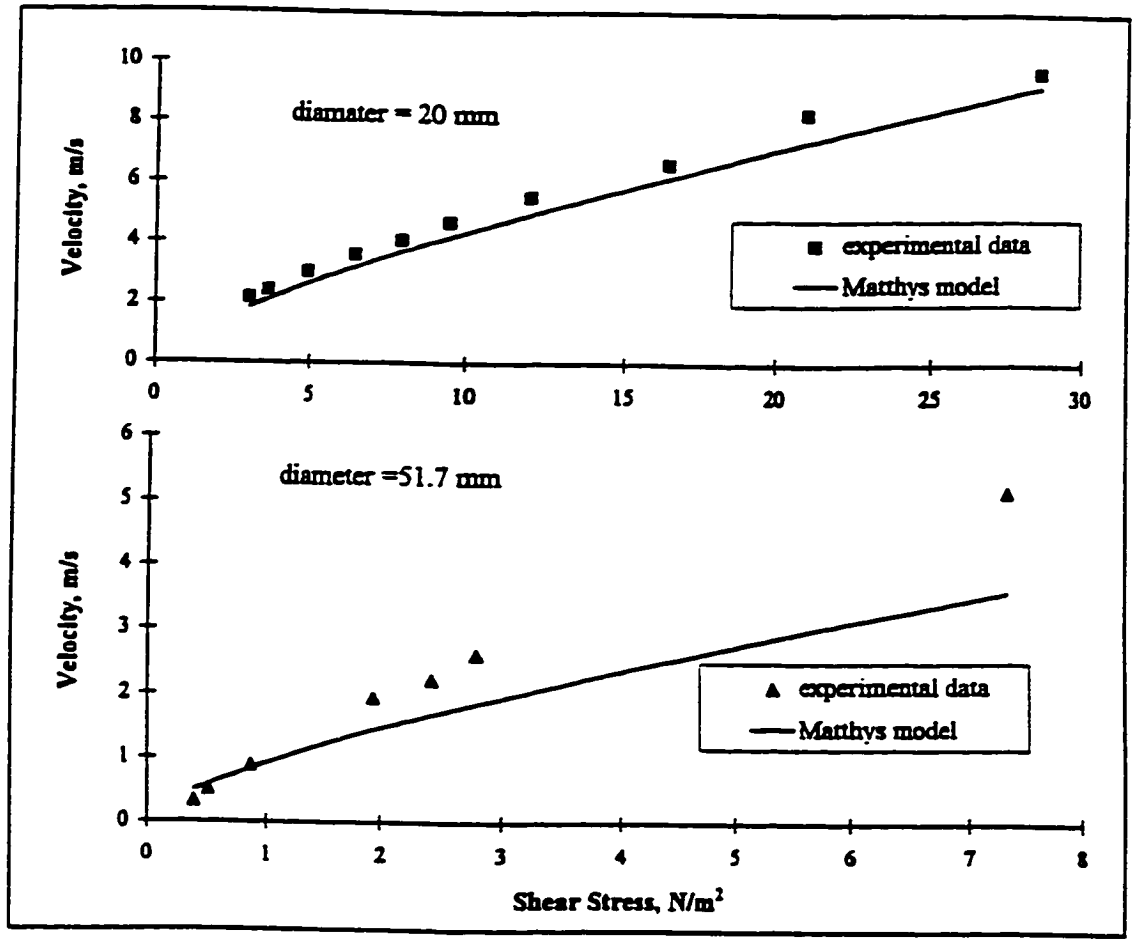

Figure 5.3 Prediction of bulk velocity in 20 mm and 51.7 mm diameter pipes using data from a 10 mm diameter tube (Matthys and Sabersky, 1982, model) (data of Gasljevic, 1995, 2300 ppm Ethoquad T13 solution)

$$DR = \left\{1 - \left(\frac{\bar{u}_s}{\bar{u}_p}\right)^2\right\} x100 \qquad \text{(at constant } \tau_w\text{)} \qquad (5.18)$$

Using the above equation, drag reduction was found to be a function of τ_w (and independent of the pipe diameter) in water-polymer, water-surfactant and oil-polymer drag reducing systems. Here we present a scale-up model which makes use of the above scale-up criteria and is based on a new hypothesis of modifying the Prandtl's mixing length for drag reducing flows.

5.2 Prandtl's Mixing Length

The concept of mixing length, as proposed by Prandtl (1952), has been successfully used in modeling turbulent flow of Newtonian fluids through circular pipes. By assuming that eddies move around in a fluid very much as molecules move around in a gas, Prandtl developed an expression for momentum transfer in a fluid in which the mixing length plays a role analogous to that of a mean free path in the kinetic theory of gases (Schlichting, 1979). This way of thinking led Prandtl to the relation for the turbulent shear stress, τ_t, which is given here without any further discussion:

$$\tau_t = \rho l^2 \left|\frac{du}{dy}\right| \frac{du}{dy} \qquad (5.19)$$

where the eddy diffusivity, ε, is defined as:

$$\varepsilon = l^2 \frac{du}{dy} \tag{5.20}$$

The mixing length, l, is a function of position. Prandtl proposed that it should be calculated as a linear function of the distance from the wall, i.e.,

$$l = Ky \tag{5.21}$$

The value of the Prandtl's mixing length constant, K, was experimentally found to be 0.40 for Newtonian fluids. This value was revalidated by Von Karman's similarity hypothesis and G.I. Taylor's vorticity transport theory (Schlichting, 1979) and was subsequently used for deriving the logarithmic velocity distribution law for flow through circular pipes. This logarithmic profile is one of the most famous results in the study of turbulent flows and is used for reliable correlation of pipe flow data for Newtonian fluids in the turbulent regime.

5.3 Mixing Length for Drag Reducing Flows

Here we will introduce the concept of a variable mixing length for drag reducing flows. According to this hypothesis, the mixing length would decrease with an increase in the additive concentration in solution, i.e., the mixing length constant, K, will take lower values with increasing concentrations in a Newtonian solvent. K will tend towards an asymptotic value as concentration increases and asymptotic drag reduction is obtained.

The following two arguments would make it clear that the mixing length for drag reducing solutions should be lower than that for Newtonian fluids:

1. The mixing length can be physically interpreted as the distance in the transverse direction which must be covered by an agglomeration of fluid particles traveling with its original mean velocity, in order to make the difference between its velocity and the velocity in the new layer equal to the mean transverse fluctuation in the turbulent flow (Schlichting, 1979). The turbulent velocity fluctuations give rise to Reynolds stresses and are responsible for the eddy viscosity, ε, in turbulent flows.

   Since in the case of the drag reducing flows, as has been proven experimentally (Virk, 1975), the velocity fluctuations are dampened in the region next to the viscous sublayer leading to a lower eddy viscosity, the distance (or the mixing length) traveled in the transverse direction by the fluid particle so that change in velocity in the new layer is equal to the velocity fluctuation also decreases. In other words, Prandtl's mixing length for drag reducing flows has a lower value compared to the mixing length for the Newtonian fluids and the mixing length should progressively decrease with increasing drag reduction (increased dampening of velocity fluctuations).

2. Turbulent shearing stress is defined by the relation,

$$\frac{\tau_t}{\rho} = \varepsilon_N \frac{du}{dy} = \varepsilon_{DR} \frac{du}{dy} \tag{5.22}$$

where ε_N and ε_{DR} are eddy diffusivities for Newtonian and drag reducing flows respectively. The contribution of molecular viscosity has been neglected in the above equation.

The effect of the drag reducing additives on the velocity profile of the solution can be understood by looking at equation (5.22) for a pure Newtonian solvent and a drag reducing solution. The presence of the drag reducing additive in solution reduces the velocity fluctuations in the elastic sublayer region. This, in turn, lowers the value of the eddy viscosity ε. But, for a given constant shear stress at the wall, τ_t, the velocity gradient would be higher for the drag reducing solution to balance the effect of a lower eddy viscosity ($\varepsilon_N > \varepsilon_{DR}$). Since ε is a product of the square of the mixing length (l^2) and the velocity gradient (equation (5.20)), it becomes clear that the mixing length for a drag reducing solution should be much lower than that for a Newtonian solvent to satisfy equation (5.22). The mixing length would progressively decrease as the additive concentration in the solution increases (and ε decreases) and finally the maximum drag reduction asymptote would be achieved where the additive concentration in the solution would no longer effect drag reduction.

5.4 Scale-up Algorithm for Drag Reduction

The dependence of the flow characteristics on Prandtl's mixing length can be demonstrated by analyzing the derivation of the Prandtl-Karman law for flow through circular pipes. From the definition of eddy diffusivity (ε_M) and the viscosity coefficient (ν), the total apparent shear stress, molecular plus turbulent, can be explained as,

$$\frac{\tau_w}{\rho} = \left(\nu + \varepsilon_M\right)\frac{du}{dy} \tag{5.23}$$

The turbulent boundary layer consists of two very distinct regions, a laminar sublayer for which we assume $\nu >> \varepsilon_M$ and a fully turbulent region for which $\varepsilon_M >> \nu$. For the fully developed region we can neglect ν relative to ε_M. The laminar sublayer is neglected for calculating the expression for the average bulk velocity since it contains a negligible amount of fluid compared to rest of the cross-section. Now equation (5.23) becomes

$$\frac{\tau_w}{\rho} = \varepsilon_M \frac{du}{dy} \tag{5.24}$$

Now we introduce Prandtl's mixing length theory. Substituting equations (5.20) and equation (5.21) into equation (5.24)

$$\frac{\tau_w}{\rho} = l^2\left(\frac{du}{dy}\right)^2 = K^2 y^2\left(\frac{du}{dy}\right)^2 \tag{5.25}$$

At this point, let us define

$$u^+ = \frac{u}{u_\tau} \tag{5.26}$$

$$y^+ = \frac{y u_\tau}{\nu} \tag{5.27}$$

$$u_\tau = \left(\frac{\tau_w}{\rho}\right)^{\frac{1}{2}} \tag{5.28}$$

Making the above substitution in equation (5.25),

$$\frac{du^+}{dy^+} = \frac{1}{Ky^+} \tag{5.29}$$

Integrating the above equation from the outer edge of the laminar sublayer:

$$\int_{u_{ls}^+}^{u^+} du^+ = \frac{1}{K}\int_{y_{ls}^+}^{y^+} \frac{dy^+}{y^+}$$

$$u^+ = \frac{1}{K}\ln y^+ + u_{ls}^+ - \frac{1}{K}\ln y_{ls}^+ \tag{5.30}$$

If equation (5.23) is integrated for the laminar sublayer in which ε_M is neglected relative to ν, then

$$\int_0^u du = \frac{\tau_w}{\mu}\int_0^y dy$$

$$u = \frac{\tau_w}{\mu} y$$

$$u^- = y^- \tag{5.31}$$

at the outer edge of the laminar sublayer

$$u_{ls}^- = y_{ls}^- \tag{5.32}$$

Substituting equation (5.32) into equation (5.30),

$$u^- = \frac{1}{K} \ln y^- + y_{ls}^- - \frac{1}{K} \ln y_{ls}^- \tag{5.33}$$

Integrating the above equation across the cross-section of the circular pipe to obtain average velocity,

$$\frac{\bar{u}}{u_\tau} = \frac{1}{K} \ln \frac{R u_\tau}{\nu} + y_{ls}^- - \frac{1}{K} \ln y_{ls}^- - \frac{1.5}{K} \tag{5.34}$$

$$\frac{\bar{u}}{u_*} = \frac{1}{K}\ln\frac{Ru_*}{\nu} + B \tag{5.35}$$

where,

$$B = y_{ls}^+ - \frac{1}{K}\ln y_{ls}^+ - \frac{1.5}{K} \tag{5.36}$$

The above equation is the general form of the Prandtl-Karman law derived from the logarithmic velocity profile for turbulent flow through a circular pipe. For Newtonian fluids, the mixing length constant K and the integration constant B have values 0.4 and 1.75 respectively (Nikuradse, 1930), and were obtained as 0.41 and 1.81 from the least square curve-fit of our velocity and shear stress data for water using equation (5.35).

Substituting 0.41 and 1.81 as values of B and K respectively in equation (5.36), the thickness of laminar sublayer $\left(y_{ls}^+\right)$ is calculated as 11.4. Various investigators have experimentally shown (Tritton, 1988) that the thickness of laminar sublayer $\left(y_{ls}^+\right)$ lies between 9.5-11.0 for Newtonian fluids, indicating that equation (5.35) predicts flow of Newtonian fluids in circular pipes reasonably well.

In our scale-up algorithm, we propose that equation (5.35) can predict not only flow of Newtonian fluids, but also drag reducing flows in circular pipes. The flow data obtained in a laboratory scale pipe would allow us to calculate K and B for the given solution concentration and subsequently, flow in a bigger pipe can be predicted using these constants. The value of K and B thus obtained can be used in equation (5.36) to calculate

increased thickness of the laminar sublayer due to drag reduction. The thickness of the laminar sublayer thus calculated has been used in the heat transfer model presented in Chapter 6.

The salient feature of our variable mixing length model is that it does not have a hypothetical elastic sublayer (Virk, 1975) with a velocity shift (the basis of *velocity profile models*) to account for the reduction in drag. This model assumes that the two layer velocity profile model, which works very well for Newtonian fluids, is valid for drag reducing flows as well, but the reduction in drag and the subsequent effective thickening of the laminar sublayer which is responsible for the reduction in convective heat transfer is explained by a reduced mixing length in the region close to the wall.

The above approach enables flow prediction in large scale pipes using pressure drop-flowrate data obtained in a small laboratory scale pipe and simple shear viscosity measurements. It is shown in Chapter 6 that an analogous approach can be used to predict heat transfer reduction as well. A variable mixing length is more practical to use as it includes the effect of the interaction of viscoelastic additive molecules with turbulence and hence the troublesome characteristic time, which is almost impossible to measure for these dilute concentrations and empirically calculated in the *correlation models*, does not come into picture.

5.5 Variable Mixing Length Model Vs Virk's Model

We integrated the velocity shift equation (equation (5.11)), by Virk (1975), across the cross-section of the circular pipe to obtain the expression for average velocity,

$$\bar{u}^{+} = 2.5 \ln R^{+} + B^{*} \tag{5.37}$$

where,

$$B^{*} = 1.75 + s^{+} \tag{5.38}$$

A comparison of equation (5.35) with equation (5.37) would indicate the basic difference between the two models. The Variable Mixing Length model uses a general form of the Prandtl-Karman equation and allows the flow behavior of a drag reducing fluid to determine the parameters K and B. Once determined, these parameters are used in equation (5.35) to predict flow in bigger pipes. In a sharp contrast, which is apparent from equation (5.37), Virk's velocity shift equation has fixed the Prandtl's mixing length constant as 0.4 (1/2.5), though this has been shown to be true only for Newtonian fluids (Schlichting, 1979). Further, unlike parameter B in equation (5.35), B^{*} does not depend on K and y_{ls}^{+} but is a function of s^{+}, which in turn depends on u_{τ} (Granville, 1978). Therefore, increased average bulk velocity in the case of drag reducing fluids is accounted for in Virk's model by parameter B^{*} (an experimentally determined function of u_{τ}), while the Prandtl's mixing length is assumed to be the same as that for Newtonian fluids.

As was discussed earlier, scale-up models based on Virk's velocity shift equation have been unsuccessful outside a narrow range of diameters. These models consistently under-predict drag reduction results in bigger pipes. The ability of the Variable Mixing Length model to predict drag reduction and a comparison with Matthys and Sabersky (1982) model is presented in the next section.

5.6 Drag Reduction Results and Model Predictions

The experiments and computations can be summarized as follows:

1. Measure the viscosity of the given drag reducing solution as a function of shear rate. For better accuracy, the measurements should be made over the range of shear rates to be encountered in the laboratory scale pipe and the bigger pipe for which the flow predictions are required.

2. Collect pressure drop and corresponding flow rate data for the given drag reducing solution in the laboratory scale pipe.

3. Use the above data to calculate shear stress (or u_τ) and average bulk velocity $(\bar{u})$.

4. Using a standard curve-fit routine and equation (5.35), obtain the best fit values for, K and B..

5. Use the values of K and B obtained above and equations (5.35) and (5.39) to predict average bulk velocity in the bigger pipe at a given u_τ by an iterative procedure

The above calculation procedure is illustrated with a specific example in Appendix 3.

The algorithm, based on the concept of a Variable Mixing Length, proposed in the previous section was tested on flow data obtained for drag reducing fluids in our experimental set-up. Details of the experimental set-up and procedures are available in Chapter 3. A 1400 ppm Ethoquad O12 solution was initially used as the test solution. Constants K and B were calculated from results obtained in the 7 mm diameter tube and

then were used to predict flow in the 10.2 mm diameter tube. The model was able to predict experimental data very well, as shown in Figure 5.4.

To test the ability of the Variable Mixing Length model to predict results in the non-asymptotic regime (where drag reduction is a function of concentration), K and B values were calculated using flow results obtained in the 7 mm tube (Figure 1.4) for 400 ppm, 500 ppm and 600 ppm Ethoquad O12 solutions and subsequently used to predict flow in the 10.2 mm tube. Estimation of parameters K and B was done using data points from Figure 1.4 which were below the critical shear stress value. Flow results obtained in 10.2 mm diameter tube and the model predictions are shown in Figure 5.5. As can be seen from Figure 5.5, the variable mixing length model is able to predict drag reduction scale-up in the non-asymptotic regime. The model works reasonably well up to the point where micelles are broken up due to the increased shear stress.

The predicted velocity and the experimental velocity for all the above concentrations for Ethoquad O12 solutions are compared in Figure 5.6. As can be seen from the Figure, the scatter in data is within 5%.

The above approach was also used on the data of Gasljevic (1995), for a 2300 ppm Ethoquad solution, to predict flow in a 20 mm diameter tube and a 51.7 mm diameter pipe from results obtained in a 10 mm diameter tube. The experimental results and model predictions are shown in Figure 5.7. A comparison between Figure 5.3 and Figure 5.7 would indicate that the Variable Mixing Length model is a better model to predict drag reduction scale-up, as compared to the Matthys model, since it can correlate experimental results reasonably well.

The ability of the two models to predict field scale data is compared in Figure 5.8. The data represented in this Figure was obtained from a 154 mm diameter Library cooling

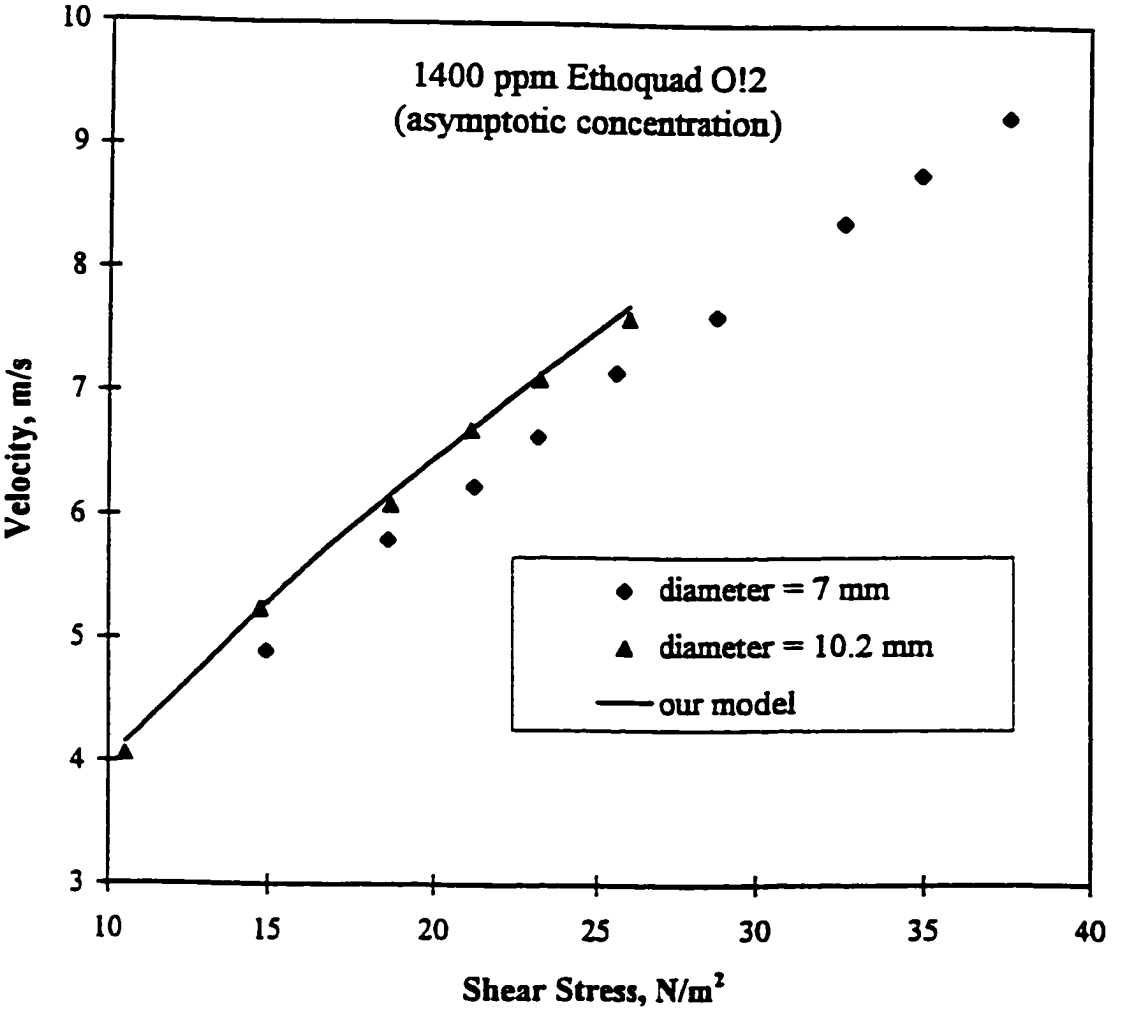

Figure 5.4 Prediction of bulk velocity in 10.2 mm diameter tube using data from a 7 mm diameter tube by variable mixing length model (our data, 1400 ppm Ethoquad O12 solution)

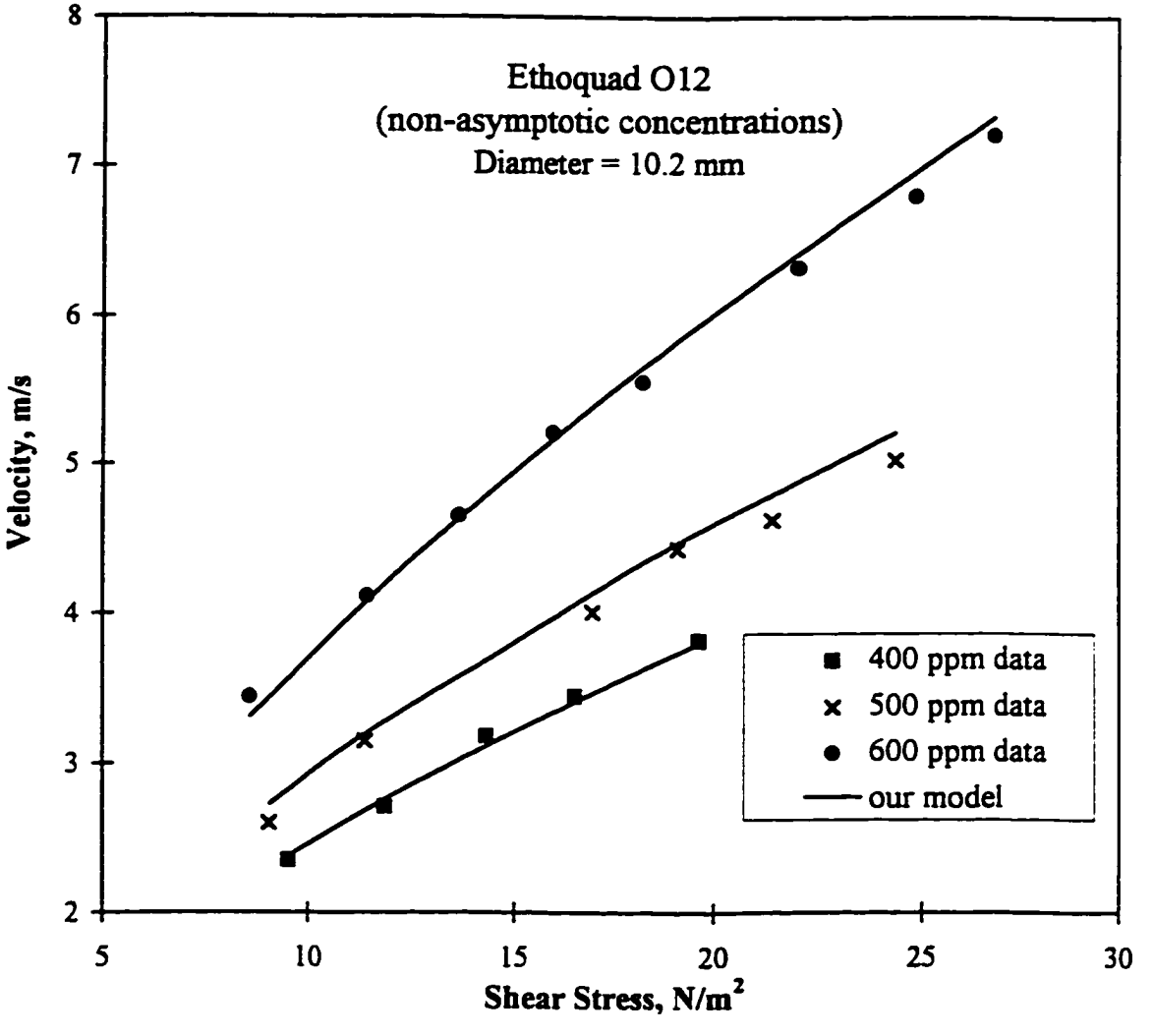

Figure 5.5 Prediction of bulk velocity in 10.2 mm diameter tube using data from a 7 mm diameter tube (Figure 1.3) by variable mixing length model (our data, 400 ppm, 500 ppm, 600 ppm Ethoquad O12 solutions)

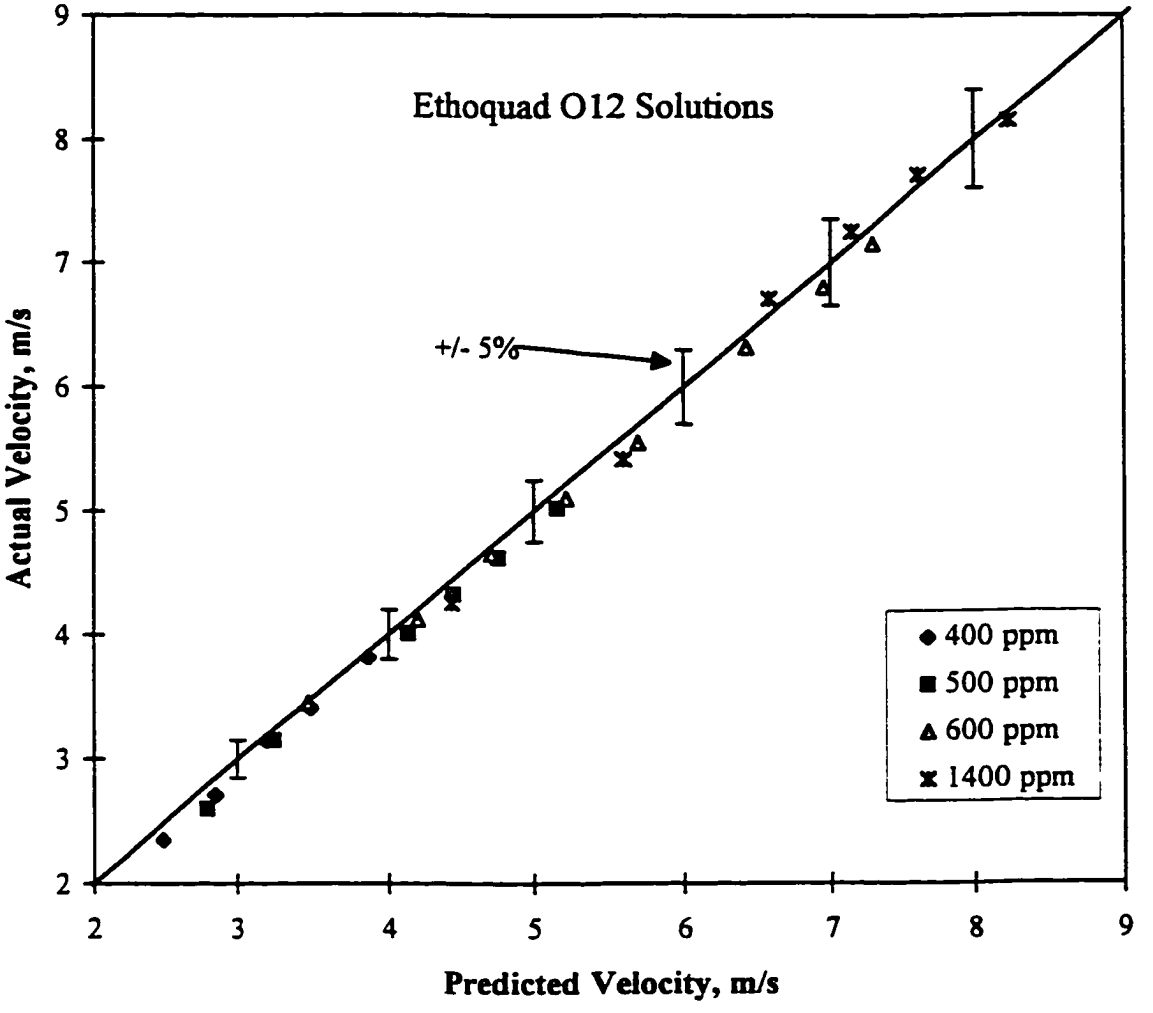

Figure 5.6 Comparison of actual and predicted bulk velocities for the 10.2 mm diameter tube for Ethoquad O12 solutions

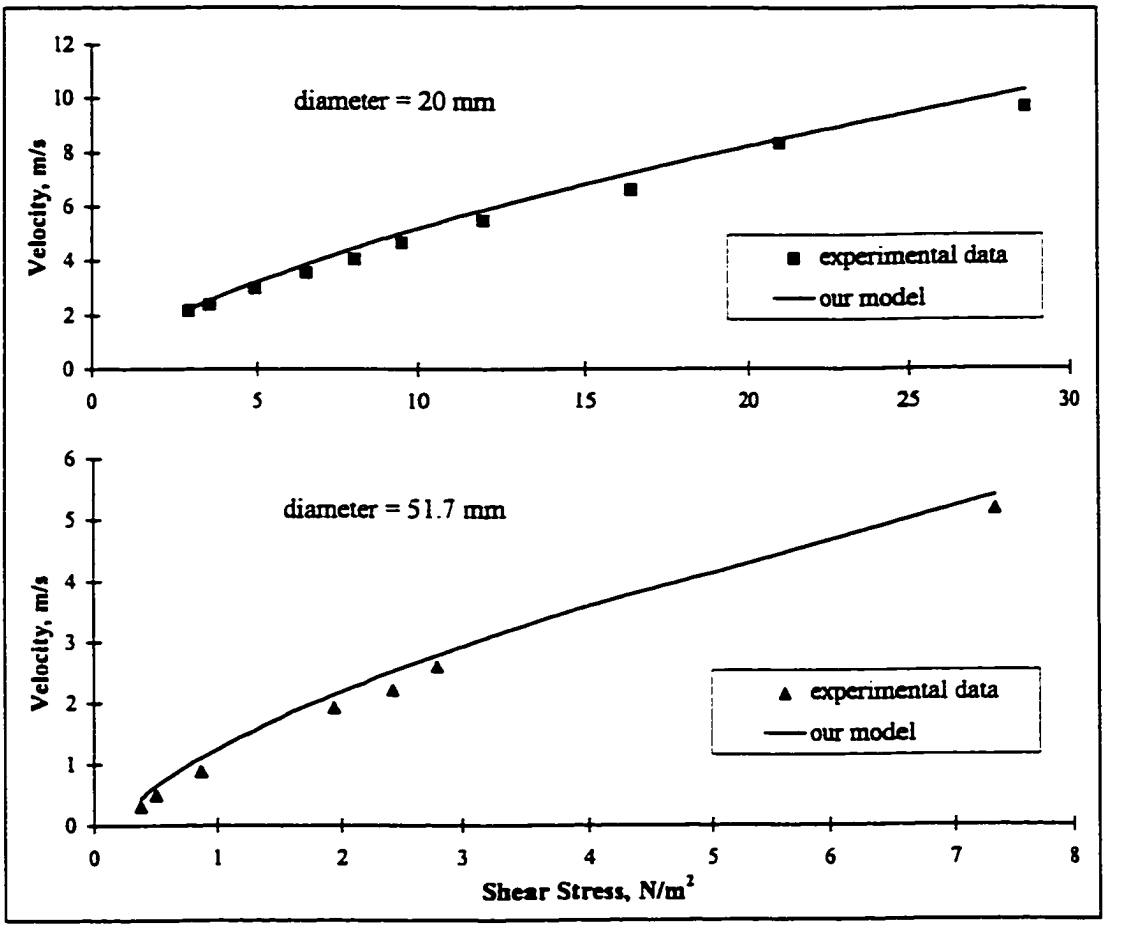

Figure 5.7 Prediction of bulk velocities in 20 mm and 51.7 mm diameter pipes by variable mixing length model using data from a 10 mm diameter tube (Figure 4.7) (data of Gasljevic, 1995, 2300 ppm Ethoquad T13 solution)

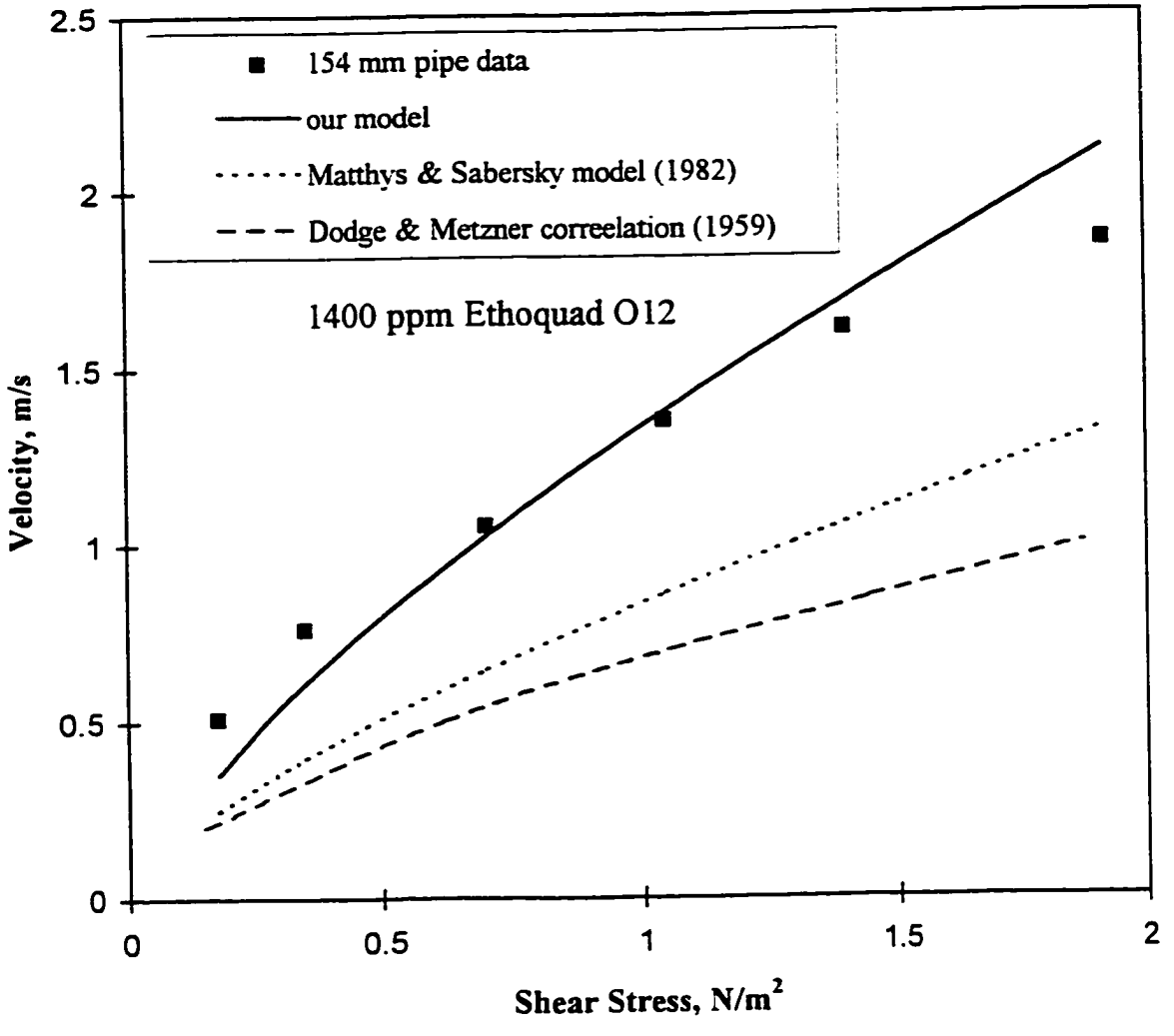

Figure 5.8 Comparison of variable mixing length model and Matthys and Sabersky (1982) model for predicting bulk velocity in a field scale (154 mm diameter) pipe using data from a 7 mm tube (Figure 5.4) (data of Young, 1996, 1400 ppm Ethoquad O12 solution)

system pipe (Young, 1996), which was running a 1400 ppm Ethoquad O12 solution. The scale-up was performed by using data obtained in the 7 mm pipe. As is clear from the figure, the Matthys and Sabersky (1982) model consistently under-predicts within an error limit of 650%, while the Variable Mixing Length Model predictions are much better in comparison.

Dodge and Metzner (1959) have presented a generalized correlation for predicting flow of non-Newtonian viscous fluids, which is given by:

$$\sqrt{\frac{1}{f}} = \left[\frac{4}{n^{0.75}} \log N_{re}' f^{\left(1-\frac{n}{2}\right)} \right] - \frac{0.40}{n^2} \tag{5.39}$$

where,

$$N_{re}' = \frac{D^n \bar{u}^{(2-n)} \rho}{K' 8^{(n-1)}} \tag{5.40}$$

n is the flow index and K' is the fluid consistency index for the power law fluids and are given by:

$$\tau_w = K' \left(\frac{-du}{dr} \right)^n \tag{5.41}$$

Equation (5.39) predicts a friction factor for pseudoplastic fluids which is lower than that for a pure Newtonian solvent. Ethoquad O12 solutions are non-Newtonian viscoelastic fluids and are pseudoplastic over a certain range of shear rates (Figures A1.1 and 1.2). Hence as a matter of interest, we wanted to see the comparison of flow prediction for the data of Young (1996) by our model (equation (5.35)) and the Dodge

and Metzner (1959) correlation (equation (5.39)). Constants n and K were calculated using viscosity data for the 1400 ppm Ethoquad O12 solution between the shear rates of 50 and 600 s^{-1} (Figure A1.1). The flow predictions obtained by the Dodge and Metzner (1959) correlation are shown in Figure 5.8. It can be seen from Figure 5.8 that the Dodge and Metzner (1959) correlation, which works well for non-Newtonian viscous fluids, performs poorly when used for non-Newtonian viscoelastic fluids.

To summarize the results presented above, the Variable Mixing Length model was successful in predicting drag reduction scale-up for a surfactant-water system over a diameter ratio of 22 (for data of Gasljevic, 1995), while the Granville model (1978) and its subsequent modifications by Matthys and Sabersky (1982) and Sellin and Ollis (1983) could reasonably predict drag reduction over a diameter ratio of only 2 or 3. This encouraged us to test the universal validity of our model.

Most of the field scale data available in literature was unsuitable for testing on this model as information about velocity dependence on shear stress and viscometric functions were not provided for the test solutions. Fortunately, Burger et al. (1982) have provided extensive data on drag reduction tests carried out on a oil-polymer system over a diameter range of 26.6 mm to 1194 mm. The drag reducing polymer additive was Conoco CDR. Using the Variable Mixing Length algorithm, constants K and B were calculated from experimental results obtained in a 26.6 mm diameter pipe. Subsequently, using these constants, drag reduction results were predicted in bigger pipes. The model was tested on 5, 10 and 20 ppm solutions for predicting flow results in 52.5, 343 mm and 1194 mm diameter pipes. The last pipe is the actual crude oil transport pipeline being run by the ARCO oil company in Alaska. The experimental data and model predictions for the 10 ppm oil-polymer system are shown in Figure 5.9. A comparison of the predicted and actual velocities for all three concentrations is shown in Figure 5.10. In this case, the

Variable Mixing Length model has been able to predict drag reduction over a diameter ratio of 45.

5.7 Velocity Profile Close to the Wall

The values for constants K and B (calculated from equation (5.35)) and thickness of the laminar sublayer, y_{ls}^{+} (calculated from equation (5.36)) for the Ethoquad O12 solutions are given in Table 5.1. The mixing length constants are plotted in Figure 5.11. As can be seen from the Figure, mixing length decreases with an increase in concentration and tends towards an asymptotic value. The thickness of the laminar sublayer also increases with an increase in concentration.

Velocity profiles close to the wall for the Ethoquad O12 solutions (as calculated from equations (5.30) and (5.31)) are shown in Figure 5.12. A comparison of Figure 5.12 with Figure 5.2 indicated the basic difference between the Variable Mixing Length model and Virk's model. While Virk's model proposed a parallel upward shift in the velocity profile with an increase in concentration, our model proposes an upward shift in the velocity profile which is not parallel to the Newtonian solvent. The slopes (or the mixing length constants) of the velocity profile curves are determined by the concentration of the solutions, with the slope becoming steeper with an increase in concentration, till the asymptotic conditions are reached.

Figure 5.13(a) shows the Laser Doppler Velocimeter measurements of velocity profiles close to the wall for a drag reducing solution and water (Rudd, 1969). The velocity profile for the Poly(acrylamide) solution is not parallel to the velocity profile for

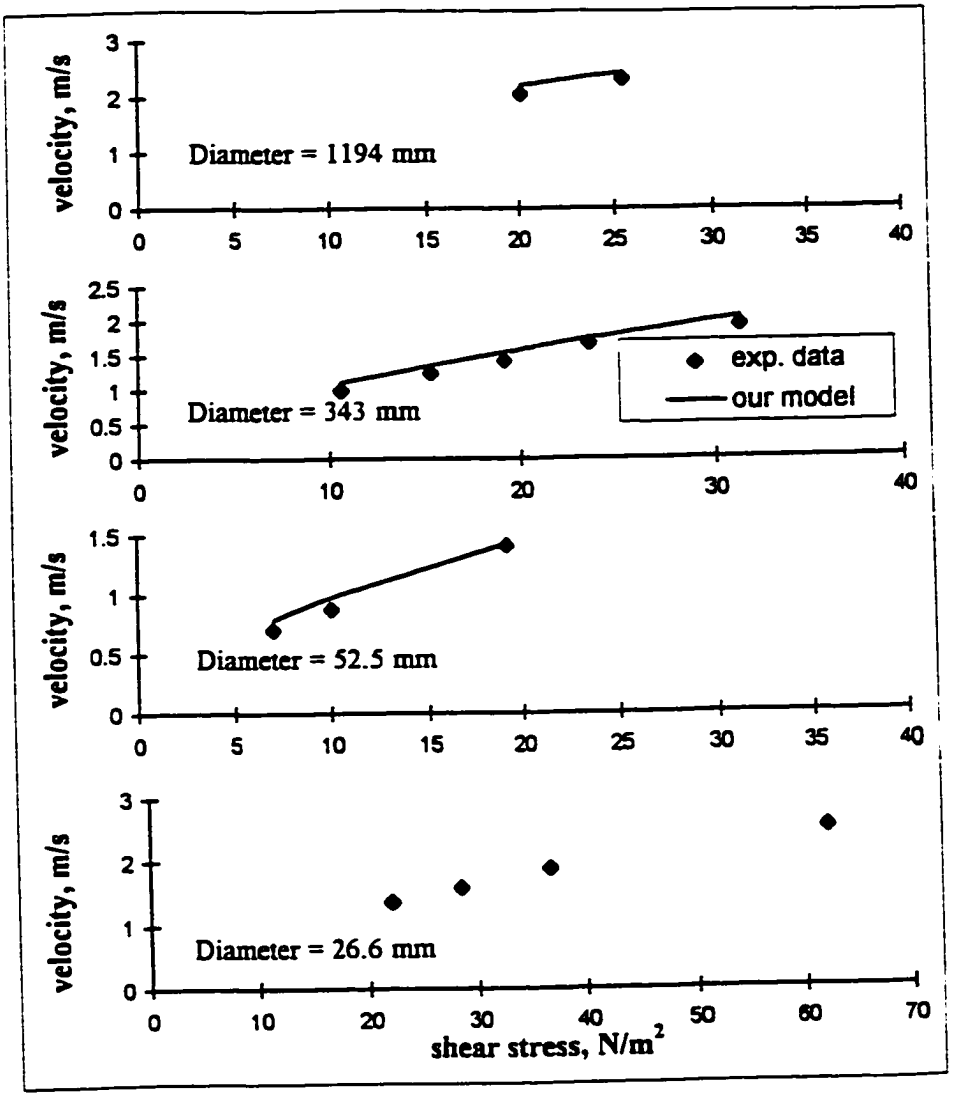

Figure 5.9 Prediction of bulk velocity in 343 mm and 1194 mm diameter pipes using data from a 26.6 mm diameter pipe by variable mixing length model (data of Burger et al., 1982. 10 ppm oil-polymer system)

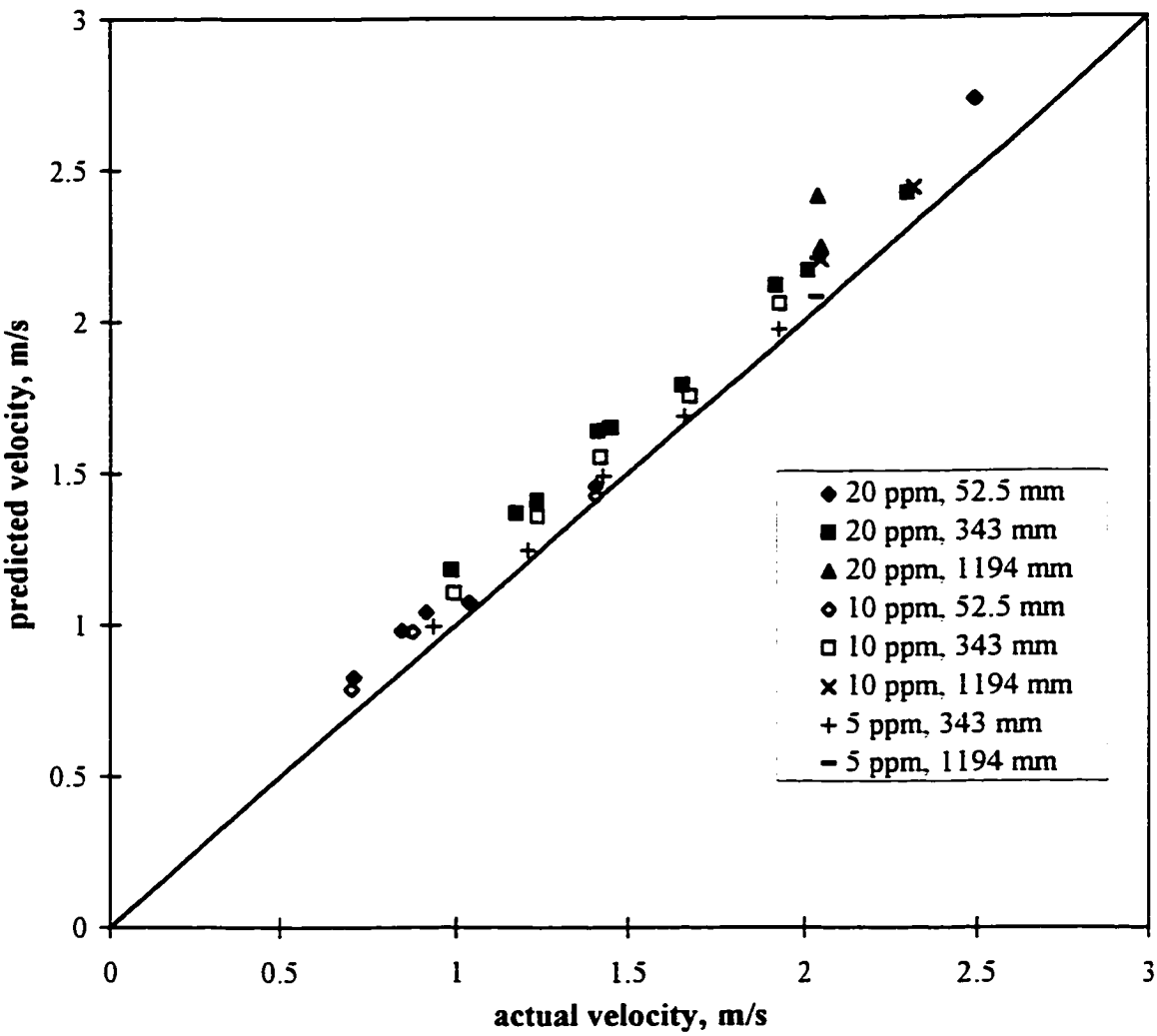

Figure 5.10 Comparison of the predicted (by variable mixing length model) and actual bulk velocities for 5, 10 and 20 ppm oil polymer system (data of Burger et al., 1982)

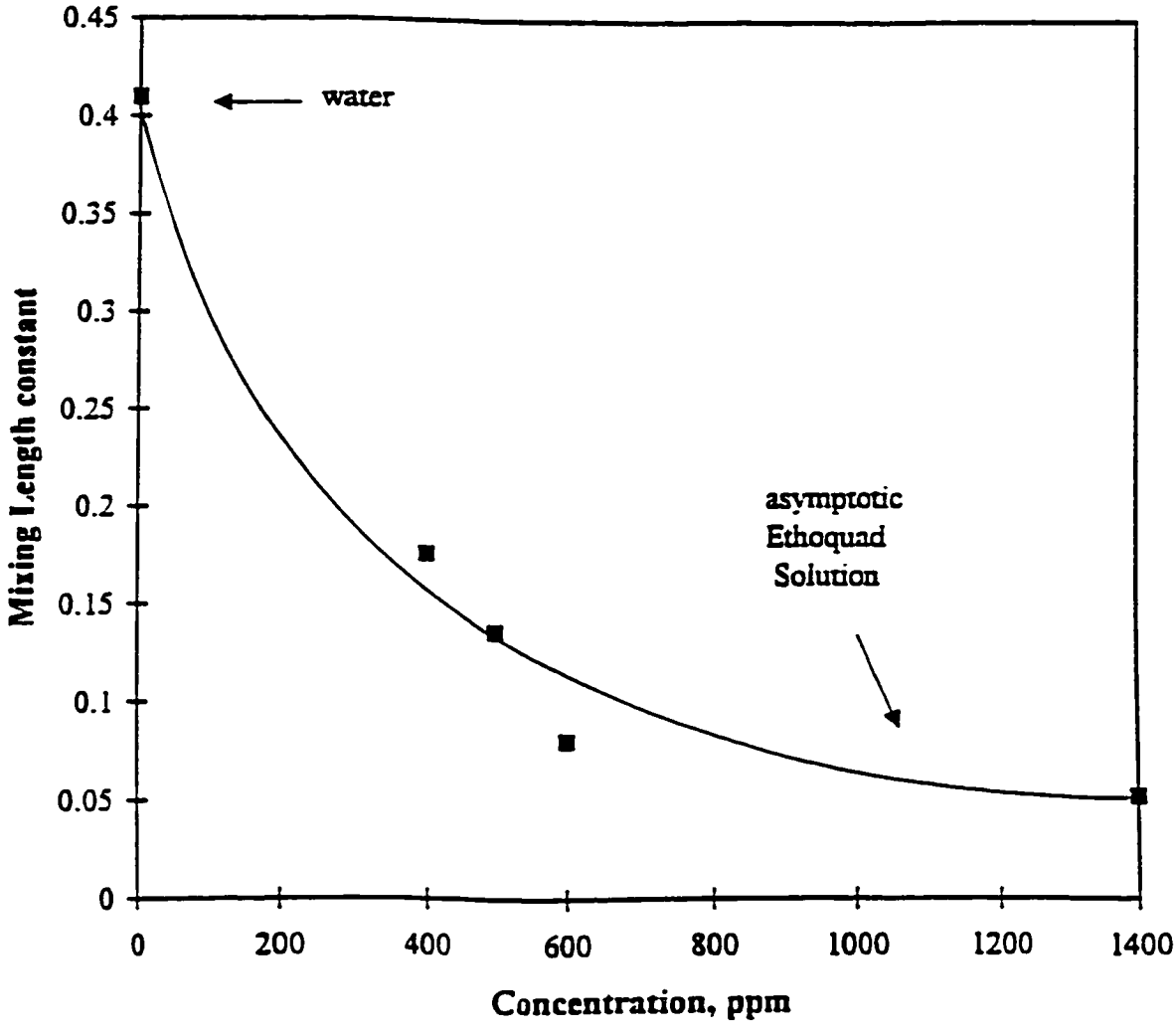

Figure 5.11 Mixing length constants for Ethoquad O12 solutions

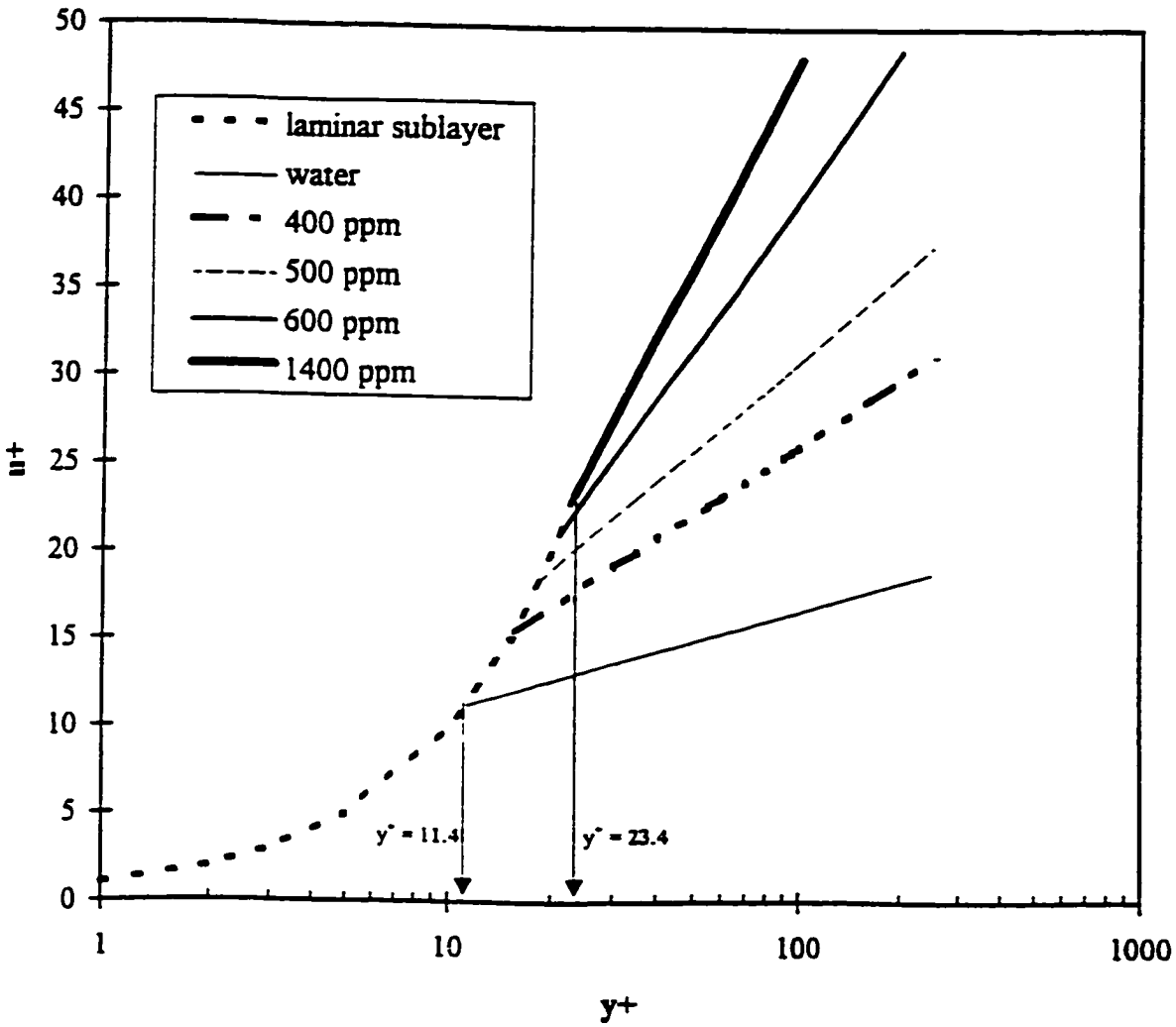

Figure 5.12 Predicted velocty profiles (close to the wall) by the variable mixing length model for Ethoquad O12 solutions

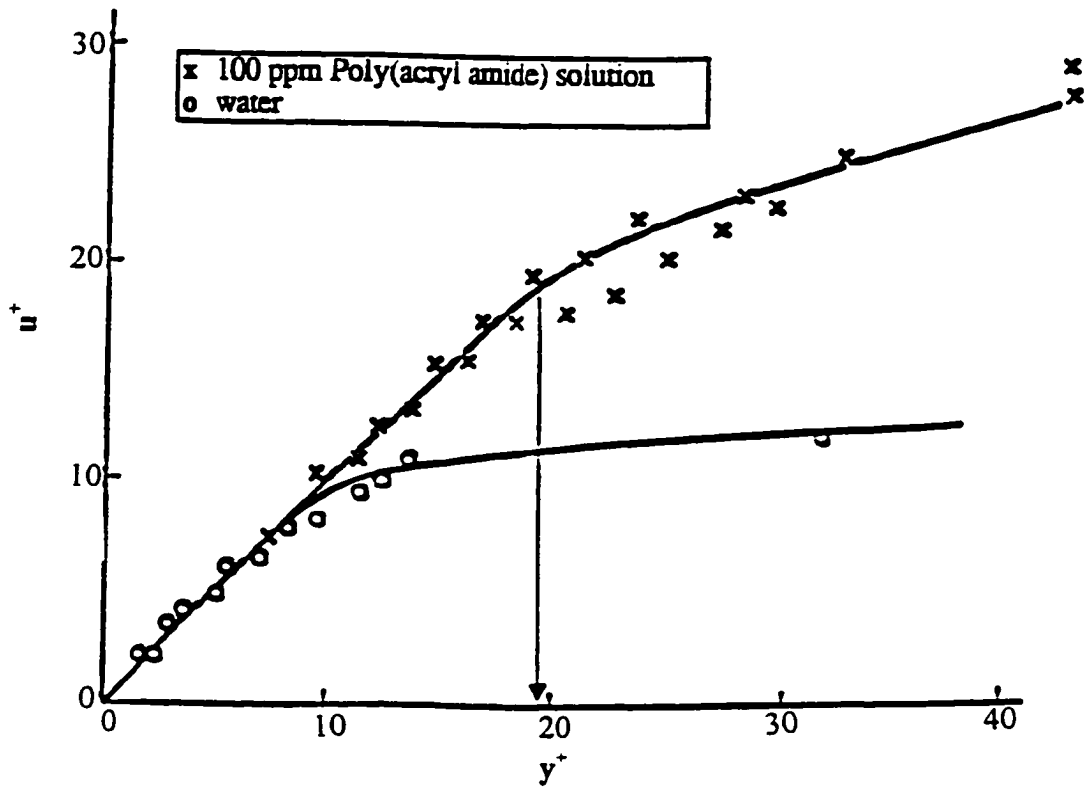

Figure 5.13(a) Velocity measurements (close to wall) for 100 ppm. Poly(acrylamide) solution and water (Rudd, 1969)

water, in the logarithmic region but is much steeper and is similar to the velocity profile calculated for the 1400 ppm Ethoquad O12 solution by the Variable Mixing Length Model (Figure 5.13(b)). Observations similar to Rudd (1969) have been reported by Zakin (1996) for drag reducing surfactant solutions.

Table 5.1 Model Constants for Water and Ethoquad O12 solutions

Concentration	K	B	y_{ls}^{-}
Water	0.41	1.81	11.4
400 ppm	0.1767	-8.5	15.5
500 ppm	0.1363	-13.91	18.5
600 ppm	0.08	-35.81	21.01
1400 ppm	0.058	-56.36	23.4

It appears from the above discussion that the Variable Mixing Length model is able to predict velocity profile in the wall region, for the drag reducing solutions, which is much closer to actual observations. It also enables the calculation of the increase in laminar sublayer thickness for drag reducing flows.

5.8 Summary

A new model for predicting drag reduction scale-up has been presented here. The model uses a physical interpretation of Prandtl's mixing length to propose that the mixing length for a drag reducing solution is lower than that for the pure solvent and is dependent only on the concentration of the solution. The scale-up algorithm calculates the mixing length constant, K, and the integration constant, B, from flow results obtained in a laboratory scale pipe and once they are established, equation (5.35) is used to predict flow in bigger pipes.

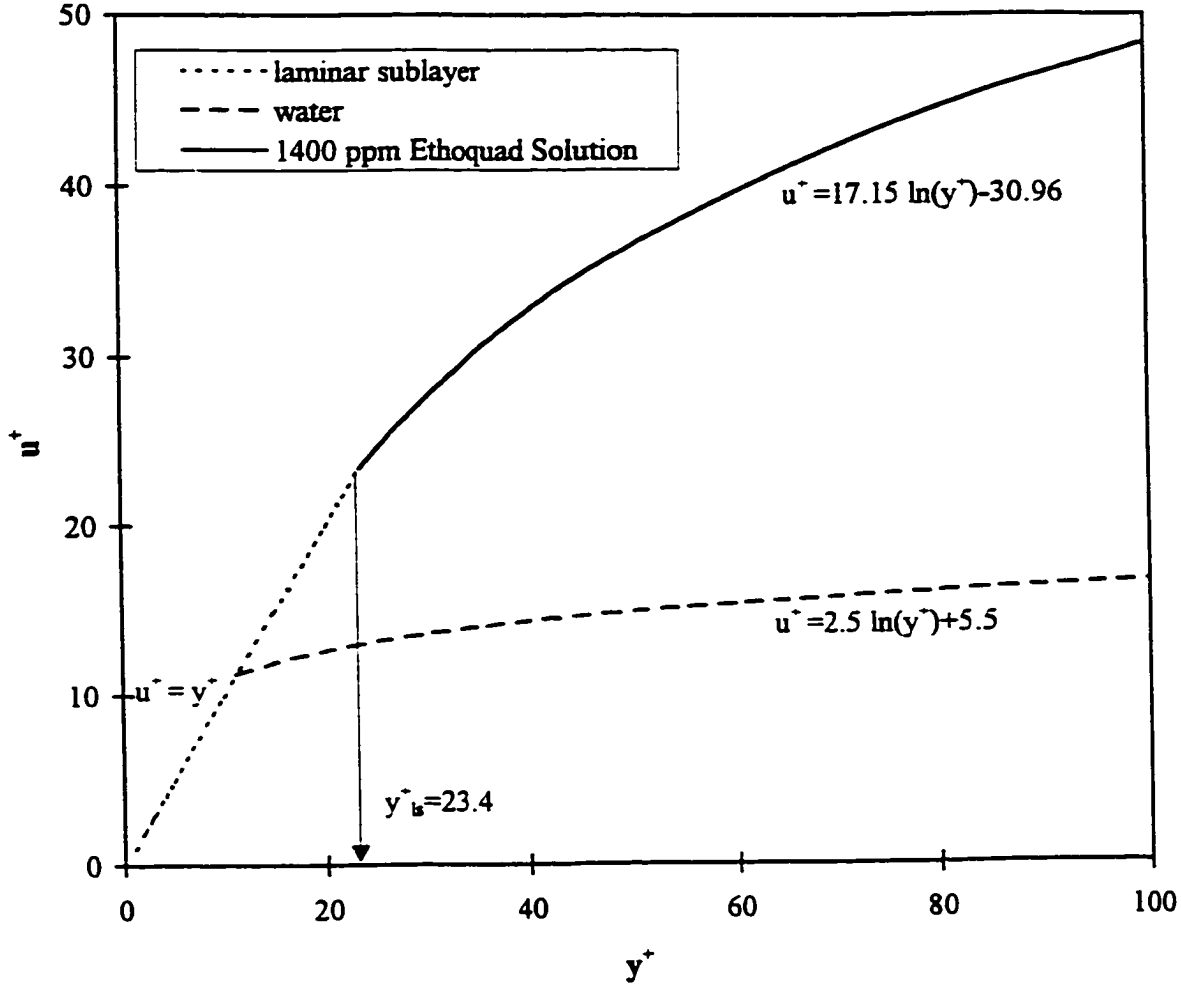

Figure 5.13(b) Velocity profile (close to wall) predicted by the variable mixing length model for a 1400 ppm Ethoquad O12 solution

The above algorithm was successfully used for predicting flow in a Library cooling system pipe (154 mm diameter) from experimental data obtained in a 7 mm diameter tube (water-surfactant system) and in the Trans Alaska Pipeline (1194 mm diameter) from experimental data obtained in a 26.5 mm diameter pipe (oil-polymer system) indicating that this is a general model which is not restricted in application to a particular system. Further, this model is simple to use as unlike other models, it does not require measurement of the troublesome characteristic time or the velocity shift correlation. A representative run carried out in a small laboratory scale pipe provides flowrate and pressure drop data, which coupled with viscosity measurements over the given shear rates enables prediction of flow in bigger pipes. This eliminates the need for carrying out expensive field tests in large industrial pipes. Other scale-up models available in published literature have been shown to be successful only over a narrow range of diameters, which makes the Variable Mixing Length model the most suitable and effective model for predicting scale-up for drag reducing flows.

The Variable Mixing Length model also predicts drag reduction results satisfactorily in the non-asymptotic regime. The mixing length, which is obtained as a function of the solution concentration, decreases with an increase in concentration and tends towards an asymptotic value. The increase in the laminar sublayer thickness with an increase in the concentration can also be calculated using equation (5.36).

The suitability of the Variable Mixing Length model as compared to Virk's hypothesis has also been examined. A comparison of the near wall velocity profiles predicted by these models with velocity measurements made with the Laser Doppler Anemometer has indicated that the Variable Mixing Length model predicts a velocity profile and thickening of the laminar sublayer which is very close to the actual observations for drag reducing solutions.

6. PREDICTION MODEL FOR HEAT TRANSFER REDUCTION

Though the problem of drag reduction has been under investigation for over four decades now, the phenomenon of convective heat transfer reduction that accompanies it has not received as much attention. Drag reducing viscoelastic solutions have heat transfer characteristics which are totally different from the Newtonian fluids. The characteristic features are briefly listed below:

- Turbulent heat transfer performance of drag reducing fluids flowing through circular pipes is characterized by thermal entrance lengths as long as 300-500 pipe diameters (Cho and Hartnett, 1982, Matthys, 1991). This is in sharp contrast to Newtonian fluids in turbulent flow, which have thermal entrance lengths of the order of 10-15 pipe diameters (Deissler, 1955). Most of the early researchers were unaware of this critical fact and hence carried out runs in relatively short tubes, leading to collection of data in the thermal entrance region rather than in the region of fully developed flow (example: Gupta et al., Astarita , 1969; 1967; Smith et al., 1969).

- Ever since Virk (1970) reported the existence of the maximum drag reduction asymptote, there were attempts to identify the corresponding maximum heat transfer reduction, or the minimum heat transfer asymptote. Correlations for predicting the minimum heat transfer asymptote were postulated by Cho and Hartnett (1982) and Matthys (1991). Based on their experimental observations, both concluded that, on relative terms, heat transfer reduction was much more than drag reduction.

- In the non-asymptotic regime, like drag reduction, heat transfer reduction is also a function of concentration and non-dimensional numbers used in the case of Newtonian fluids have been found to be insufficient to correlate the heat transfer results in different diameter pipes.

6.1 Previous Work on Scale-up Modeling

Very little work has been done in the field of scale-up modeling (or predicting the Diameter Effect) for heat transfer reduction. Two models are available in literature which are discussed below:

A prediction technique for heat transfer reduction was developed by Matthys and Sabersky (1982) which was based on Virk's (1975) three layer velocity profile model for drag reducing solutions. Virk's model has been shown in the previous Chapter to be inadequate for predicting drag reduction scale-up in industrial size pipes. Hence, a heat transfer reduction scale-up model based on the above velocity profile model would not be able to predict scale-up satisfactorily. The model, in fact, was not tested on experimental data by the authors at that time.

Yoon and Ghajar (1988) developed another prediction technique for heat transfer reduction which was analogous to the Correlation Models for drag reduction mentioned in the last Chapter. This model was based on the interaction of the additive molecules with energy dissipating eddies. But again, the model is empirical in nature since the molecular characteristic time cannot be measured for these dilute solutions. Moreover, the model treats heat transfer and friction separately. The model was tested by Yoon and Ghajar (1988) on their experimental data over a narrow range of Reynolds number and was found to be satisfactory. The model was not tested on any other drag reducing system to check

for universal applicability.

It can be inferred from the above discussion that not many attempts have been made to develop a scale-up model for heat transfer reduction. Matthy's and Sabersky (1982) model is based on Virk's velocity profile model and Yoon and Ghajar (1988) model is based on correlations, concepts which have been shown to be unsatisfactory in predicting drag reduction scale-up (Chapter 5).

The ability of the Variable Mixing Length model to predict drag reduction scale-up for industrial size pipes encouraged us to apply the same principles in predicting heat transfer reductions scale-up. An analogous model is presented in the next section, which uses the constants K and B calculated from velocity-shear stress data to predict heat transfer reduction.

6.2 Variable Mixing Length Model for Heat Transfer Reduction

Similar to the expression for the total apparent shear stress at the wall (equation (5.23)), an equation can be written to represent the total heat flux, laminar and turbulent (Kays and Crawford, 1980):

$$\frac{q_w}{\rho C_P} = -(\alpha + \varepsilon_H)\frac{dt}{dy} \tag{6.1}$$

$$\int_{t_w}^{t} dt = -\frac{q_w}{\rho C_P}\int_0^y \frac{dy}{\alpha + \varepsilon_H} \tag{6.2}$$

where,

$$\alpha = \frac{k}{\rho C_P} \tag{6.3}$$

Introducing non-dimensional variables:

$$y^+ = \frac{y u_\tau}{\nu}$$

$$t^+ = \frac{(t_w - t) u_\tau}{(q_w / \rho C_P)}$$

Making the above substitutions in equation (6.2),

$$t^+ = \int_0^{y^+} \frac{dy^+}{\frac{1}{N_{\mathrm{Pr}}} + \frac{\varepsilon_H}{\nu}} \tag{6.4}$$

Following the same procedures as were used for the momentum boundary layer in Chapter 5, let us consider a two-layer model for the thermal boundary layer with a laminar sublayer and a fully turbulent region. Let y_{ls}^+ be the thickness of the laminar sublayer. Now

equation (6.4) becomes

$$t^+ = \int_0^{y_{ls}^+} \frac{dy^+}{\frac{1}{N_{\mathrm{Pr}}} + \frac{\varepsilon_H}{\nu}} + \int_{y_{ls}^+}^{y^+} \frac{dy^+}{\frac{1}{N_{\mathrm{Pr}}} + \frac{\varepsilon_H}{\nu}} \tag{6.5}$$

If we were to follow precisely the procedure used in Chapter 5 to calculate $\overline{t^+}$, that is difference between the wall temperature and the average bulk temperature, we would neglect the first integral for the laminar sublayer. But in reality, there is a large temperature gradient across the laminar sublayer, which provides the resistance for convective heat transfer from the wall. Hence the first integral cannot be neglected. The first integral representing the laminar sublayer was neglected for calculating the average velocity since a very little fraction of the total flow across a cross-section is contained in the laminar sublayer.

To be able to solve the above equation analytically, we made the following simplifying assumptions:

1. In the laminar sublayer, (first integral in equation (6.5)) we neglect ε_H since viscous forces are dominant and molecular conduction is responsible for heat transfer.

2. In the second integral (in equation (6.5)), the fully turbulent region, the situation is reversed. It has been shown (Kays and Crawford, 1980) that for $N_{Pr} > 0.5$, the molecular conduction term can be neglected. Since for drag reducing dilute polymer and surfactant solutions N_{Pr} is usually in the range of 6-14, neglecting $(1/N_{Pr})$ in the second integral would be a safe assumption.

Now equation (6.5) takes the form,

$$t^+ = \int_0^{y_{ls}^+} N_{\Pr} dy^+ + \int_{y_{ls}^+}^{y^+} \frac{dy^+}{\varepsilon_H / \nu} \tag{6.6}$$

If we use equation (5.24) and equation (5.25) to determine the eddy diffusivity for momentum (ε_M), we obtain the relation,

$$\frac{\varepsilon_M}{\nu} = Ky^+ \tag{6.7}$$

Turbulent Prandtl number $N_{\Pr_t}$ is defined as,

$$N_{\Pr_t} = \frac{\varepsilon_M}{\varepsilon_H} \tag{6.8}$$

For $N_{Pr} > 1.0$, it has been experimentally shown that $N_{\Pr_t} = 1.0$ (Kays and Crawford, 1980), that is, the Reynolds Analogy is true. Using this result to combine equation (6.7) and equation (6.8),

$$\frac{\varepsilon_M}{\nu} = Ky^+ = \frac{\varepsilon_H}{\nu} \tag{6.9}$$

Making the above substitution in equation (6.6),

$$t^+ = N_{Pr} y_{ls}^+ + \int_{y_{ls}^+}^{y^+} \frac{dy^+}{Ky^+} \tag{6.10}$$

$$t^- = \frac{1}{K} \ln y^- + \left(N_{Pr} y_{ls}^- - \frac{1}{K} \ln y_{ls}^- \right) \tag{6.11}$$

for the centerline temperature,

$$T^- = \frac{(t_w - t_C)u_\tau}{q_w / \rho C_P} = \frac{1}{K} \ln R^- + N_{Pr} y_{ls}^- - \frac{1}{K} \ln y_{ls}^- \tag{6.12}$$

Combining equations (6.11) and equation (6.12),

$$t^- = T^- - \frac{1}{K} \ln \frac{R}{y} \tag{6.13}$$

Integrating the above equation across the cross-section of the pipe to obtain the difference between wall temperature and the average bulk temperature,

$$\overline{t^+} = T^+ - \frac{1.5}{K} \tag{6.14}$$

Substituting the expression for T^+ (equation (6.12)) in the above equation,

$$\frac{(t_w - \bar{t})u_\tau}{(q_w / \rho C_P)} = \frac{1}{K}\ln\frac{Ru_\tau}{\nu} + N_{Pr}y_{ls}^+ - \frac{1}{K}\ln y_{ls}^+ - \frac{1.5}{K} \tag{6.15}$$

We know that,

$$q_w = h(t_w - \bar{t}) \tag{6.16}$$

Hence equation (6.15) reduces to the form given below:

$$h = \frac{u_\tau \rho C_P}{\left(\frac{1}{K}\ln\frac{Ru_\tau}{\nu} + N_{Pr}y_{ls}^+ - \frac{1}{K}\ln y_{ls}^+ - \frac{1.5}{K}\right)} \tag{6.17}$$

The above equation can be used to predict the local convective heat transfer

coefficient. This is an extension of the Variable Mixing Length model presented in the last Chapter. Measurement of heat transfer is not required in a small laboratory scale pipe to predict heat transfer in an industrial scale pipe. The flow measurements ($\bar{u}$, u_τ) in the small pipe are used to calculate the constants K and B in equation (5.35). Thickness of the laminar sublayer (y_{ls}^-) for the given solution is calculated from equation (5.36). These constants along with the known fluid properties (ρ, C_P, ν, k) are used in equation (6.17) to predict the heat transfer coefficient in a pipe of any diameter.

The algorithm for predicting heat transfer coefficients for drag reducing solutions is summarized below:

1. Make flowrate and pressure drop measurements in a small laboratory scale pipe.
2. Calculate $\bar{u}$ and shear stress (or u_τ).
3. Make shear viscosity measurements.
4. Perform a least square error fit of the velocity and shear stress data to obtain K and B from equation (5.35).
5. Calculate y_{ls}^+ form equation (5.36).
6. Use K and y_{ls}^+ in equation (6.17) along with the known fluid properties (ρ, C_P, ν, k) to obtain the heat transfer coefficient.

The above calculation procedure has been illustrated with a specific example in Appendix 4.

6.3 Heat Transfer Results and Model Predictions

We carried out heat transfer measurements for water and 1400 ppm Ethoquad O12

solution in the 7 mm and 10.2 mm diameter tubes. The results for the 1400 ppm Ethoquad solution have already been shown in Figure 4.10. To test the validity of the model presented in the last section, constants K, B and y_{ls}^{+} were calculated using the least squares error fit of the velocity and shear stress data in equations (5.35) and (5.36). The values of these constants were found to be the same as those listed in Table 5.1. Knowing these constants and the fluid properties (except μ, all other properties are same as that of water), heat transfer coefficients were calculated for water and the surfactant solution using equation (6.17). The experimental results and model predictions are shown in Figure 6.1 and Figure 6.2 for the 7 mm and 10.2 mm diameter tubes respectively. As can be seen from Figure 6.3, the model fit is within the error limits of $\pm$ 10%, which is considered to be a good fit for heat transfer models.

The heat transfer model was also tested on Poly(acrylamide) solutions in water (10 ppm, 100 ppm, 300 ppm, and 1000 ppm) to test the universal applicability of the model and its ability to predict heat transfer reduction in the non-asymptotic regime. The data for the 10 ppm and 1000 ppm solutions was obtained from Cho and Hartnett (1982) and for the 100 ppm and 300 ppm solutions from Yoon and Ghajar (1988). The flow results were used for calculating the constants K, B and y_{ls}^{+} (listed in Appendix 5), and equation (6.17) was used for calculating the heat transfer coefficients. Viscosity data for these solutions (Hartnett and Kwack, 1985) is shown in Appendix 1 The experimental results and model predictions are shown in Figure 6.4. An error analysis is done in Figure 6.5, which indicates that the model is able to reasonably predict the experimental results with a little scatter.

6.4 Analogy Between Momentum and Heat Transfer for Drag Reducing Fluids

Reynolds Analogy assumes that eddy diffusivities for momentum and heat transfer

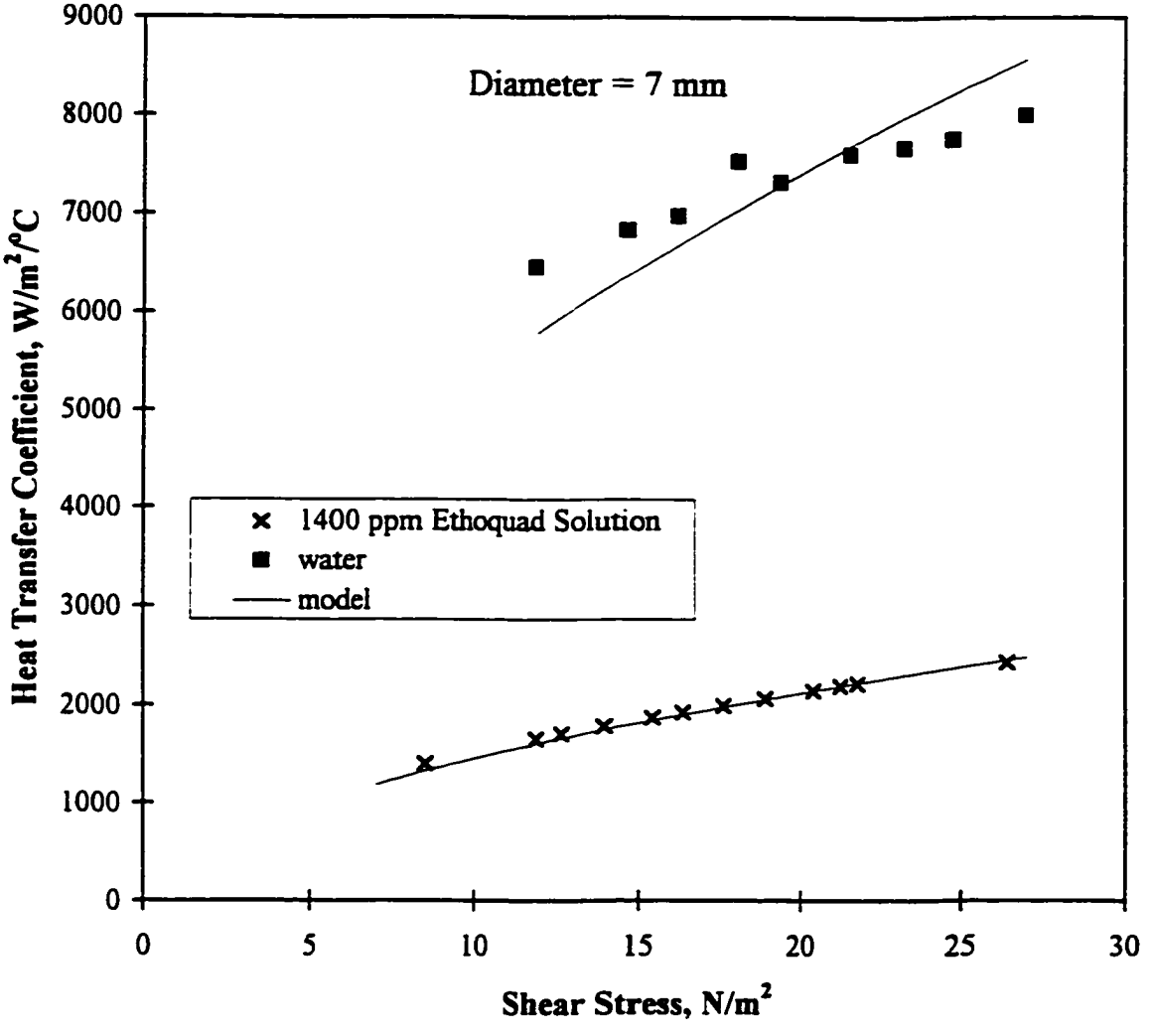

Figure 6.1 Prediction of heat transfer results in the 7 mm diameter tube using equation (6.17) (our results,water and 1400 ppm Ethoquad O12 solution)

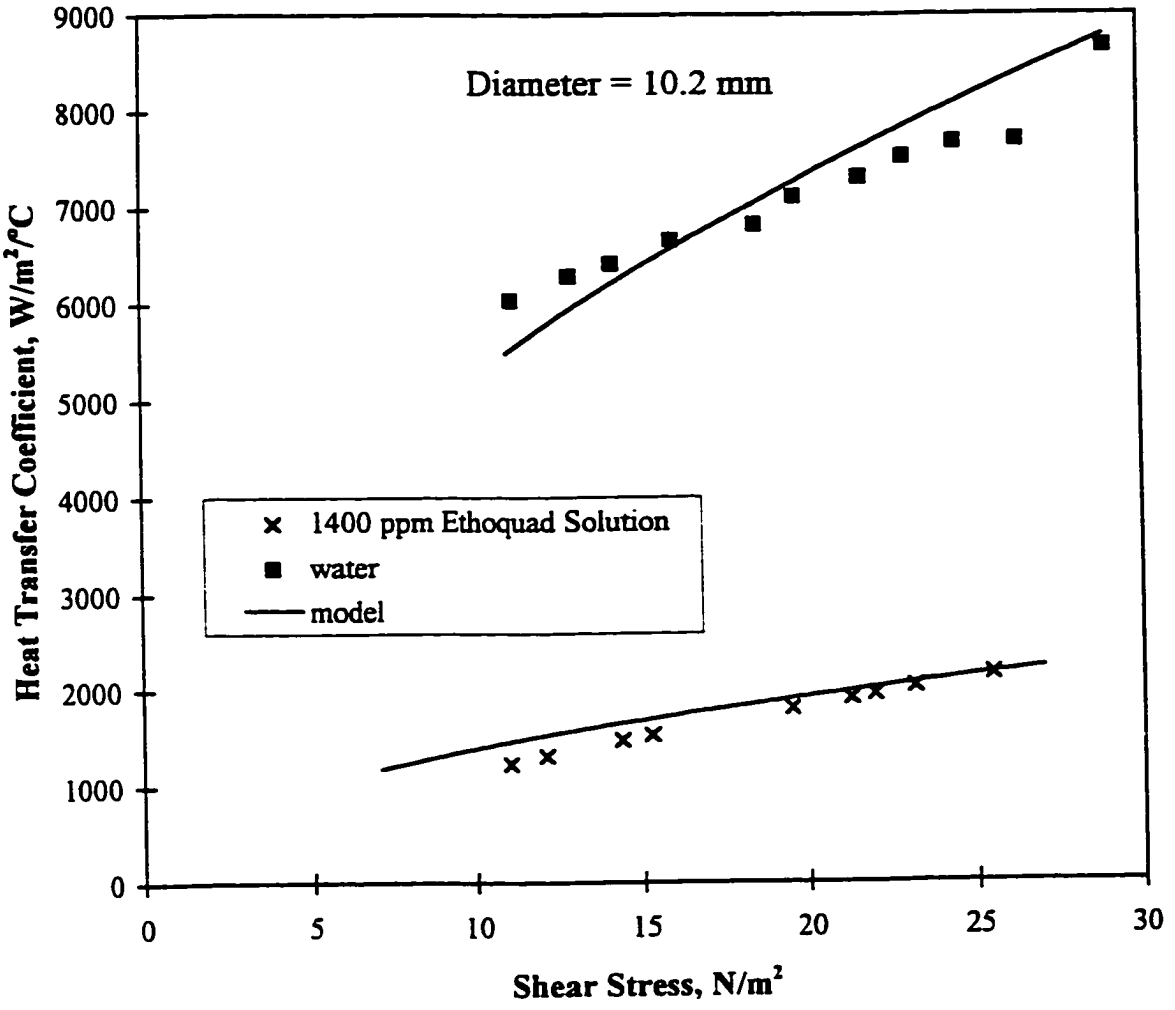

Figure 6.2 Prediction of heat transfer results in the 10.2 mm diameter tube using equation (6.17) (our results,water and 1400 ppm Ethoquad O12 solution)

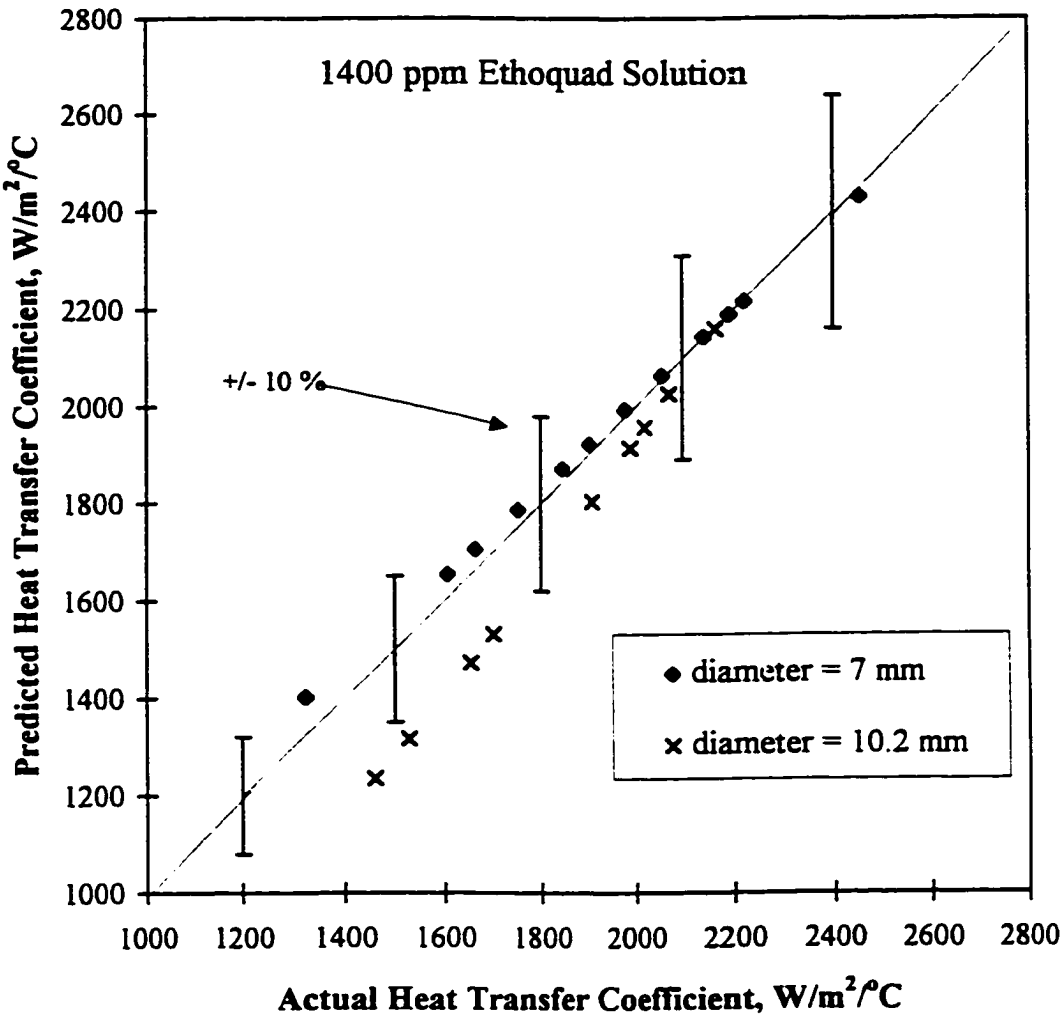

Figure 6.3 Comparison of actual and predicted heat transfer coefficients for 1400 ppm Ethoquad O12 solution

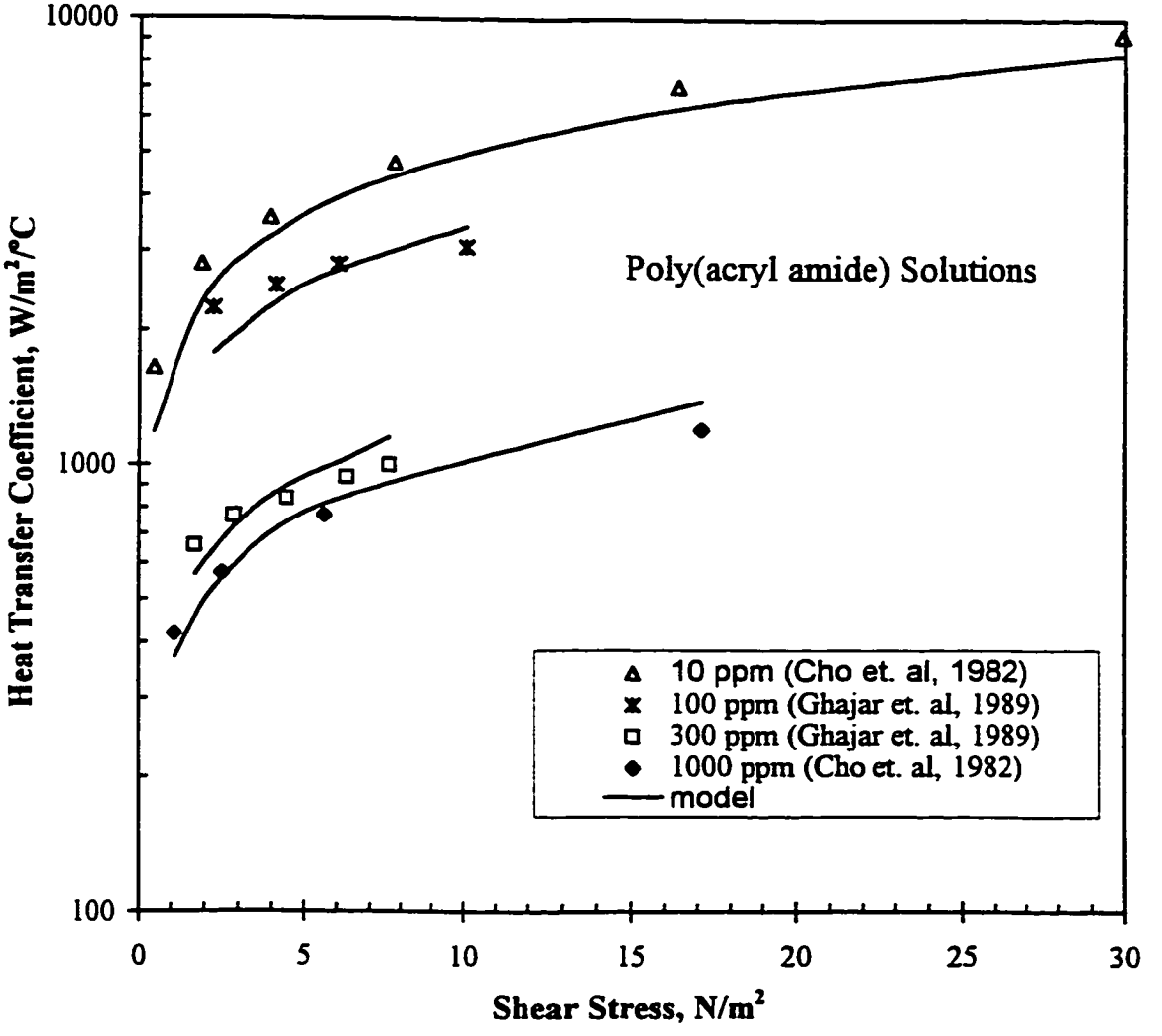

Figure 6.4 Prediction of heat transfer results for a polymer-water system (data of Cho and Hartnett, 1982; Ghajar and Yoon, 1989, Poly(acrylamide) solutions)

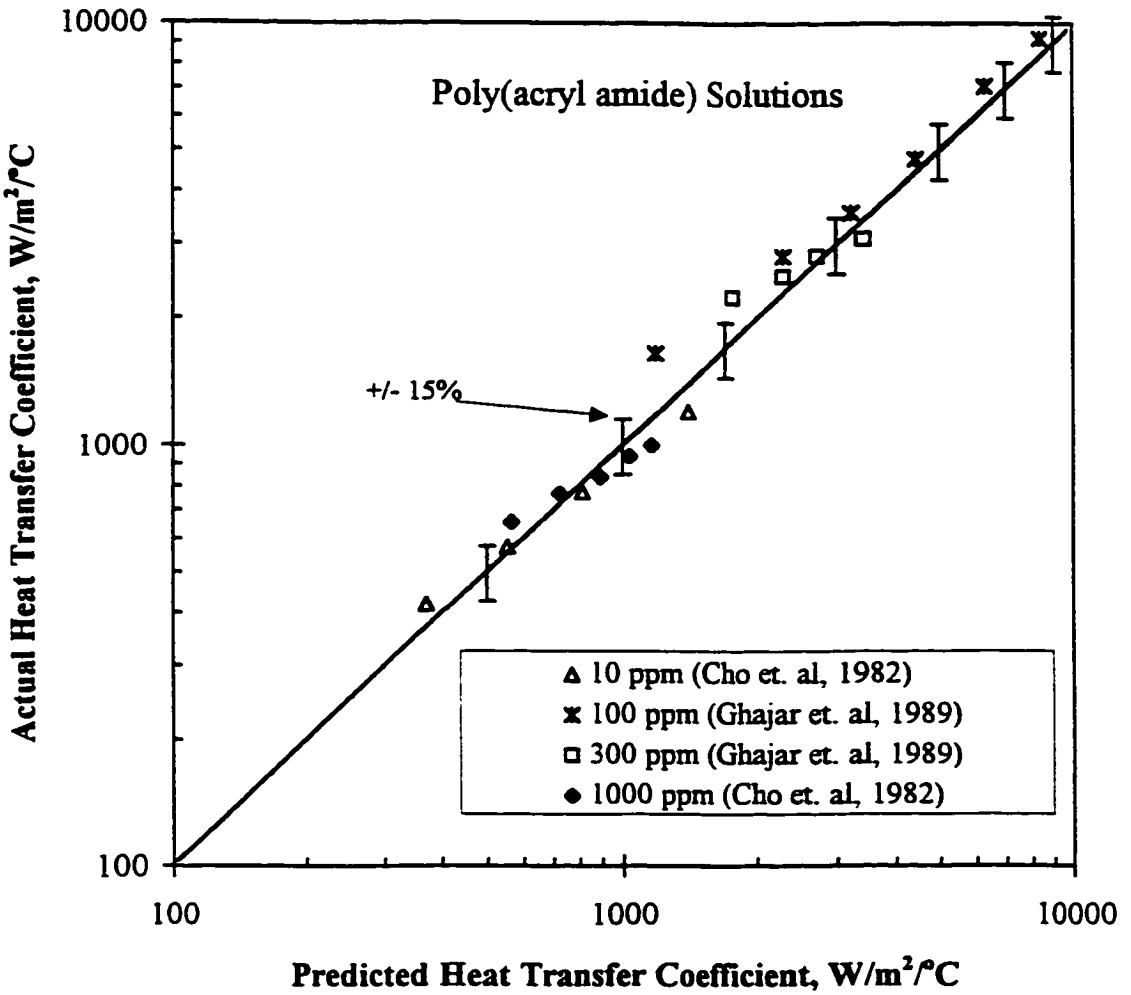

Figure 6.5 Comparison of actual and predicted heat transfer coefficients for Poly(acrylamide) solutions (data of Cho and Hartnett, 1982; Ghajar and Yoon, 1989)

are approximately equal for Newtonian fluids. It is based on the concept that the physical mechanisms leading to the transport of momentum and energy by mixing are very similar.

But this analogy is valid roughly at best due to the following reason. The momentum exchange process in fully developed turbulent flow takes place primarily through pressure acting on a fluid element as a result of impact with the surrounding fluid. Viscous forces are obviously present, but apparently play a minor role since the turbulent shear stress is independent of viscosity. On the other hand, heat exchange process must be by molecular conduction since there is no mechanism for heat transfer analogous to the impact-pressure mechanism for heat transfer (Kays and Crawford, 1980).

Validity of the Reynolds Analogy for drag reducing viscoelastic solutions has been the subject of controversy for many years. Early investigators (Kale, 1977, Pruitt et al., 1966, Wells, 1968, Meyer, 1966 and Corman, 1970) assumed the analogy between momentum and heat transfer to be valid, but the correlations proposed by them were rather complicated and required detailed knowledge of the boundary layer structure. In general, they could not be used in standard engineering practice.

Later experimental observations indicating that heat transfer reduction was relatively more than drag reduction gave rise to the general acceptance that eddy diffusivity for momentum was much more than eddy diffusivity for heat. An interesting contribution was also made by Khabakhpashev and Perepelitsa (1973). They measured the temperature and velocity profiles for aqueous solutions of Poly(acrylamide) by means of thermocouples inserted into the flow field. The eddy diffusivities of momentum and heat were calculated based on the experimentally determined velocity and temperature profiles and it was found that the turbulent Prandtl number (N_{Pr_t}), defined as the ratio of the eddy diffusivity of momentum to that of heat, exceeded unity for a substantial part of the square test section. But there was an error in their experiments which was common at that time.

They used a square pipe as the test section which was only 200 diameters in length, while it has been shown experimentally and accepted universally (Cho and Hartnett, 1982) that drag reducing viscoelastic solutions have an entrance length of 300-500 diameters. Hence their conclusions were based on observations made while the thermal boundary layer was still developing.

In the development of our heat transfer model, the turbulent Prandtl number (N_{Pr_t}) has been taken to be 1.0, which means that the eddy diffusivity of momentum has been assumed to be equal to the eddy diffusivity of heat. The decrease in drag and heat transfer is accounted for by a reduced mixing length and the subsequent thickening of the laminar sublayer. The mechanisms leading to the transport of momentum and heat are still assumed to be the same as that for Newtonian fluids.

The fact that heat transfer reduction is relatively more than drag reduction can be understood by analyzing the role of fluid viscosity in these phenomenon. The contribution of the fluid viscosity is negligible towards friction in turbulent pipe flow and dampening of turbulent velocity fluctuations are solely responsible for the reduction in fluid drag. On the other hand, for heat transfer from the wall to the fluid, there is a large temperature gradient (drop) across the laminar sublayer. Since the laminar sublayer is thicker for drag reducing fluids, the temperature gradient is bigger. In addition, the dampening of velocity fluctuations results in a decreased transport of energy due to mixing, which is reflected by the decrease in the mixing length. The above two factors, that is, thicker laminar sublayer and a decrease in transport of energy due to mixing contribute together to reduce the convective heat transfer relatively much more than drag reduction.

The assumption in the development of our model that eddy diffusivity of momentum is equal to the eddy diffusivity of heat appears to be valid since the model has predicted experimental results reasonably well. But more experimental work, where eddy

diffusivity of momentum and heat are actually measured, is needed to confirm this assumption.

6.5 Summary

A model for prediction of heat transfer results for drag reducing fluids has been proposed, which is an extension of the scale-up model for drag reduction presented in the last Chapter. The heat transfer coefficient can be calculated without any prior knowledge about the heat transfer behavior of the fluid. Using velocity and shear stress data obtained in a small laboratory scale pipe, constants K, B and y_{ls}^{+} are calculated from equations (5.35) and (5.36). These constants and the fluid properties (C_P, ν, k) are used in equation (6.17) to calculate the heat transfer coefficients. The model has been tested with reasonable success on our experimental data for the surfactant Ethoquad O12 (1400 ppm solution) and data available in published literature for the polymer Poly(acrylamide) (10 ppm, 100 ppm, 300 ppm, 1000 ppm solutions). This indicates that the model is not restricted to a particular type of drag reducing fluid but has universal applicability.

The validity of the Reynolds Analogy is still a subject of debate which can only be clarified by sound experimental observations. In our analysis, we have assumed the analogy to be valid and the reduction in convective heat transfer has successfully been correlated by a reduced mixing length and a thicker laminar sublayer.

7. STUDIES ON MICELLAR BREAK-UP

In the past few years, surfactants have been recognized as very promising drag reducers. But drag reduction by additives in turbulent flow is always accompanied by heat transfer reduction, which is usually larger than the reduction in drag itself (Matthys, 1991). Heat transfer reduction is useful in heating and cooling systems because it helps to reduce the thermal energy losses in the pipes. The Trans Alaska Pipeline (Burger et al., 1982) is a good example where convective heat transfer losses were minimized and reheating costs for the crude oil transportation over 1300 kms were significantly reduced by use of drag reducing additives.

However, good heat transfer in heat exchangers is an important consideration for heating and cooling systems. If the heat transfer reduction effect is not overcome in heat exchangers by breaking up the surfactant micelles, increased heat transfer area would be required leading to an increase in the fixed capital cost, which would cut into cost savings due to the drag reduction effect.

For cooling systems, in most designs water flows on the tube side under turbulent conditions. The refrigerant is on the shell side, whose flow is accompanied by a relatively high heat transfer due to phase change. Any reduction in heat transfer on the water side due to the presence of surfactant additives would result in a proportional reduction in the overall heat transfer coefficient. Similarly for heating systems, where most designs have water flowing under turbulent conditions in banks of tubes along the boiler walls, reduced heat transfer on the water side can be a serious problem.

It appears from the above discussion that for successful application of the

surfactant additives in heating or cooling systems, intentional degradation of the micelles would be necessary to prevent drag reduction and the associated heat transfer reduction in heat exchangers.

So far only a few studies (discussed in section 7.1) have been reported in literature where the intentional degradation of surfactant micelles for heat transfer enhancement has been investigated. All of them have focused on practical aspects or the economic consequences of breaking up the micelles for increased heat transfer in heat exchangers. Studies on the fundamental aspects of micellar break-up and recovery and factors controlling them have not been reported.

We carried out experiments to study the dependence of micellar break-up and recovery on pressure drop across the shearing device and flow conditions in the test tube. Theoretical considerations and experimental results are discussed in sections 7.2 and 7.3, respectively. A methodology to calculate the recovery time has also been presented in section 7.3.

7.1 Previous Work

A number of experimental studies have been conducted on the implementation of surfactant additives to heating and cooling systems. The studies have primarily focused on the economic viability of using these additives in closed circulation systems.

Rouse et al. (1989) used surfactant additives in a building heating system. The maximum drag reduction achieved in their system was about 70%, but the overall drag reduction was somewhat lower than expected. They attributed the reduced overall drag reduction to possible laminar flow in parts of the circulation loop and the micellar

breakage due to high shear stress levels in bends and fittings.

Steiff et al. (1989) reported a field scale implementation of surfactant additives in a district heating system with the main transport pipeline being 2.4 km long (0.45 m diameter). Optimum levels of drag reduction were reported. They also encountered problems with the loss of heat transfer in heat exchangers due to the presence of these additives.

Gasljevic and Matthys (1992) have reported a study on effect of drag reducing surfactant solutions on the performance of centrifugal pumps. They also carried out a feasibility study on the use of drag reducing surfactant additives in a closed circulation heating or cooling system to reduce pumping power.

Pollert et al. (1994) have reported on the use of friction reducing surfactant additives in a district heating system in Czech Republic. Later experiments on the same system by Zakin (1996) have indicated drag reduction lower than that predicted by Virk's Asymptote.

Gasljevic (1995) carried out a study on heat transfer aspects of using surfactant additives for closed circulation systems. Heat transfer in different types of heat exchangers and the effects of additives on pumps and valves were also investigated. Use of flow obstructing inserts was proposed as a means of enhancing heat transfer on the tube side. However, significantly large pressure drops have been reported in their experiments with these inserts, indicating that this might not be the most economical alternative.

Young (1996) used surfactant additives in a library cooling system and drag reduction levels of 70% and above were reported. The same surfactant solution (Ethoquad O12) has been used in the closed circulation system for over four years, confirming the

durability and excellent resistance of these solutions to mechanical degradation. Increased heat transfer in the heat exchanger was achieved by throttling the inlet valve of the heat exchanger to break-up the surfactant micelles by high shearing stresses.

7.2 Theoretical Description of Factors Affecting Micellar Break-up and Recovery

Heat transfer enhancement by placing inserts (Gasljevic, 1995) in the tube flow of drag reducing fluids (internal demicellation) inside a heat exchanger is useful only as an operational concept. The use of inserts is disadvantageous in a closed circulation system since once they are placed inside the tubes of the heat exchanger, they can only be removed after a total shutdown of the heating or cooling system. Moreover, once the positions and the total number of inserts necessary for the desired heat transfer enhancement are optimized for a given operating condition, any change in the operating condition might result in an unnecessary pressure drop across the heat exchanger.

Based on the observations in their experimental set-up, Young (1996) concluded that using a throttling valve (external demicellation), or a device that produces high shear comparable to a throttling valve, at the inlet to the heat exchanger would be preferable to internal demicellation for the following reasons:

1. Internal demicellation can only be used with a shell and tube heat exchanger, while the use of external demicellation is not restricted by the type of heat exchanger since it breaks up the micelles at the inlet and not inside the heat exchanger.

2. External demicellation allows for adjustment of the applied level of shear stress to the minimum necessary to achieve micellar break-up. Unnecessary pressure drop across the heat exchanger can thus be avoided.

3. External demicellation in their system was able to enhance heat transfer across the entire length of the heat exchanger tubes.

A survey of literature available on demicellation has indicated that studies have not been conducted so far on factors which affect micellar break-up and recovery. Following two questions need to be answered to optimize the use of surfactant additives in closed circulation heating or cooling systems:

- Does pressure drop across the shearing device have any role in recovery of micelles further downstream?
- What role, if any, do flow conditions play in the recovery of micelles?

7.2.1 Effect of Pressure Drop Across the Shearing Device

Micellar aggregates are composed of charged surfactant molecules. As pressure drop across the shearing device (ΔP_{sh}) is increased, micelles would break-up into individual molecules once the shear stress is high enough (critical shear stress) to overcome the intermolecular forces binding the molecules together. The micellar structures would recover further downstream.

Gasljevic (1995) observed in their experiments that prohibitively high pressure drops were required across a wire mesh plug in their system to prevent the micelles from recovering in the heat exchanger (140 diameters in length). Based on the above observations, they proposed that at higher values of (ΔP_{sh}), the degree of micellar break-up would be more extensive and recovery would take a longer time. But their conclusions were based on the observations made in a relatively short pipe in which high velocities (4-7 m/s) were maintained. Due to the short length of the pipe, recovery of micelles could

not be studied and the role of flow conditions in micellar recovery was not investigated.

In our view, pressure drop across the shearing device is a measure of the energy dissipation and the shearing stress experienced by the solution as it passes through the screens. As pressure drop across the shearing device is increased and the critical shear stress is exceeded, micelles would disintegrate into individual molecules and any further increase in shear stress would not increase the degree of dissociation. In other words, the recovery of micelles would depend upon the concentration of the solution and flow conditions further downstream and would be totally independent of the pressure drop across the shearing device.

To verify the above hypothesis, a study of micellar break-up was carried out in our experimental set-up (details discussed in chapter 3) which was maintained under constant flux heating conditions. A wire mesh plug was placed at the inlet to the test section and the solution was subjected to varying degrees of shear by using different numbers of wire meshes in the plug. Micelles were broken up as they passed through the plug and their recovery further downstream was analyzed by observing the wall temperature profile. Since our test-section was about 600 diameters long, we were able to observe micellar break-up and recovery and could correlate them with ΔP_{sh} The results are discussed in section 7.3.2.

7.2.2 Role of Flow Conditions in Micellar Recovery

Surfactant molecules consist of two parts, one which is polar and highly soluble in the medium concerned and the other which is insoluble. Micelles are formed by the aggregation of surfactant molecules in solution due to Van der Waal forces, so that they present a hydrophilic surface to the solvent while the core is hydrophobic in nature.

Let us consider a surfactant solution containing micelles and flowing through a pipe under turbulent conditions. When the solution is subjected to a shearing force (across a wire mesh or a throttling valve) which is strong enough to overcome the intermolecular forces holding the micelles together, the micelles would break-up into individual molecules. Since the concentration of surfactant molecules is high enough to thermodynamically favor micelle formation (as discussed in Chapter 2), the molecules would tend to regroup once they are past the shearing device.

A hypothesis is presented below to explain the recovery of micellar structures downstream of the shearing device:

The process of molecular regrouping would be controlled by the turbulent flow conditions. In a turbulent flow field, irregular fluctuations are superimposed on the main stream. These fluctuations give rise to eddies and a mixing motion, which continuously transports energy from the main flow into larger eddies. These large eddies subsequently break-up into successively smaller eddies till they are small enough to be destroyed by the action of fluid viscosity. For the small energy dissipating eddies in a circular pipe, their characteristic length (l_E) and frequency of occurrence (Ω) are approximately represented by the following expressions (Davies, 1972) :

$$l_E = 20dN_{re}^{-0.78} \tag{7.1}$$

$$\Omega = 0.02\bar{u}N_{re}^{0.56}d^{-1} \tag{7.2}$$

l_E and Ω are plotted in Figure 7.1 as the function of bulk velocity for a 7 mm

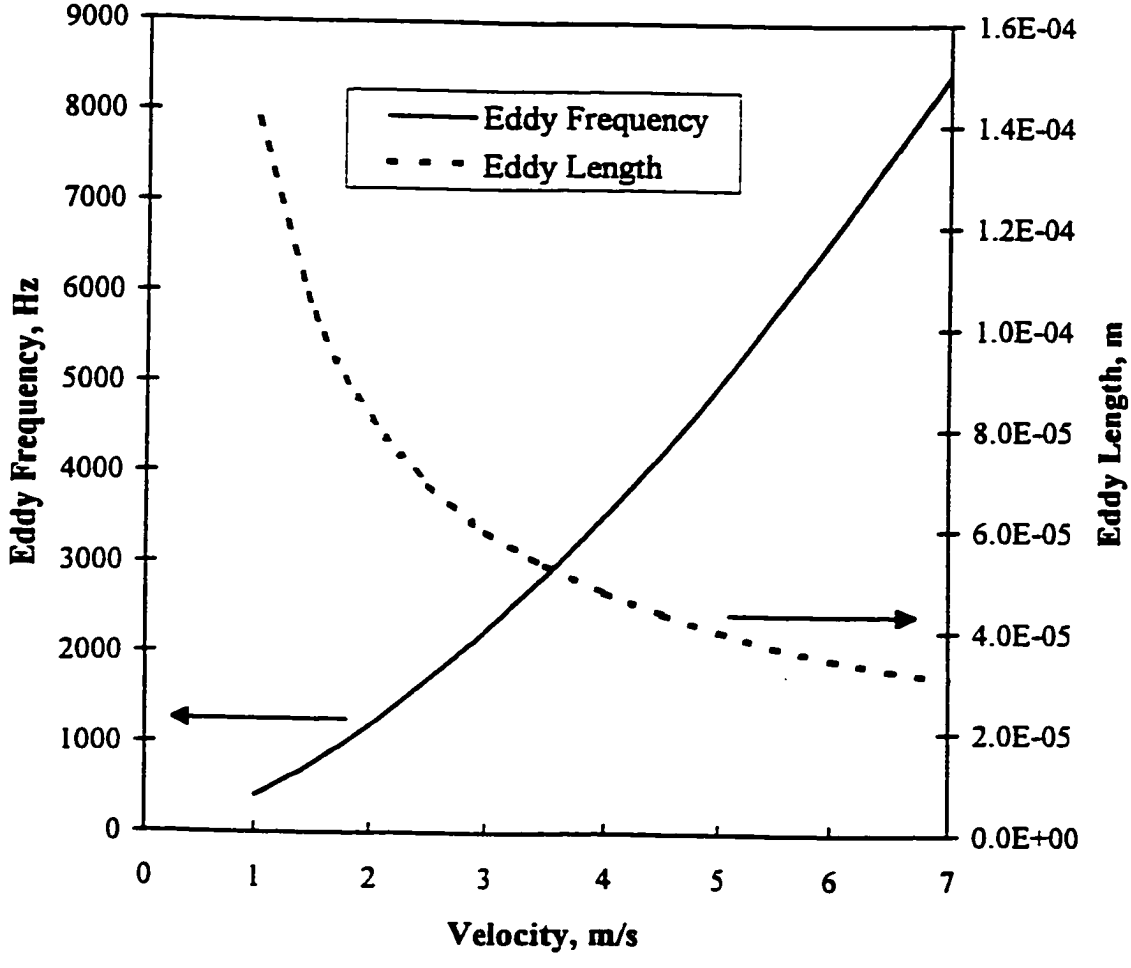

Figure 7.1 Length and frequency of energy dissipating eddies as a function of bulk velocity (7mm diameter tube)

diameter pipe. As can be seen from the Figure, size of the smallest energy dissipating eddy is of the order of 10^{-5} m . It has also been shown (Dill, 1984) that the size of individual surfactant molecules is approximately 10^{-8} m, i.e., a thousand times smaller than the smallest eddy. Hence initially when the micelle breaks up into smaller molecules, the collision frequency of the molecules would be low because each molecule would in all probability be a part of an eddy which is much bigger in size. As a few molecules get attached to each other, the aggregates grow and become comparable in size to the energy dissipating eddies and are now able to absorb kinetic energy from these eddies, making their movements more random and thus increasing the probability of collision with other molecules.

A fully formed micelle contains 50-100 molecules and has a radius of gyration of the order of 10^{-5} m (Dill, 1984), which is same as the size of energy dissipating eddies. When size of the energy dissipating eddies becomes comparable to the size of the viscoelastic polymer molecule (or surfactant aggregate) energy dissipation decreases and a reduction in drag is achieved (Virk, 1975).

Figure 7.1 shows that as the Reynolds number (or velocity) of the flow increases, i.e., the flow becomes more turbulent, length (l_E) of the energy dissipating eddies decreases and their frequency (Ω) of occurrence increases, which means that for surfactant molecules trying to regroup, the collision frequency should increase with an increase in turbulence. An increase in the collision frequency would lead to a faster rate of recovery for the micelle.

The validity of the hypothesis presented above was tested in our experimental set-up. Micellar break-up and their subsequent recovery was analyzed for different fluid velocities (increasing Reynolds number) in the turbulent flow regime. The flow experiments were conducted in the 7 mm diameter tube under constant flux heating

conditions and using a wire mesh plug containing 12 screens. The wall temperature profiles gave an indication of micellar break-up and their rate of recovery. The results are discussed in section 7.3.3.

7.3 Results and Discussion

External demicellation was chosen as the method for breaking up the surfactant micelles in our experiments as it has certain advantages over internal demicellation (as discussed in section 7.2) from a practical point of view.

Micelles were broken up by placing a wire mesh plug, upstream of the test section (at 0 l/D). The number of wire mesh screens could be varied in the plug. The screens used for our study had 20 by 20 meshes per cm^2, with a wire diameter of 0.23 mm. Constant heat flux conditions were maintained across the test-section (7 mm diameter tube) which was 600 diameters in length. Wall temperature was measured at 17 points along the length of the tube and also the inlet and outlet fluid bulk temperatures. Construction of the thermocouples and their placement on the test tube are discussed in detail in Chapter 3.

7.3.1 Observing Micellar Break-up and Recovery From Temperature Profiles

Figure 7.2 illustrates the difference between wall temperature profiles for water, surfactant solution (micelles not intentionally broken up at inlet) and surfactant solution with micelles intentionally broken up at the inlet by a wire mesh plug (12 screens).

It can be seen from the Figure, that for water the wall temperature profile does not

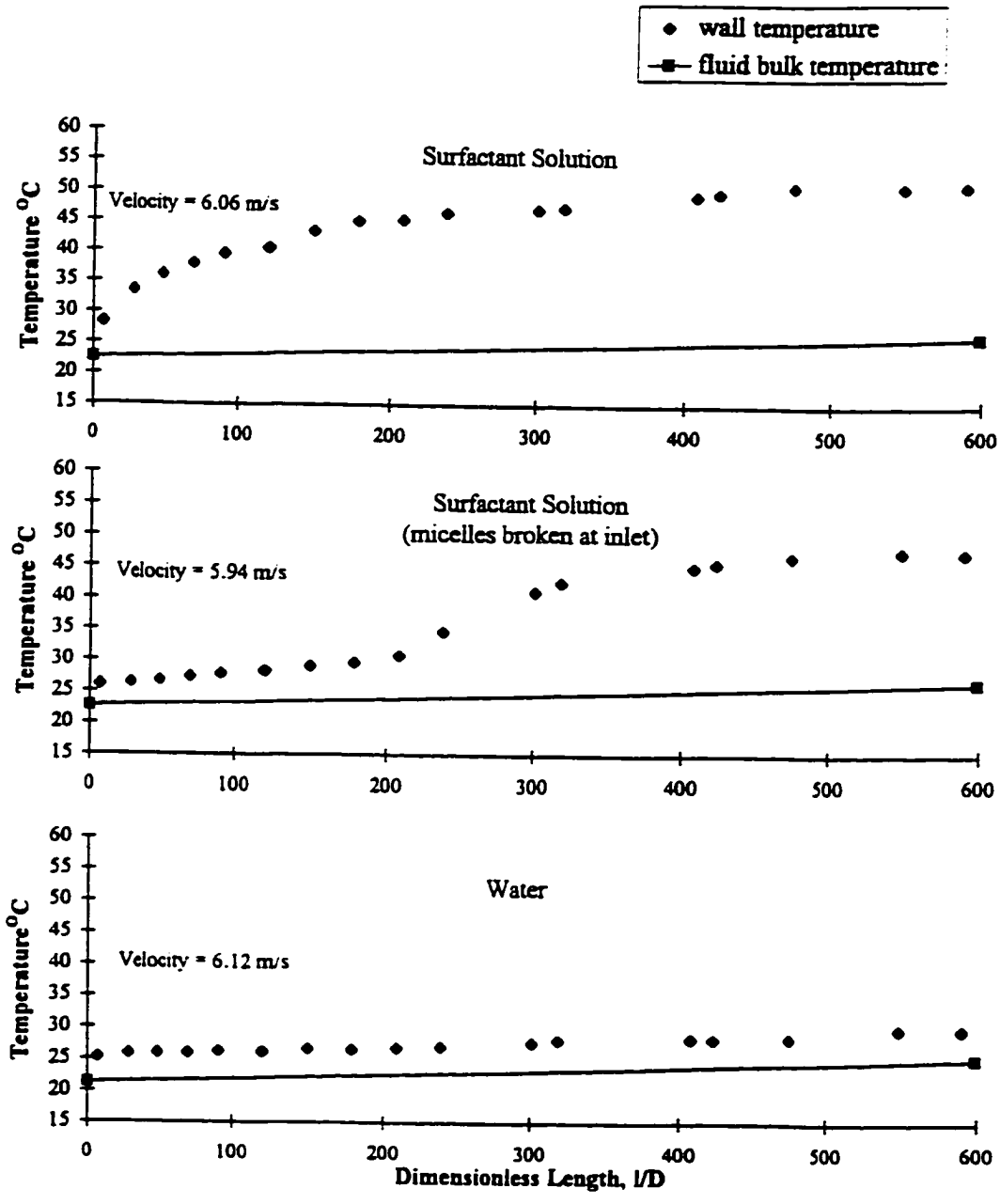

Figure 7.2 Comparison of temperature profiles for water, 1400 ppm Ethoquad O12 solution and 1400 ppm Ethoquad O12 solution (micelles broken at inlet), heat flux = 43 kW/m^2

show any entrance region. This was expected as Newtonian fluids generally have an entrance region of only 10-15 diameters (Deissler, 1955) and in our experiments the placement of thermocouples along the length of the tube was made at 12.5 diameters or more apart. The difference between wall temperature and the fluid bulk temperature was approximately 5°C for the entire length of the tube, indicating a high heat transfer coefficient.

The temperature profile for the surfactant solution (micelles not intentionally broken up at inlet) showed an entrance length of about 250 diameters and a temperature difference of about 25°C in the fully developed region; indicating a low heat transfer coefficient due to the heat transfer reduction effect.

The temperature profile for the surfactant solution with micelles intentionally broken-up at the inlet showed a temperature profile similar to water for about 200 diameters with a temperature difference of about 5°C. At this point, the micelles seemed to regroup and the wall temperature profile showed a sudden change in slope as the heat transfer reduction effect developed. The temperature difference increased to about 25°C by the time the solution left the test section.

7.3.2 Effect of Pressure Drop Across Shearing Device

Pressure drop across the shearing device (wire mesh plug in our case) is a measure of the flow energy loss over the plug and therefore is a measure of energy dissipated in the fluid. Calculating the shear stress on the fluid as it passes through a wire mesh plug, in which the screens are packed closely together, is a difficult proposition. Though all the losses in the fluid as it passes through the plug are due to viscous stresses, we cannot calculate the shear stress as we cannot associate any area to it since the screens are packed

closely in the plug.

Shear stress can indeed be estimated across a single screen as the area of flow can be calculated from the wire thickness and wire spacing. However, we did not concern ourselves with these calculations because, as we have discussed in Chapter 1, critical shear stress needed to break-up the micelles for a given concentration can be calculated from pressure drop-flow rate data. By using different number of screens in the wire mesh plug we intended to subject the surfactant solution to varying degrees of shear above the critical shear stress needed to break-up the micelles and study whether the amount of excessive shearing had any role in recovery of the micelles further downstream.

We conducted a set of flow experiments in which different wire mesh combinations (1, 3, 6, 9 and 12 screens) were used in the plug. For each wire mesh combination, three different flow rates were maintained (5.0, 5.5 and 6.0 m/s) in the test loop. The wall temperature profiles obtained for all the runs are shown in Figure 7.3 (a, b, c).

Let us look at Figure 7.3(a) in which an average bulk velocity of 5.0 m/s was maintained in the test loop. As number of screens in the wire mesh plug were increased from 1 to 12, a higher pressure drop resulted across the plug. In other words, as the number of screens were increased for a given bulk velocity, the solution was subjected to higher degrees of shear. It can be observed from the Figures that as the number of screens (or shear stress across the plug) was increased for a given bulk velocity, the point at which the micelles began to recover was approximately the same (within ±50 l/D). Apparently, the degree of shearing in the wire mesh plug did not have any noticeable effect on micellar recovery. Similar observations can be made from Figure 7.3(b, c). These observations contradict the hypothesis by Gasljevic (1995), which proposed that if the degree of shearing in the plug was increased for a given velocity, the micelles would recover further downstream.

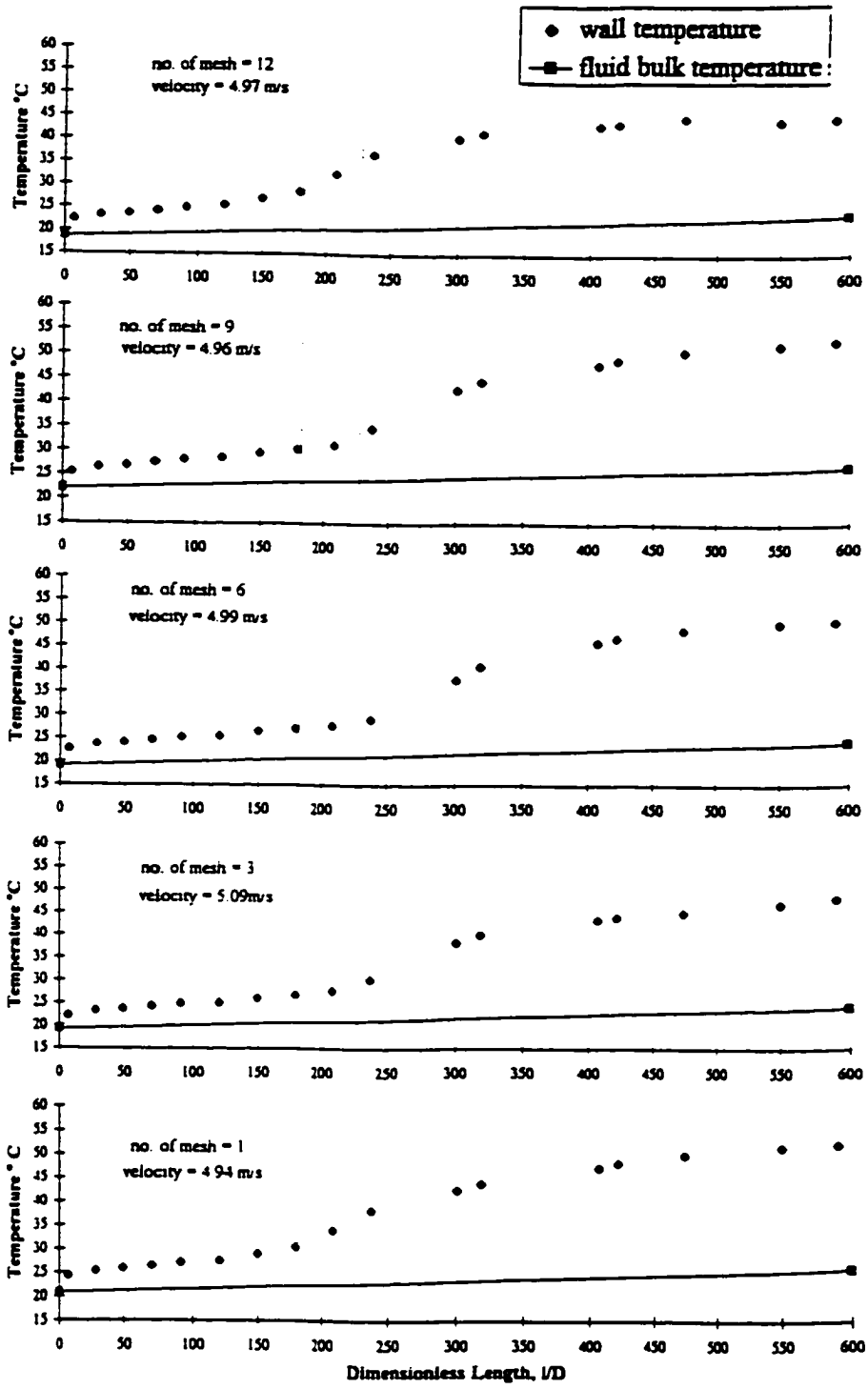

Figure 7.3(a) Effect of pressure drop across the shearing device on micellar recovery length for a 1200 ppm Ethoquad O12 solution (average bulk velocity ~ 5 m/s) (micelles broken at inlet by a wire mesh plug containing 1, 3, 6, 9, 12 screens respectively), heat flux = 43 kW/m^2

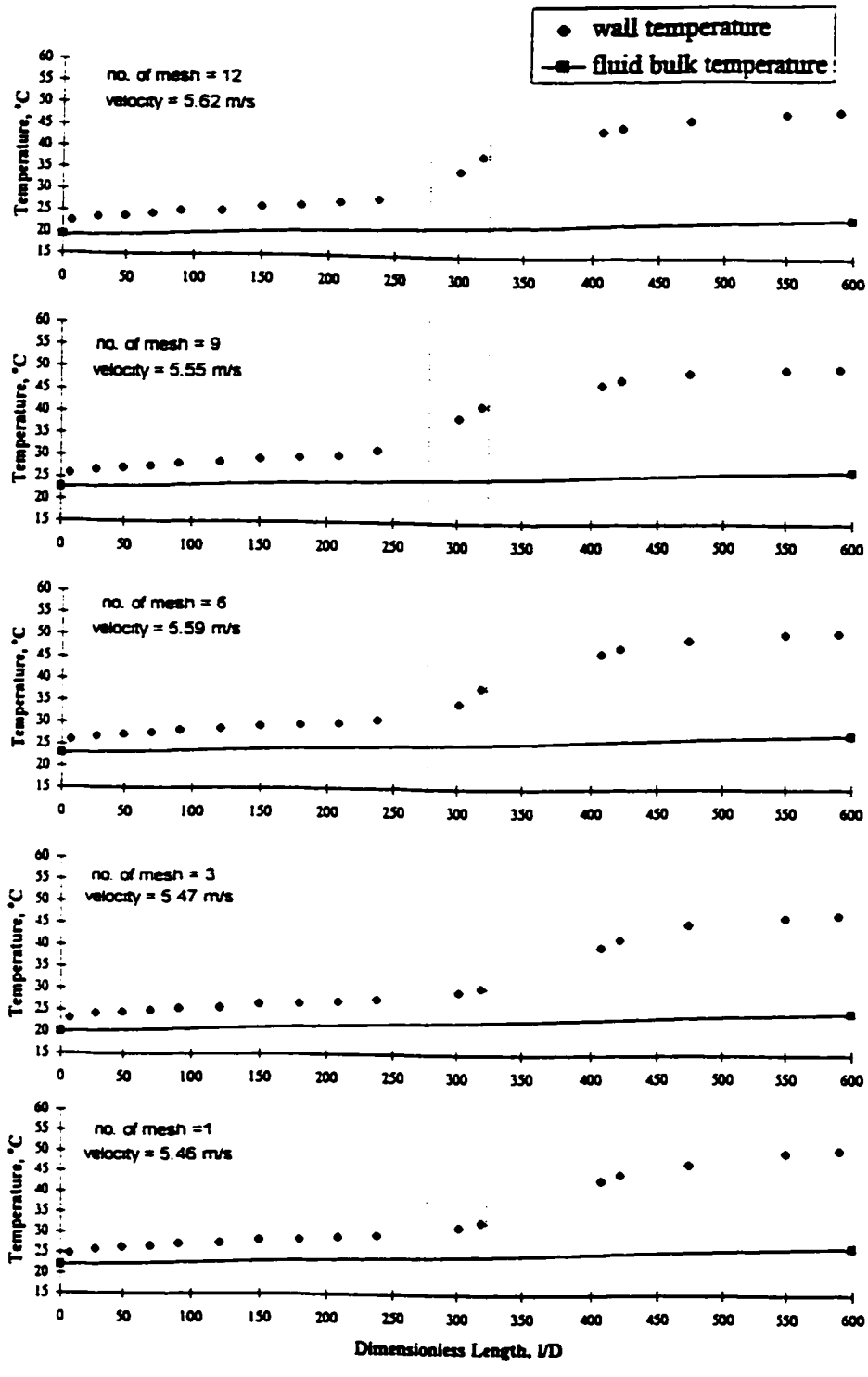

Figure 7.3(b) Effect of pressure drop across the shearing device on micellar recovery length for a 1200 ppm Ethoquad O12 solution (average bulk velocity ~ 5.5 m/s) (micelles broken at inlet by a wire mesh plug containing 1, 3, 6, 9, 12 screens respectively), heat flux = 43 kW/m^2

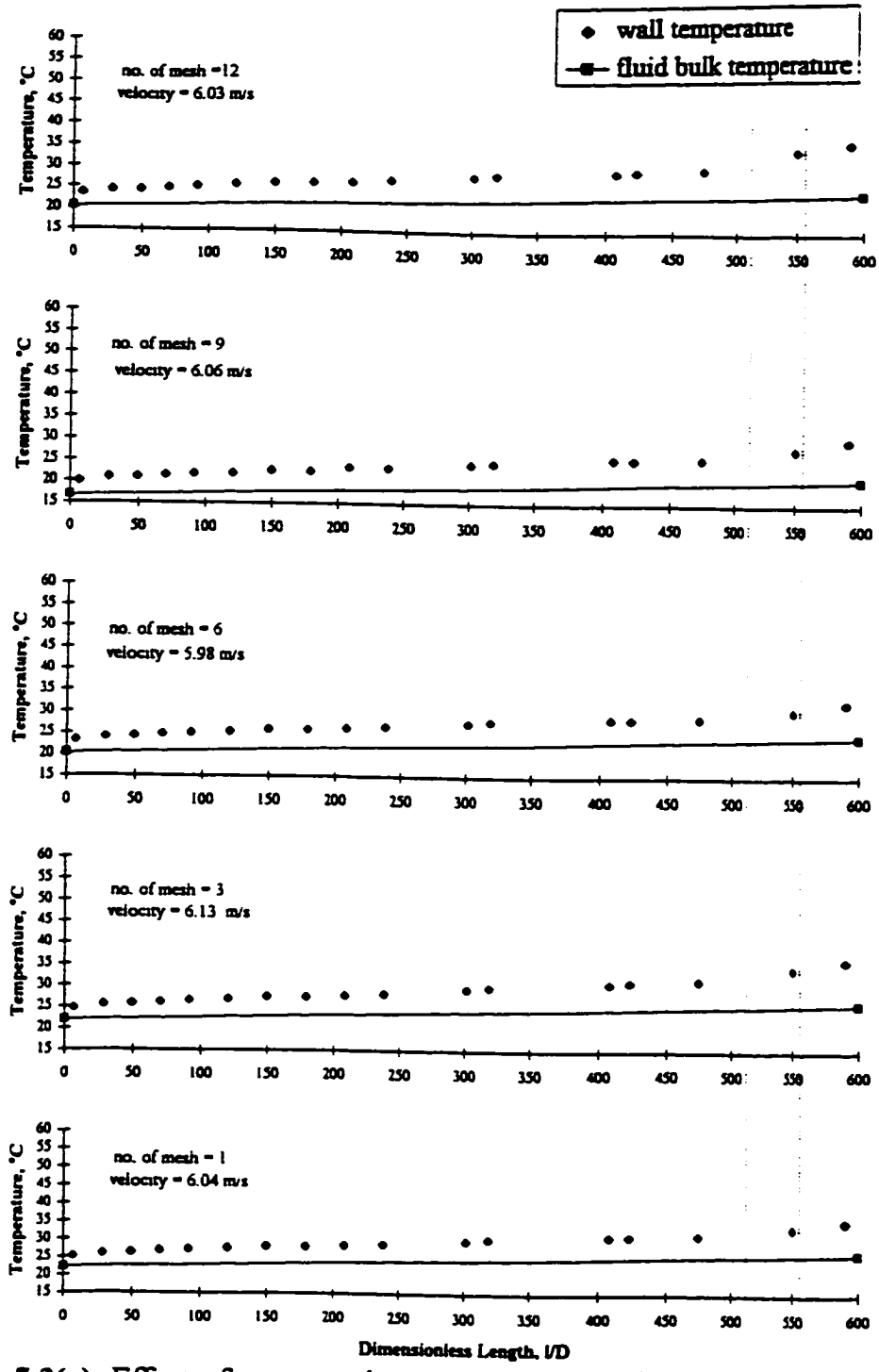

Figure 7.3(c) Effect of pressure drop across the shearing device on micellar recovery length for a 1200 ppm Ethoquad O12 solution (average bulk velocity ~6 m/s) (micelles broken at inlet by a wire mesh plug containing 1, 3, 6, 9, 12 screens respectively), heat flux = 43 kW/m^2

We had proposed in section 7.2.1 that shear stress across the plug was only responsible for breaking up the micelles but has no role in their recovery downstream. Increasing the shear stress across the plug above the critical shear stress needed to break the micelles would not delay the recovery of the micelles, but would only contribute to an unnecessary pressure loss. The hypothesis has been justified by the observations in Figure 7.3 (a, b, c). Since for a given velocity, the micelles have recovered at approximately the same distance down the tube irrespective of the degree of shearing in the wire mesh plug.

7.3.3 Role of Flow Conditions in Micellar Recovery

It was discussed in section 7.2.2 that an increase in turbulence would decrease the size of energy dissipating eddies and increase their frequency of occurrence (Figure 7.1). These conditions would increase collision frequency of the surfactant molecules and the rate of recovery for the micellar structures would be more rapid.

We conducted a set of experiments in which different flow rates (varying from 5 m/s to 6.5 m/s) were maintained in the flow loop. The micelles were broken-up by a wire mesh plug (12 screens) at the inlet of the test section and steady state temperature profiles (for constant heat flux conditions) were analyzed. The results are shown in Figures 7.4(a,b).

It can be observed from Figure 7.4 (a) that immediately downstream of the wire mesh plug the difference between wall temperature and the average bulk temperature was about 5-8°C, indicating a high heat transfer coefficient. As the micelles recovered further downstream, the wall temperature profile pulled away due to the heat transfer reduction effect.

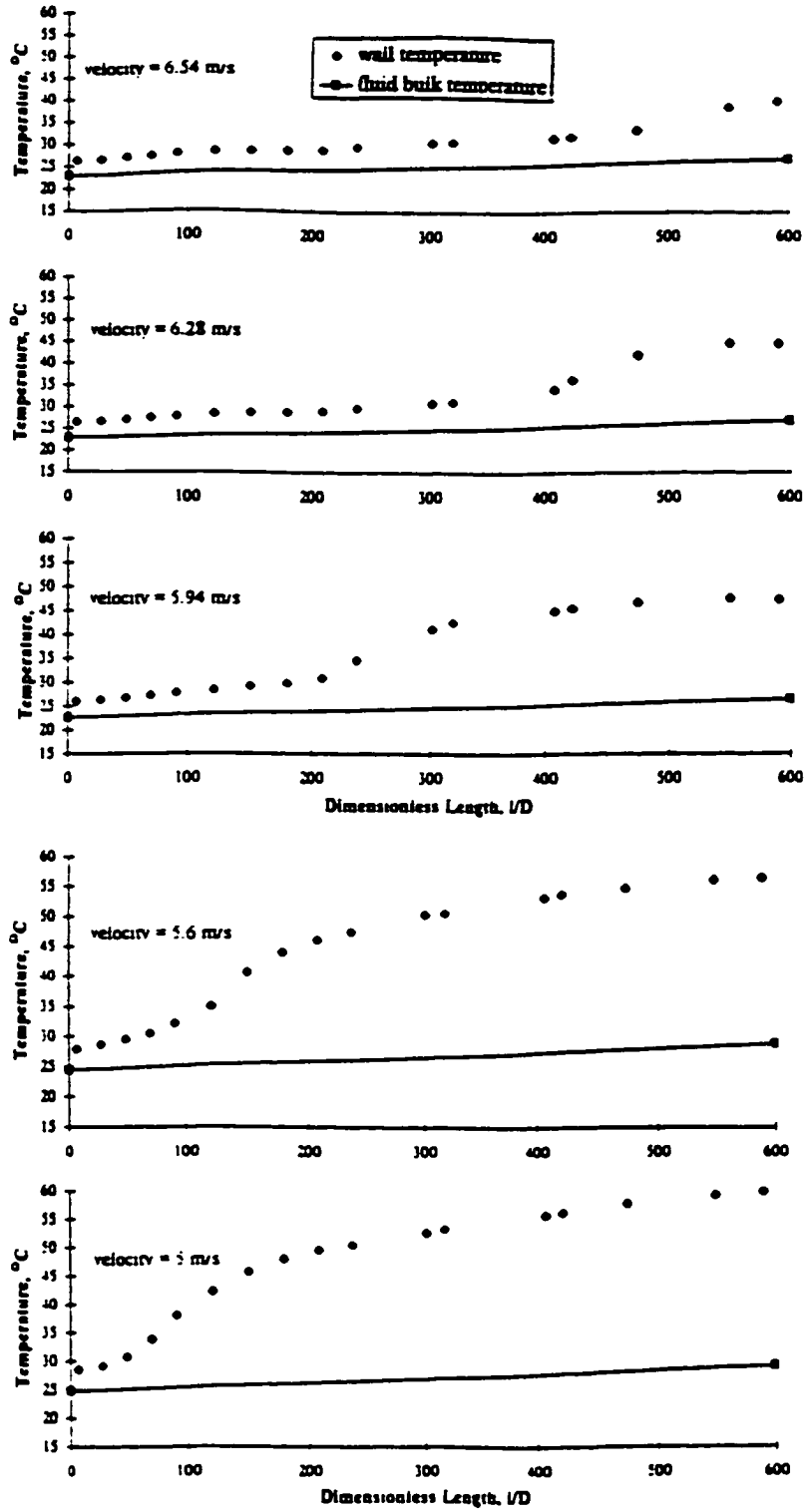

Figure 7.4(a) Effect of increasing turbulence on the rate of recovery of micelles for a 1400 ppm Ethoquad O12 solution (micelles broken at inlet by a wire mesh plug containing 12 screens), heat flux = 43 kW/m^2

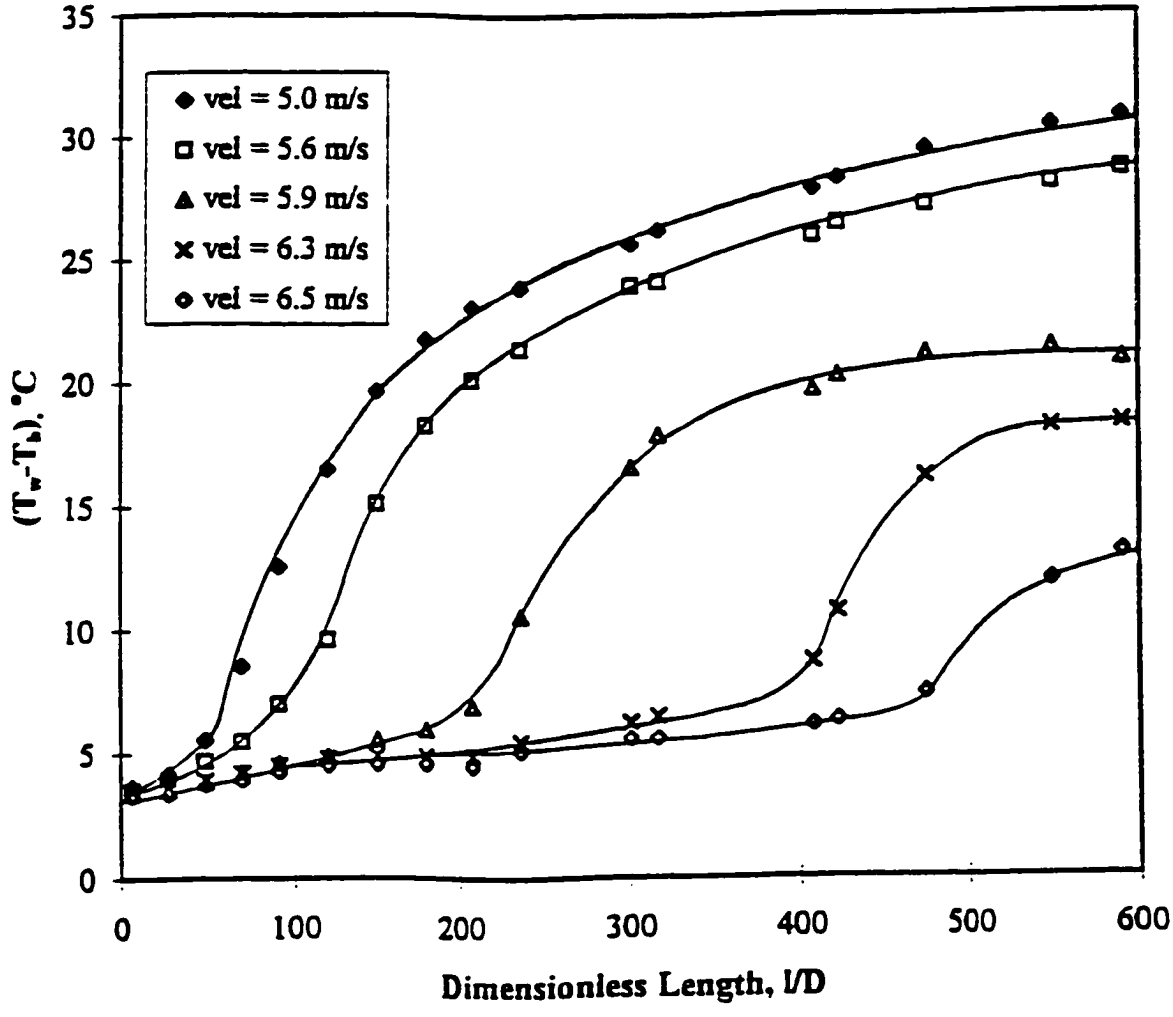

Figure 7.4(b) (T_w - T_b) vs l/D for a 1400 ppm Ethoquad O12 solution (micelles broken at inlet by a wire mesh plug containing 12 screens), heat flux = 43 kW/m^2

The results presented in Figure 7.4(a) are plotted again in Figure 7.4(b), which gives a better indication of the variation of the temperature difference between wall and the bulk fluid (T_w -T_b) with dimensionless distance (l/D) down the tube. It can be seen clearly from Figure 7.4(b) that for velocities 5.0 m/s and 5.6 m/s, (T_w -T_b) curves rise gradually and have positive slopes which indicates that the temperature profiles were still developing at the exit of the test section (600 diameters). As the flow rate was increased further (5.9 and 6.3 m/s), two effects were noticed. The point at which the micelles began their recovery moved further down the tube but now the recovery of the heat transfer reduction effect was more rapid. The temperature profiles (and hence, the micelles) were clearly fully developed and the (T_w -T_b) curves were parallel to the x-axis (Figure 7.4(b)) before exiting the test-section, indicating that due to increased turbulence the micelles were able to recover at a faster rate.

For the results shown in Figures 7.4(a,b), flow velocity was increased from 5 m/s up to 6.5 m/s. It can be observed from Figure (7.1) that when the velocity is increased from 5 m/s to 6.5 m/s in a 7 mm tube, the frequency (Ω) of energy dissipating eddies increases by almost 50 %. An increase of such a magnitude in Ω would certainly increase the collision frequency of the surfactant molecules and thus the recovery of micelles would take place at a faster rate.

The above observations verify our hypothesis (section 7.2.2) that flow conditions past the shearing device play an important, perhaps decisive role in recovery of micelles.

7.3.4 Calculation of Recovery Time for Micelles

Micelles are formed in a surfactant solution once the Critical Micellar Concentration is exceeded at the given temperature. These micelles are in a dynamic

equilibrium (Everett, 1988) with the surfactant molecules in solution, i.e., surfactant molecules continually enter and leave a micellar structure, but the net rate is zero.

Once the micelles are broken up into individual molecules by shear, the process by which they regroup can be represented by the reversible reactions:

$$\underset{\text{(surfactant molecules)}}{50\ A} \Leftrightarrow \underset{\text{(spherical micelles)}}{B} \qquad (7.3A)$$

$$\underset{\text{(spherical micelles)}}{B} \Leftrightarrow \underset{\text{(cylindrical micelles)}}{C} \qquad (7.3B)$$

The stoichiometric coefficient (α) for A has been shown to be 50 in the above equation, though the number of molecules forming the micellar aggregate could be anywhere in the range of 50-100 depending upon the type of surfactant. But there is no necessary connection between 'order' of the reaction and stoichiometric coefficients in the reaction equation; for example, it is not required that $\alpha=1$ for a first order reaction (Smith, 1970). The order of the reaction is determined by comparison of experimental data with the rate equation.

When surfactant molecules (A) combine to form micelles, spherical micelles (B) are formed initially, which do not produce drag reduction (or, heat transfer reduction) (Figure 7.5). Transition of spherical micelles to cylindrical micelles (C) coincides with the manifestation of the drag reduction (or, heat transfer reduction) (point P, Figure 7.5) effect. From a practical standpoint, the reaction represented by equation (7.3A) is of considerable interest as it is desirable to design a heating or cooling system in such a way that the first reaction (equation (7.3A)) proceeds to completion in the heat exchanger and the cylindrical micelles would be formed immediately downstream.

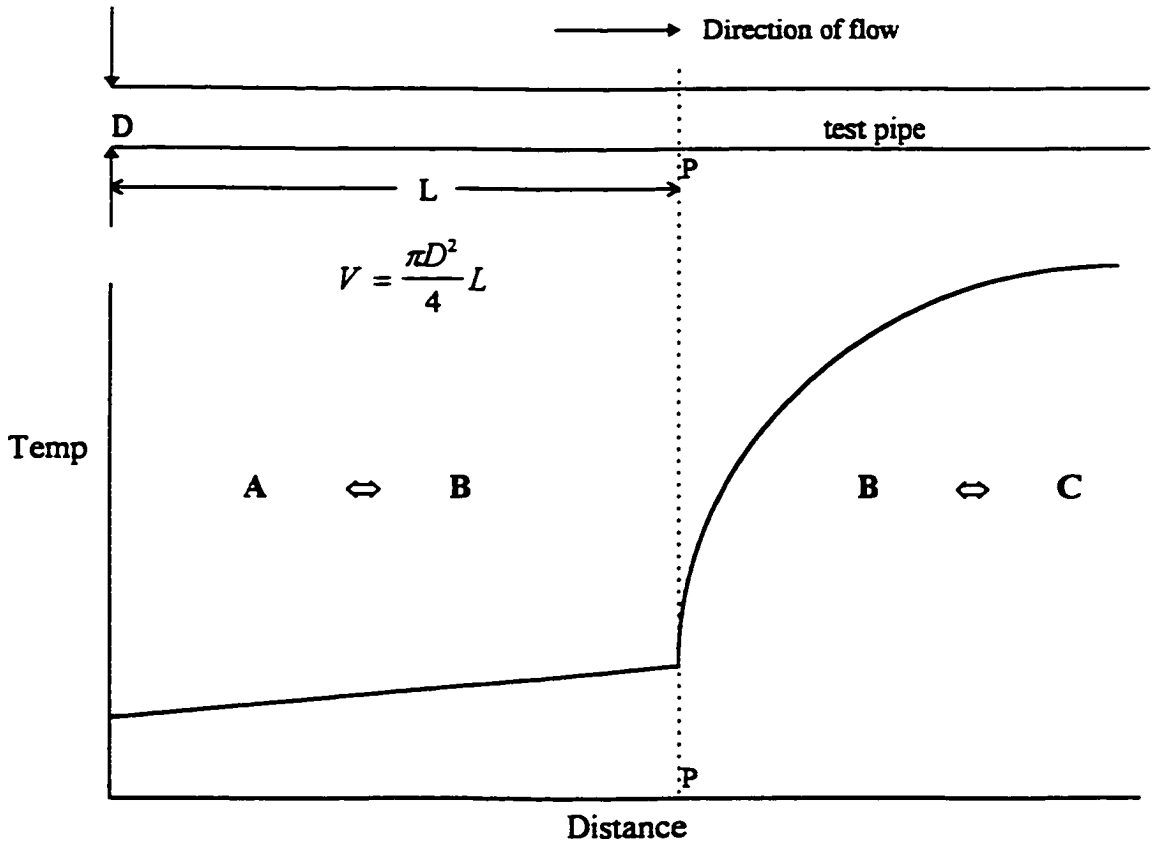

Figure 7.5 Hypothesis to explain micellar break-up and recovery

To gather insight into the kinetics of the reaction represented by equation (7.3A), let us assume that it is a first order reversible reaction. Following the method outlined by Smith (1970), a rate expression similar to that for an irreversible first order reaction can be obtained for equation (7.3A), i.e.,

$$r_A = \frac{dC'_A}{dt} = -k_R C'_A \tag{7.4}$$

where,

$$C'_A = C_A - C_{Ae} \tag{7.5}$$

C_{Ae} is the concentration of A in the solution as the reaction proceeds to equilibrium.

Our experimental set-up can be looked upon as a plug flow reactor in which the above reaction (equation (7.3)) is taking place. Writing the material balance equation over a differential volume for the plug flow reactor in terms of the molar flow rate:

$$Input = Output + Accumulation + disappearance \tag{7.6}$$

for the control volume,

Input : $F_{ao}(1-X)$

Disappearance : $(r_A)dV'$

Output : $F_{Ao}(1 - X-dX)$

Accumulation : 0

making the above substitutions in equation (7.6),

$$k_R = \frac{F_A}{V(C_{Ao} - C_{Ae})} \ln \frac{1}{1 - X} \tag{7.7}$$

X is the fractional conversion given by the relation,

$$X = 1 - \frac{C_A - C_{Ae}}{C_{Ao} - C_{Ae}} = \frac{C_{Ao} - C_A}{C_{Ao} - C_{Ae}} \tag{7.8}$$

where C_{Ao} is the original total concentration of A.

Equation (7.7) and (7.8) can be used to calculate the rate constant, k_R. From Figures 7.3 (a,b,c) we have a set of data in which for each given bulk velocity (or, F) we know the length (or, V) of the reactor at which the heat transfer reduction effect begins to manifest itself. This length (or, V) corresponds to the point at which the wall temperature profile exhibits a sudden change in slope and also represents the fact that the conversion of surfactant molecules to spherical micelles is almost complete.

For the 1200 ppm Ethoquad O12 solution results shown in Figure 7.3 (a,b,c), we have:

C_{Ao}= 3 moles/m^3

C_{Ae} = 0.4 moles/m^3 (Young, 1996)

If we assume that 90% of the surfactant molecules have been converted into spherical micelles at the point where the wall temperature profile shows a sudden change in slope, i.e., the reaction represented by equation (7.3A) has almost proceeded to completion, then:

$X = 0.90$

$C_A = 0.65$ moles/m^3

Using the values of C_{Ao}, C_{Ae}, C_A and X calculated above, we can calculate the rate constant (k_R) for the data shown in Figure 7.3 (a,b). Figure 7.3 (c) was not used as the micelles did not recover for the entire length of the tube and it was difficult to reliably guess the point at which the micelles began to recover. The calculated values of the rate constant are listed in Table 7.1.

It can be observed from Table 7.1 that there is no steady trend in the calculated values of the rate constant, but there is a little scatter. The absence of a steady trend is significant because it indicates that the initial assumption of first order reversible reaction mechanism is valid (Smith, 1970). Hence the average rate constant is,

$k_R = 7.72$ /s (standard deviation = 1.02)

Knowing k_R, recovery time (t_R) can be calculated by integrating equation (7.4), i.e.,

$$\ln(C_A - C_{Ae}) = -k_R t + \text{constant} \qquad (7.9)$$

The constant in the above equation can be calculated using the boundary condition:

at $t = 0$, $C_A = C_{Ao}$

Now equation (7.9) becomes,

$$t_R = -\frac{1}{k_R}\ln\frac{(C_A - C_{Ae})}{(C_{Ao} - C_{Ae})} \tag{7.10}$$

Substituting C_A, C_{Ae}, C_{Ao} and k_R calculated earlier into equation (7.10) we get for the 1200 ppm Ethoquad O12 solution,

t_R = 0.303 sec

We have demonstrated in this section that it is possible to calculate the recovery time for micelles if the pipe is treated as a plug flow reactor and the process of micellar formation is represented by a first order reversible reaction (equation (7.3)). Combining Equations (7.7) and (7.10) we get,

$$t_R = \left(\frac{V}{F_A}\right)\frac{C_A - C_{Ae}}{X}\ln\left(\frac{C_A - C_{Ae}}{C_{Ao} - C_{Ae}}\right) \tag{7.11}$$

It can be seen from equation (7.11) that recovery time is dependent upon the solution concentration the molar flow rate. If the above equation is formulated for two different diameter pipes and a given surfactant solution, then,

$$\left(\frac{V}{F_A}\right)_{dia1} = \left(\frac{V}{F_A}\right)_{dia2} = \text{constant} \tag{7.12}$$

The above equation signifies that the ratio (VF_A) is independent of the pipe diameter for a given solution concentration. Hence, once the ratio (VF_A) is determined for a given surfactant solution, it can be used to calculate the micellar recovery length in any diameter pipe for a given flow rate.

Recovery time calculations facilitate the design of heat exchangers for industrial size heating or cooling systems using drag reducing surfactant additives. The systems can be so designed that the residence time of the fluid in the heat exchanger is equal to or slightly less than the recovery time of the surfactant micelles. Conversely, the concentration of the additive can be selected in such a way that its recovery time is equal to or slightly more than the residence time of the fluid inside the heat exchanger.

7.3.5 Economic Aspects

There are two important cost considerations regarding the use of drag reducing surfactant additives in heating or cooling systems, i.e., the amount of additive required and the pressure drop needed across the shearing device to break the surfactant micelles as they enter the heat exchanger.

Gasljevic (1995) observed that very high pressure drop across a wire mesh plug (300 to 400 kPa) was required in their experimental set-up to prevent the micelles from regrouping within the heat exchanger tubes (140 l/D in length). Based on these observations it was proposed that breaking up the surfactant micelles would be an expensive proposition, which would greatly offset the savings due to the reduced power requirements for operating the pump.

One reason for the prohibitively high pressure drop requirements in their system

could be the high concentration of the surfactant additive used. They used a 2300 ppm Ethoquad solution, while we have shown that 600 ppm concentration provided asymptotic drag reduction in our experimental system (Chapter 1). At 2300 ppm level, higher shear stress (or higher pressure drop) would be needed to break-up the surfactant micelles. The micelles would also have a tendency to quickly recover once they are past the shearing device since there is a high concentration of molecules in the solution.

We have shown in Figure 7.3(c) that at a velocity of 6 m/s, the micelles were not able to recover almost along the entire length of the test-section (600 l/D) for a 1200 ppm Ethoquad O12 solution irrespective of the number of screens used in the wire mesh plug. Pressure drop required across the plug for the cases shown in Figure 7.5(c) are listed in Table 7.2, where it can be seen that they are significantly lower than the pressure drop observed in Gasljevic (1995) system.

The above discussion leads to the conclusion that use of shearing devices (valve or a plug) to break-up micelles in a heating or cooling system in order to enhance heat transfer in the heat exchanger is a viable alternative. The pressure drop needed across the shearing device would be low (as seen from Table 7.2) if a lower concentration of the additive is used. For example, we have used a 1200 ppm solution while Gasljevic(1995) used a 2300 ppm solution though both solutions produce asymptotic drag reduction. Further, the concentration of additive (as discussed in the last section) should be such that its recovery time is equal to or slightly in excess of the residence time in the heat exchanger.

7.4 Summary

Use of drag reducing surfactant additives in a closed circulation heating or cooling

system reduces the power consumption required for operating the pump. But the additives pose a problem in the heat exchangers, where more heat transfer area would be required to overcome the heat transfer reduction effect.

A simple solution to the above problem appears to be the use of a shearing device (a throttling valve) at the inlet to the heat exchanger, which would break-up the micelles as they enter the heat exchanger. Contrary to the discussions presented in the published literature, we have been able to show for a 1200 ppm Ethoquad O12 solution that pressure drop across the shearing device is responsible only for breaking up the micelles and has no role in their recovery further downstream. The subsequent recovery of the micelles is controlled by turbulence levels in the flow downstream of the shearing device, with the rate of recovery increasing with an increase in turbulence.

We also observed that the recovery length of micelles for a given bulk velocity was constant and was independent of pressure drop across the shearing device or the number of screens in the wire mesh plug.

We also presented a methodology for calculating the recovery time of the micelles. The test tube was considered to be an ideal plug flow reactor in which a reversible first order reaction was taking place, i.e., conversion of surfactant molecules to micelles. The recovery time for a 1200 ppm Ethoquad O12 solution was calculated to be 0.303 sec assuming that 90% of the spherical micelles were formed at the point where the wall temperature profile showed a sudden change in slope.

The above methodology is based on the simplifying assumption that the surfactant molecules are first converted into spherical micelles and then to cylindrical micelles. The point at which the heat transfer reduction effect can be seen (from the wall temperature profile) has been assumed to signify that the conversion of surfactant molecules to

spherical micelles is complete and the spherical micelles are being transformed into cylindrical micelles. The calculations shown for the 1200 ppm Ethoquad O12 solution should be considered preliminary. Since micellar recovery length is observed from the wall temperature profile, more extensive measurements using more closely spaced thermocouples would enable reliable calculations and form the basis for designing heat exchangers for large scale heating and cooling systems.

The pressure drop needed across the shearing device to break-up the micelles was found to be much lower than the pressure drop reported in the literature, which showed that use of such a device on an industrial scale could be a viable alternative.

For a given surfactant additive, the recovery time for the micelles can be obtained as a function of solution concentration and molar flow rate by carrying out micellar break-up and recovery experiments in a laboratory scale experimental set-up. The test section is assumed to be a plug flow reactor in which a first order reversible reaction (formation of micelles from surfactant molecules) is taking place. The optimum concentration for use in a given industrial system can thus be selected by calculating the residence time of a fluid particle in the heat exchanger and then selecting the concentration which has a recovery time equal to or a little more than the residence time.

Table 7.1 Calculation of Recovery Time

Bulk Velocity (v) (m/s)	Molar Flow rate (F) (moles/s)x10^{-4}	l/D (fig 7.3 a,b) for X = 0.90	Volume of Reactor (V) (m^3)x10^5	k_R (/s)
4.97	5.8	200	5.48	9.38
4.96	5.79	235	6.29	8.16
4.99	5.82	265	7.26	7.11
5.09	5.94	250	6.85	7.69
4.94	5.76	200	5.48	9.31
5.62	6.56	275	7.53	7.72
5.55	6.48	275	7.53	7.62
5.59	6.52	285	7.94	7.28
5.47	6.38	325	9.18	6.15
5.46	6.37	300	8.35	6.76

Average k_R = 7.72 /s

Std. Deviation = 1.02

Table 7.2 Pressure Drop Across the Plug (Figure 7.5(c))

Number of Screens	Pressure Drop Across the Plug (kPa)
12	79.9
9	72.3
6	48.5
3	33.1
1	21.5

8. CONCLUSIONS AND RECOMMENDATIONS

8.1 Conclusions

An experimental and theoretical study has been completed on drag reduction and heat transfer reduction associated with turbulent pipe flow of dilute polymer/ surfactant solutions. Experimental runs were carried out with and without constant heat flux input at the wall for various concentrations of Ethoquad O12 solutions in two SS 304 tubes of internal diameter 0.00704m and 0.0102m respectively.

The following general conclusions were drawn from the detailed summaries provided at the end of Chapters 4, 5, 6 and 7:

1. Drag reduction results obtained in different diameter pipes fall on to the same curve, provided drag reduction is calculated at the same shear stress using equation (4.6). The above observation was verified using our experimental data and also data available in published literature on polymer-water, surfactant-water and polymer-oil systems.

2. Heat transfer reduction results obtained in our experimental set-up appear to be independent of the pipe diameter when heat transfer reduction is calculated at a constant shear stress.

3. A new model for predicting drag reduction scale-up has been presented, which uses a physical interpretation of Prandtl's mixing length and proposes that the mixing length for a drag reducing solution is lower than that for the pure solvent and is dependent only on the concentration of the solution. Flow experiments carried out in a small

laboratory scale pipe, along with viscosity measurements enable the calculation of the model constants K and B for the given drag reducing solutions. These constants can then be used for predicting flow in any diameter pipe.

The above algorithm was successfully used for predicting flow in a 154 mm diameter pipe from experimental data obtained in a 7 mm diameter tube for a surfactant-water system and in a 1194 mm diameter pipe from experimental data obtained in a 26.5 mm pipe for a polymer-oil system.

4. The mixing length for the Ethoquad O12 solutions decreases with an increase in solution concentration and tends towards are asymptotic value.

5. The suitability of the variable mixing length model as compared to Virk's three-layered velocity profile model has also been examined. A comparison of the near wall velocity profiles predicted by these models with velocity measurements made with Laser Doppler Anemometer has indicated that the variable mixing length model predicts a velocity profile and thickening of the laminar sublayer which is close to the actual observations.

6. A model for predicting heat transfer results for drag reducing fluids has been presented. The heat transfer coefficients can be calculated without any prior knowledge about the heat transfer behavior of the fluid. Velocity and shear stress data obtained in a small laboratory scale pipe are used for calculating the constants K, B and y^+_{ls}, which are used along with the fluid properties to calculate the heat transfer coefficients.

The model has been tested with reasonable success on our experimental data for the Ethoquad O12 solution and data available in published literature for the Poly(acrylamide) solutions.

7. A study on micellar break-up and recovery was conducted. The micelles were broken up by placing a wire mesh plug at the entrance to the test section, which was maintained under constant heat flux conditions. The wall temperature profile downstream of the wire mesh gave an indication of micellar recovery. It was observed that the recovery length of micelles for a given bulk velocity was constant and was independent of pressure drop across the shearing device.

8. A methodology for calculating the recovery time of the micelles has been presented. The test tube was considered to be an ideal plug flow reactor in which a reversible first order reaction was taking place, i.e., conversion of surfactant molecules to micelles. Preliminary calculations for a 1200ppm Ethoquad O12 solution have been shown.

8.2 Recommendations for Future Work

1. The variable mixing length model allows for the calculation of the modified Prandtl's mixing length constant for drag reducing solutions. The new mixing length can be used for numerically solving the Navier-Stokes equation for turbulent flow through a circular pipe. A comparison of flow prediction by the variable mixing length model and the numerical solution of the Navier-Stokes equation with actual experimental data would be of considerable interest.

2. The model presented for calculating the heat transfer coefficients for drag reducing solutions assumes that the Reynolds Analogy is valid for these solutions. Since the magnitude of heat transfer reduction is much more than drag reduction, it has been speculated in the published literature that Reynolds Analogy is not valid for drag reducing solutions. Actual measurement of eddy diffusivities for momentum and heat

transfer close to the wall under fully developed conditions should be carried out to determine whether the Reynolds Analogy holds for drag reducing solutions.

3. A methodology for calculating the recovery time of micelles was presented along with preliminary calculations for a 1200ppm Ethoquad O12 solution. The methodology should be further evaluated using experimental data over a range of concentrations. More extensive wall temperature measurements should be carried out to accurately determine the recovery length. The methodology should be eventually tested on field scale data.

9. REFERENCES

Astarita, G., Greco, G., Jr. and Nicodemo, L., "Phenomenological Interpretation and Correlation of Drag Reduction", AIChE J., Vol. 15, 4:564 (1969)

Astarita, G., "Possible Interpretation of the Mechanism of Drag Reduction in Viscoelastic Fluids", I & EC Fundamentals, Vol. 4, 3:354 (1965)

Burger, E.D., Chorn, L.G. and Perkins, T.K., "Studies of Drag Reduction Conducted Over a Broad Range when Flowing Prudhoe bay Crude Oil", J. of Rheology, Vol 24, 5:603 (1982)

Berman, N.S., "Drag Reduction by Polymers", Ann. Rev. Fluid Mech., Vol. 10: 47 (1978)

Carreau, P.J., "Rheological Equations from Molecular Network Theories", Trans. Soc. Rheol. 16:99 (1972)

Cho, Y.I., and Hartnett, J.P., "Non-Newtonian Fluids in Circular Pipe Flow", Adv. Heat Transfer, Vol. 15:59 (1982)

Corman, J.C., "Experimental Study of Heat Transfer to Viscoelastic Fluids", Ind. Eng. Chem. Process Des. Dev. 2:254 (1970)

Darby, R. and Chang, H.D., "Generalized Correlation for Friction Loss in Drag Reducing Polymer Solutions", AIChE J., Vol. 30, 2:274 (1984)

Darby, R. and Pivsa-Art, S., "An Improved Correlation for Turbulent Drag Reduction in Dilute Polymer Solutions", Can. J. Chem. Eng., Vol. 69:1395 (1991)

Davies, J.T., Turbulence Phenomena, Academic Press, New York (1972)

Day, S., Hydraulic Drag and Heat Transfer Properties of Dilute Aqueous Surfactant Solutions Under Turbulent Flow Conditions, BSc Honour's Thesis, St. Mary's University, Halifax, Canada (1991)

Deissler, R.G., "Turbulent Heat Transfer and Friction in the Entrance Regions of Smooth Passages", Trans ASME, Vol. 77:1221 (1955)

Dill, K.A., Nature Vol. 309:42 (1984)

Dodge, D.W. and Metzner, A. B., "Turbulent Flow of Non-Newtonian Systems", AIChE J., Vol.5:189 (1959)

El'Perin, I.T., Smol'skii, B.M. and Leventhal, L.I., "Decreasing the Hydrodynamic Resistance of Pipelines", Int. J. Chem. Eng., Vol. 7:276 (1967)

Everett, D.H., Basic Principles of Colloidal Science, Royal Society of Chemistry, Burlington House, London, UK (1988)

Fabula, A.G., "Fire-fighting Benefits of Polymeric Friction Reduction", J. Basic. Eng., Trans. ASME, Series D, 93(4):453 (1971)

Gadd, G.E., "Turbulence Damping and Drag Reduction Produced by Certain Additives in Water", Nature, Vol. 206:463 (1965)

Gadd, G.E., "Differences in Normal Stress in Aqueous Solutions of Turbulent Drag Reducing Additives", Nature, Vol. 212:1348 (1966)

Gasljevic, K., An Experimental Investigation of Drag Reduction by Surfactant Solutions and its Implementation in Hydronic Systems, PhD. Thesis, UC Santa Barbara, USA (1995)

Gasljevic, K. and Matthys. E.F., "On Saving Pumping Power in Hydronic Thermal Distribution Systems Through the Use of Drag-Reducing Additives", Energy and Buildings, Vol. 20: 45 (1993)

Gasljevic, K. and Matthys. E.F., "Effect of Drag-Reducing Surfactant Solutions on Centrifugal Pumps Performance", in Recent Advances in Non-Newtonian Flows, AMD-Vol. 153:49 (1992)

Gasljevic, K. and Matthys. E.F., "A Feasibility Study of the Use of Drag Reducing Additives to Reduce Pumping Power in Hydronic Thermal Distribution Systems", Industrial Applications of Fluid Mechanics, ASME, N.Y., Vol. FED-132:57 (1991)

Golda, J., "Hydraulic Transport of Coal in Pipes with Drag Reducing Additives", Chem. Eng. Commun., Vol. 43:53 (1986)

Green, H.L., Mostardi, R.F. and Wokes, R.F., "Effects of Drag Reducing Polymers on Initiation of Arteriosclerosis", Polym. Eng. Sci., Vol. 20:499 (1980)

Granville, P.S., "Scaling-up of Pipe Flow Frictional Data for Drag Reducing Polymer Solutions", 2nd Int. Conf. on Drag Reduction, Cambridge, UK (1978)

Gupta, M.K., Metzner, A.B. and Hartnett, J.P., "Turbulent Heat Transfer Characteristics of Viscoelastic Fluids", Int. J. Heat Mass Transfer, Vol. 10:1211 (1967)

Hartnett, J.P. and Kwack, E.Y., "Prediction of Friction and Heat Transfer for Viscoelastic Fluids in Turbulent Pipe Flow", Proc. 9th Symposium on Thermophysical Properties, June 24-27, Boulder, Colorado, USA, pp 53 (1985)

Hartnett, J.P. and Cho, Y.I., "Non-Newtonian Fluids in Circular Pipe Flow", Adv. Heat transfer Vol. 15:59 (1982)

Hoffman, H., Rehage, H., Platz, G., Schorr, W., Thurn, H. and Ulbricht, W., "Investigations on a Detergent System with Rod-Like Micelles", Colloid and Poly. Sci., 260, 1042-1056 (1982)

Hoyt, J.W., "The Effect of Additives on Fluid Friction", J. Of Basic Engineering, Vol. 94:258 (1972)

Kale, D.D., An Analysis of Heat Transfer to Turbulent Flow of Drag Reducing Fluids, Int. J. Heat Mass Transfer Vol. 20:1077 (1977)

Kays, W.M. and Crawford, H.R., Convective Heat and Mass Transfer, McGraw Hill, New York, USA (1980)

Khabakhpasheva, E.M. and Perepelitsa, B.V., "Turbulent Heat Transfer in Weak Polymeric Solutions", Heat Transfer-Sov. Res., Vol. 5:117 (1973)

Kulicke, W.M., Koetter, M. and Graeger, H., "Drag Reduction Phenomenon With Special Emphasis on Homogeneous Polymer Solutions", Advances in Polymer Science, Vol. 89:1, Springer Verlag (1989)

Little, R.C., "Flow Properties of Polyox Solutions", Ind. Eng. Chem. Fundam., Vol. 8:520 (1969)

Lumley, J.L, "Drag Reduction in Turbulent Flow by Polymer Additives", J. Polym. Sci. Macromol. Rev., Vol. 7:263 (1973)

Lumley, J.L, "Drag Reduction by Additives", Ann. Rev. Fluid Mech., Vol. 1:367 (1969)

Lumley, J.L., "Turbulence in Non-Newtonian Fluids", Phys of Fluids, Vol. 7:335 (1964)

Matthys, E.F., "Heat Transfer, Drag Reduction and Fluid Characterisation for Turbulent Flow of Polymer Solutions: Recent Research Needs", J. of Non-Newtonian FM, Vol. 38:313 (1991)

Matthys, E.F. and Sabersky, R.H., "A Method of Predicting the Diameter Effect for Heat Transfer and Friction of Drag Reducing Fluids", Int. J. Heat Mass Transfer, Vol. 25(9):1343 (1982)

Meyer, W.A., A Correlation of the Friction Characteristics for Turbulent Flow of Dilute Viscoelastic Non-Newtonian Fluids in Pipes, AIChE J., Vol. 12:522 (1966)

Nikuradse, J., "Laws of Resistance and Velocity Distribution for Turbulent Flow of Water in Smooth and Rough Tubes", Pro. 3rd Int. Cong. For Appl. Mech., Stockholm, Vol. 1:239 (1930)

Prandtl, L., "Motion of Viscous Fluids: Turbulence: Fluid Resistance: Practical Applications" in Essentials of Fluid Dynamics, Hafner Publishing Company, New York , USA (1952), pp. 118.

Pollert, J.,. Zakin, J.L., Myska, J and. Kratochvil, P "Use of Friction Reducing Additives in District Heating System Field Test at Kaldno-Krocehlavy, Czech Republic", Proc. Int. District Heating and Cooling Conf., Seattle, Vol. 85:141 (1994)

Pruitt, G.T., Whitsitt, N.F. and Crawford, H.R., "Turbulent Heat Transfer to Viscoelastic Fluids", Contract No. NA7-369, The Western Company (1966)

Rochefort, W.E., McHugh, R. and Middleman, S., "Xanthan Gum Drag Reduction in a Rectangular Flow Loop: Multiple-Pass Stability Studies", Drag Reduction in Fluid Flows, Eds. Sellin and Moses, pp. 319-325, Ellis Horwood Ltd. Chichester, England (1989)

Rouse, G.D., and Foster, K.L., "Drag Reduction and Rheological Properties of Cationic Viscoelastic Surfactant Formulations", J.Non-Newtonian Fluid Mechanics, Vol. 31:59 (1989)

Rudd, M.J., "Measurements Made on a Drag Reducing Solution with a Laser Velocimeter", Nature, Vol. 224:587 (1969)

Savins, J.G., " Drag Reducing Additives Improve Drilling Fluid Hydraulics", Oil and Gas J., Mar 13, pp 79(1995)

Savins, J.G. and Seyer, F.A., "Drag Reduction Scale-up Criteria", Phys of Fluids, Vol. 20:578 (1977)

Schlichting, H., Boundary Layer Theory, McGraw Hill, New York, USA (1979)

Sellin, R.H.J., and Ollis, M., "Effect of Pipe Diameter on Polymer Drag Reduction", Ind. Eng. Chem. Prod. Res. Dev., Vol. 22:445 (1983)

Sellin, R.H.J., Hoyt, J.W., Pollert, J. and Scrivener, O., "The Effect of Drag Reducing Additives on Fluid Flows and Their Industrial Applications and Future Proposals", J. Hydraulic Res., Vol. 20:235 (1982)

Seyer, F.A. and Metzner, A.B, "Turbulent Flow Properties of Viscoelastic Fluids", Can. J. Chem. Eng., Vol. 45:121 (1967)

Shenoy, A.V., "A Review on Drag Reduction with Special Reference to Micellar Systems"; Colloid and Poly. Sci. Vol. 262:319 (1984)

Singh, R.P., Singh, J., Deshmukh, S.R. and Kumar, A., "Novel Applications of Drag Reducing Polymers in Agriculture", Drag Reduction in Fluid Flows, Sellin, R.H.J. and Moses, R.T. (Eds), Ellis, Horwood, Chichester, pp 223 (1989)

Smith, K.A., Keuroghlian, P.S. Virk, P.S. and Merrill, E.W., "Heat Transfer to Drag Reducing Polymer Solutions", AIChE J.,Vol. 15:294 (1969)

Smith, J.M., Chemical Engineering Kinetics, McGraw Hill, New York, USA (1970)

Sood, A., Reduction in Drag and Heat Transfer, MSc Thesis, Univ. of Calgary, Canada (1993)

Steiff, A., Althaus, W., Weber, M. and Weinspach, P.M. in "Drag Reduction in Fluid Flows", Ellis Horwood, Chichester, pp 61-67 (1989a)

Steiff A., Althaus, W., Weber, M. And Weinspach, P.M., "Application of Drag-Reducing Additives in District Heating Systems", in: Sellin, R.H. and Moses, R.T. (Eds), Drag Reduction in Fluid Flows, Ellis Horwood, Chichester, pp. 247-254 (1989b)

Toms, B.A., "Some Observations on the Flow of Linear Polymer Solutions Through Straight Tubes at Large Reynolds Numbers", Proc. 1st Int. Congr. on Rheology, Amsterdam (1948)

Tritton, D.J., Physical Fluid Dynamics, Oxford Press, New York, USA (1988)

Usui, H. And Saeki, T., "Drag Reduction and Heat Transfer Reduction by Cationic Surfactants", Journal of Chemical Engineering of Japan, Vol. 26:103 (1993)

Virk, P.S., "Drag Reduction fundamentals", AIChE J., Vol. 21:625 (1975)

Virk, P.S., "Drag Reduction in Rough Pipes", J. Fluid Mech., Vol. 45:225 (1971)

Virk, P.S. "The Ultimate Asymptote and Mean Flow Structure in Toms Phenomenon", ASME J. Appl. Mech., Vol. 37:488 (1970)

Virk, P.S., H.S. Merrill, H.S. Mickley, K.A. Smith and E.L. Mollo-Christensen, "The Toms Phenomenon-Turbulent Pipe Flow of Dilute Polymer Solutions", J. Fluid Mech. Vol. 30:305 (1967).

Walsh, M., "Theory of Drag Reduction in Dilute High Polymer Flows", Int. Shipbuilding Prog., Vol. 14:134 (1967)

Wells, C.S., Jr., "Turbulent Heat Transfer in Drag Reducing Fluids", AIChE J. Vol. 14:406 (1968)

Whitsitt, N.F., Harrington, L.J. and Crawford, H.R., "Effect of Wall Shear Stress on Drag Reduction of Viscoelastic Solutions", in "Viscous Drag Reduction", Ed. C.S. Wells, Plenum, New York, pp 265 (1969)

Yoon, H.K. and Ghajar, A.J., "A Method for Correlating the Diameter and Concentration Effects on Friction and Heat Transfer in Drag-Reducing Flows", AIAA San Antonio, June 27-29 (1988)

Young, John, C.O'C., "Advanced Fluids Applications to District Cooling Systems", Contract Report, Natural Resources Canada, CANMET-ERL Division (1996)

Zakin, J.L., "New Limiting Drag Reduction and Velocity Profile Asymptotes for Non-polymeric Additive Systems, AIChE J., Vol. . 42:3544 (1996)

APPENDIX 1

Viscosity Data

A) Viscosity data for Ethoquad T13 2300 ppm solution (25 °C, Gasljevic, 1995) and Ethoquad O12 1400 ppm solution (20 °C) are shown in Figure A1.1.

B) Viscosity data for Ethoquad O12 400, 500 and 600 ppm solutions (20 °C) are shown in Figure A1.2.

C) Viscosity data for 10, 100, 300 and 1000 ppm Poly(acryl amide) solutions (Hartnett and Kwack, 1985) are shown in Figure A1.3.

D) Viscosity data for the 5, 10 and 20 ppm Conoco-CDR solutions (oil-polymer system) have not been reproduced here and are available in a tabular form elsewhere (Burger et al., 1982).

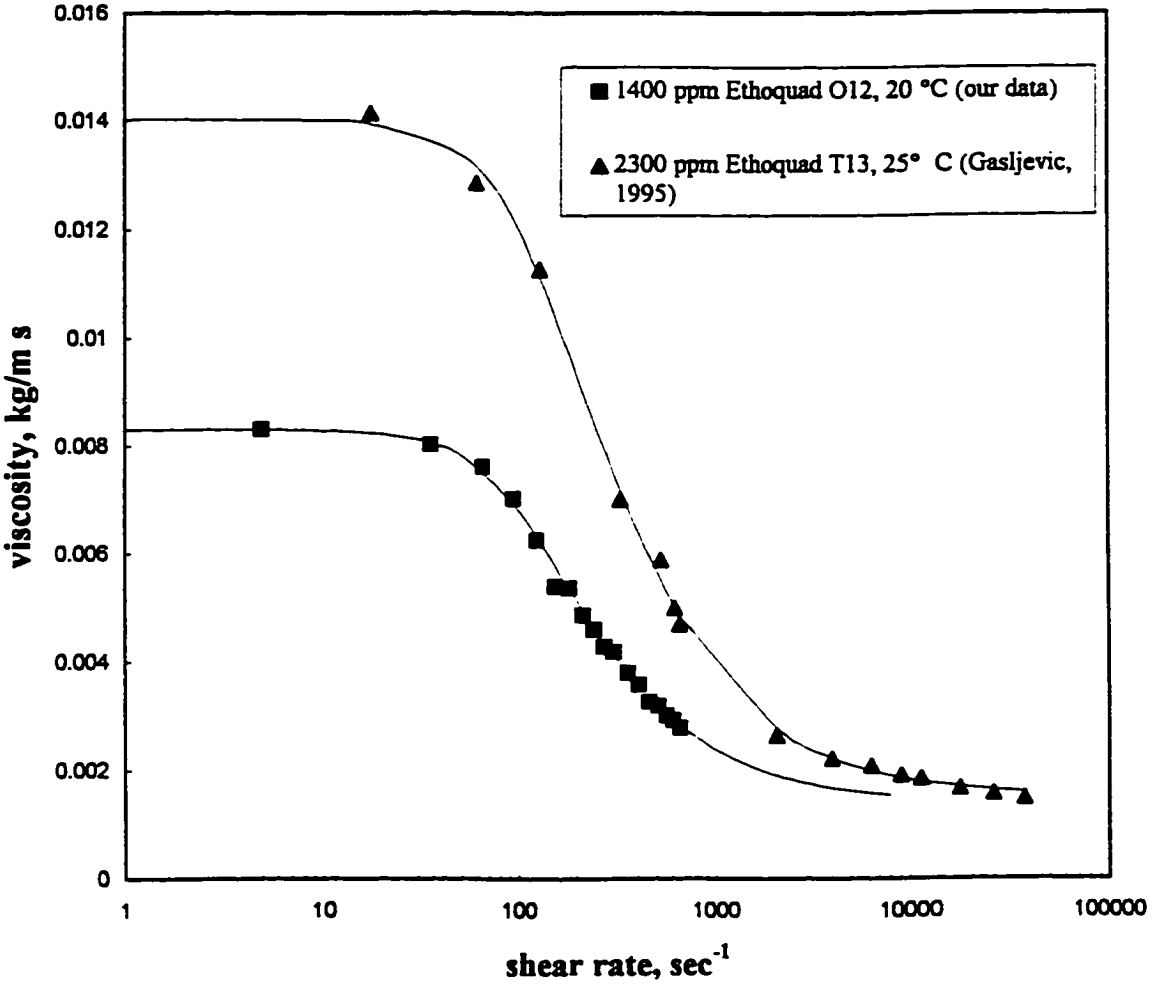

Figure A1.1 Viscosity data for 1400 ppm Ethoquad O12 solution (20 °C) and 2300 ppm Ethoquad T13 solution (25 °C)

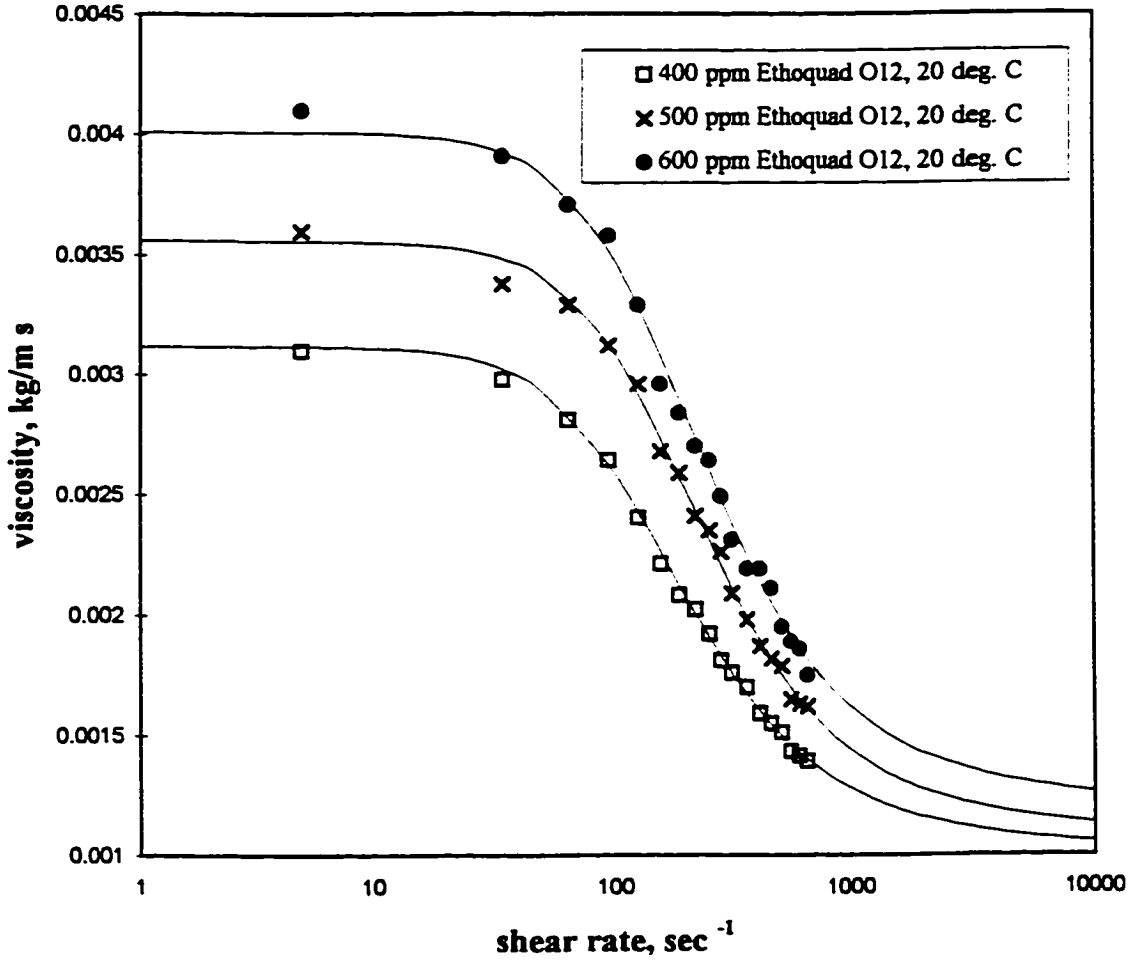

Figure A1.2 Viscosity data for 400, 500 and 600 ppm Ethoquad O12 solutions (20 °C)

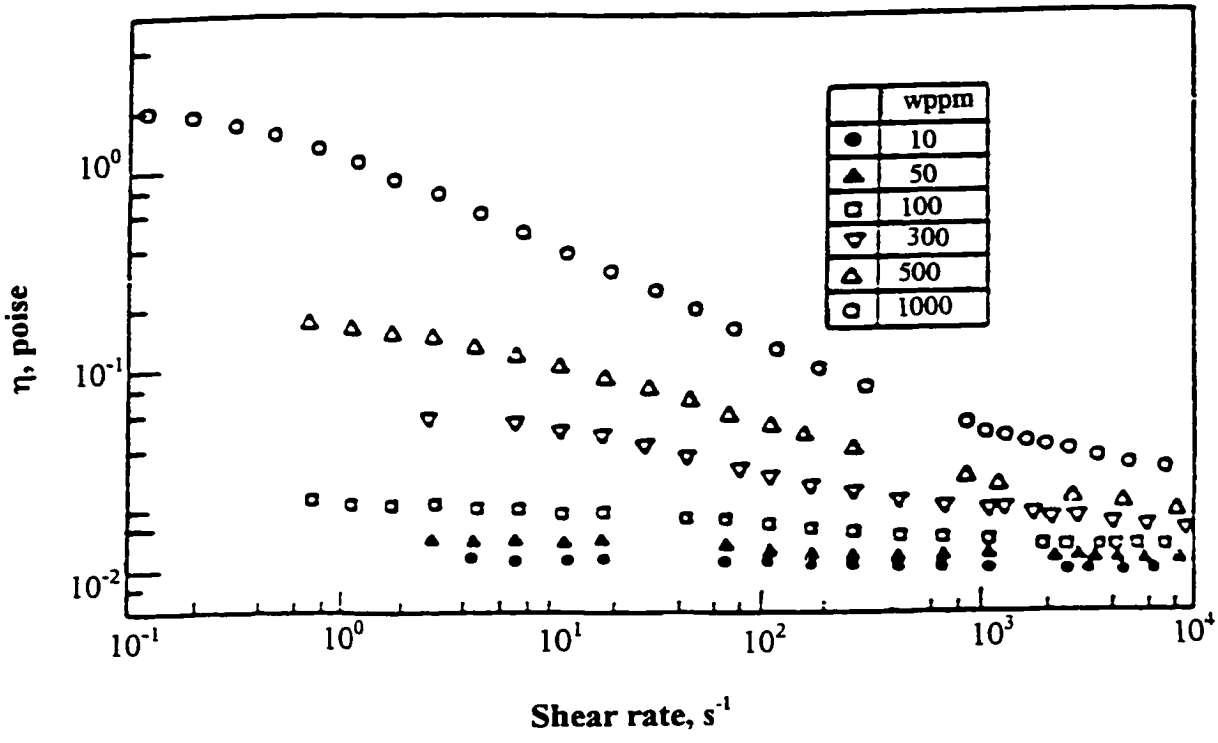

Figure A1.3 Viscosity data for 10, 100, 300 and 1000 ppm Poly(acryl amide) solutions (Hartnett and Kwack, 1982; Yoon and Ghajar, 1988)

APPENDIX 2

Calibration Results

A) Friction results for water are shown in Figure A2.1 and are correlated well by the Prandtl-Karman law (equation A2.1).

$$\frac{\bar{u}}{u_\tau} = \left(\frac{1}{0.41}\right) \ln \frac{R u_\tau}{\nu} + 2.0 \qquad \text{(A2.1)}$$

B) Heat transfer results for water are shown in Figure A2.2 and are correlated within ±13% by the Seider-Tate equation (equation A2.2).

$$N_{Nu} = 0.023 N_{re}^{0.8} N_{\mathrm{Pr}}^{1/3} \left(\frac{\mu_b}{\mu_w}\right)^{0.14} \qquad \text{(A2.2)}$$

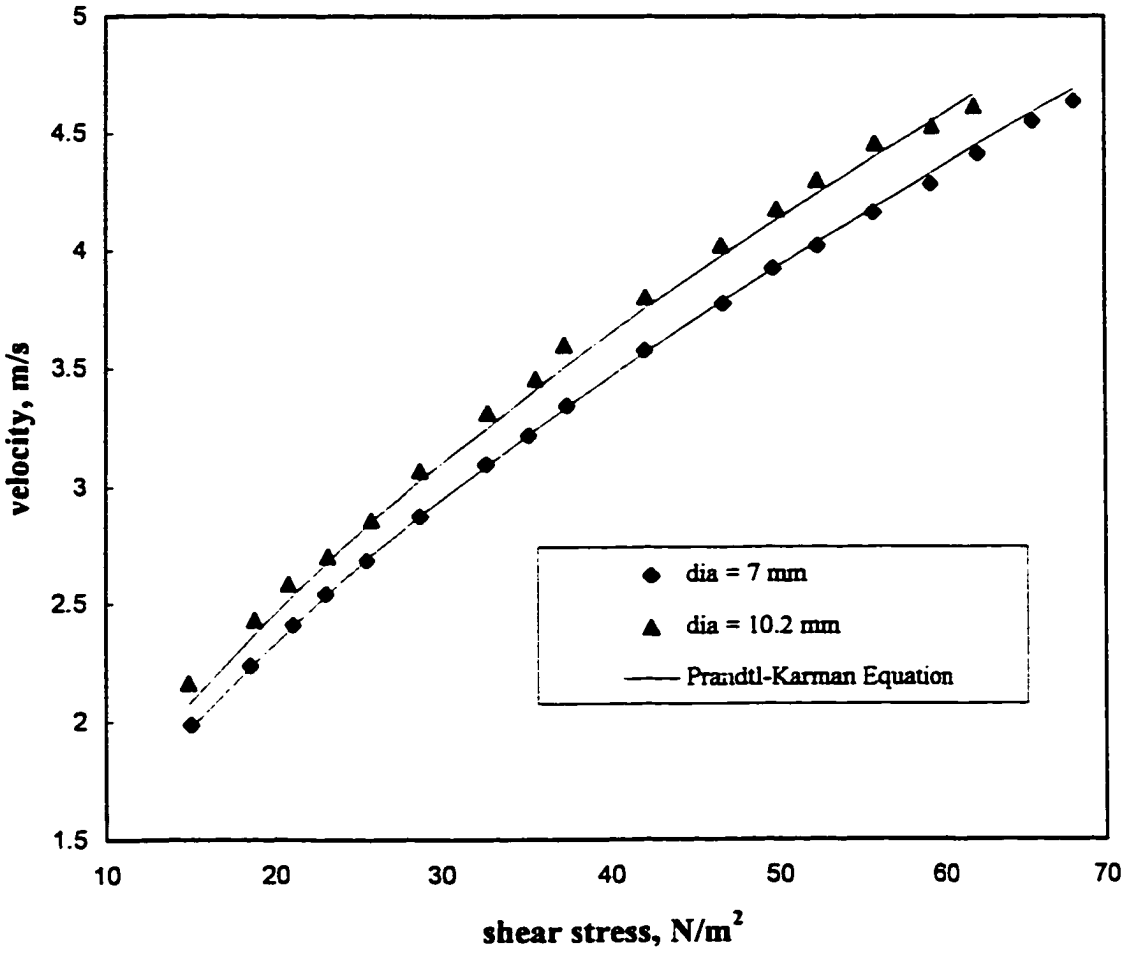

Figure A2.1 Friction results for water

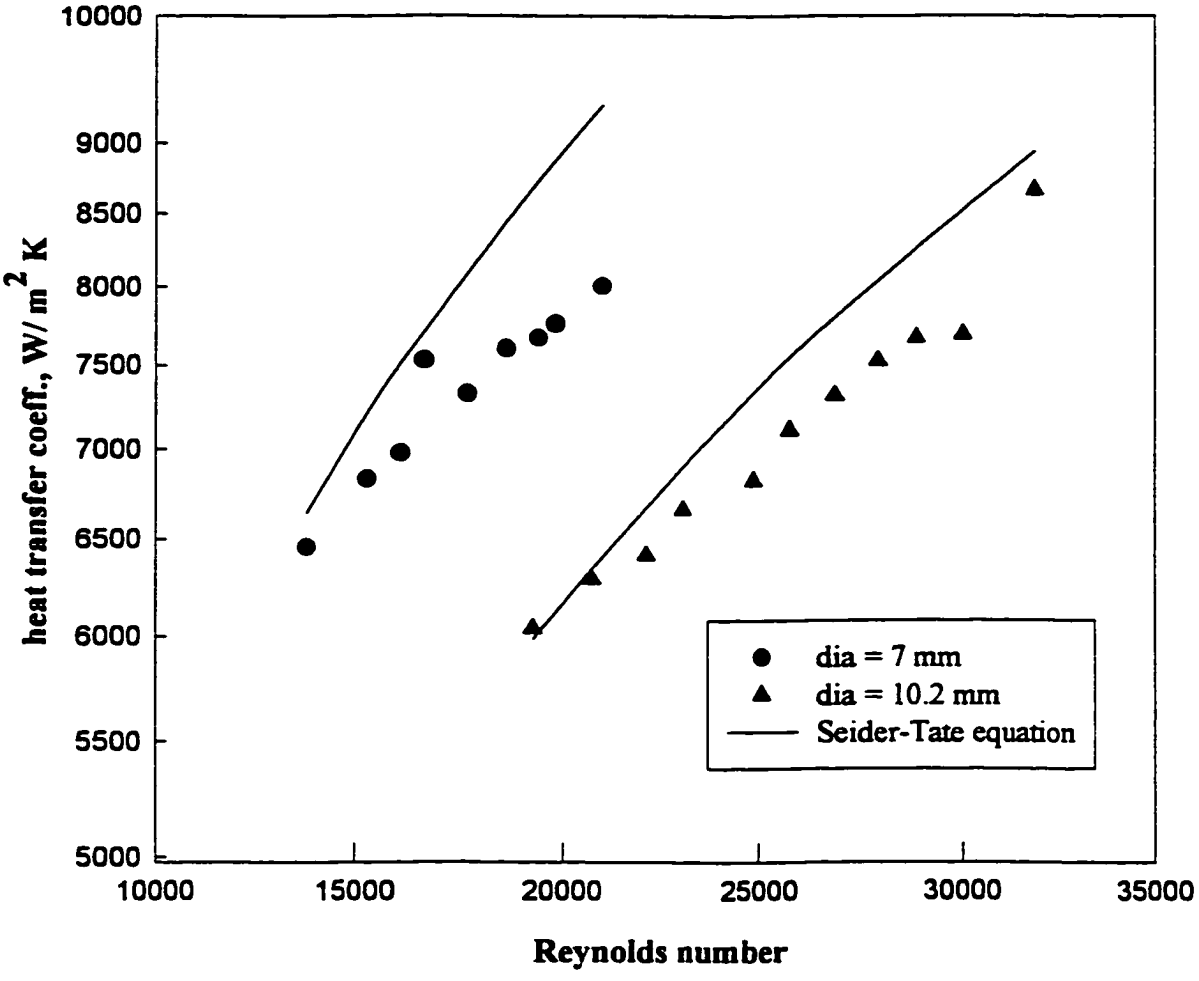

Figure A2.2 Heat transfer results for water

APPENDIX 3

Methodology for Drag Reduction Scale-up

(A) The computations involved in predicting drag reduction scale-up by the variable mixing length model are illustrated below with a specific example. The steps can be summarized as follows:

1. Measure the viscosity of the given drag reducing solution as a function of shear rate. For better accuracy, the measurements should be made over the range of shear rates to be encountered in the laboratory scale pipe and the bigger pipe for which the flow predictions are required. e.g., for the 1400 ppm Ethoquad O12, the viscosity is correlated well by a Carreau (1972) type of equation (Figure A1.1):

$$\mu = 0.001401 + \frac{(0.0083 - 0.001401)}{\left[1 + 0.00007\left(\frac{8\bar{u}}{D}\right)^2\right]^{0.459}} \qquad \text{(A3.1)}$$

It should be noted here that commercially available viscometers measure apparent viscosity as a function of the wall shear rate. For using equation (A3.1) in our scale-up algorithm, we have used the average bulk velocity $(\bar{u})$ for calculating the shear rate $(8\bar{u}\ D)$, which is a reasonable approximation.

2. Collect pressure drop and corresponding flow rate data for the given drag reducing solution in the laboratory scale pipe.

3. Use the above data to calculate shear stress (or u_τ) and average bulk velocity ($\bar{u}$). For the above 1400 ppm Ethoquad O12 solution, $\bar{u}$ and shear stress data for the 7 mm diameter pipe are shown in Figure 5.4

4. Using a standard curve-fit routine and u_τ, $\bar{u}$ and μ data in Equation (5.35), obtain the best fit values for, K and B. For the above 1400 ppm Ethoquad O12 solution, K = 0.0583 and B = -56.36 from the 7 mm diameter pipe.

5. Use the values of K and B obtained above and Equations (5.35) and (A3.1) to predict average bulk velocity in the 154 mm diameter pipe (Figure 5.8) at a given u_τ by an iterative procedure as described in the example below:

- For the above 1400 ppm solution, we want to predict bulk velocity corresponding to τ_w = 1.045 N/m^2 in the 154 mm pipe. Let us guess a value for $\bar{u}$, say 0.5 m/s.
  From Equation (A3.1), $\mu = 8.15 \times 10^{-3}$ kg/m s
- Assuming density of water, from Equation (5.35) we get $\bar{u}$ (new) = 1.34 m/s
  Calculate a new value for μ using $\bar{u}$ (new), i.e. μ (new) = 7.4×10^{-3} kg/m s and so on.
- The iteration is continued till successive calculated values of $\bar{u}$ do not change significantly.
- Hence for the 154 mm diameter pipe and τ_w= 1.045 N/m^2, $\bar{u}$ predicted by the model is 1.4 m/s.
  The $\bar{u}$ obtained by Young (1996) was 1.36 m/s (Figure 5.8).

(B) The viscosity of the drag reducing solution has been expressed in the above methodology as a function of wall shear rate $\left(8\bar{u}/D\right)$. In reality, $\left(8\bar{u}/D\right)$ represents the wall shear rate only for laminar viscometric measurements in a rotating cylinder viscometer, but is valid approximately for turbulent flow through pipes since the velocity at the boundary of the laminar sublayer is very close to the average bulk velocity.

Another method for performing the scale-up calculations is being presented here, in which instead of wall shear rate, the viscosity is expressed as a function of the wall shear stress. As has been discussed in Chapter 4, velocity fluctuations close to the wall are quantified by shear stress at the wall and representation of the viscosity as a function of the wall shear stress would also be consistent with the concept of using wall shear stress as a "scale-up criteria" (Chapter 5). The methodology would now be as follows:

1. Obtain viscosity as a function of wall shear stress. For the 1400 ppm Ethoquad O12 solution, the viscosity has been shown as a function of wall shear stress in Figure A3.1

2. Collect pressure drop and corresponding flow rate data for the given drag reducing solution in the laboratory scale pipe.

3. Use the above data to calculate shear stress (or u_τ) and average bulk velocity ($\bar{u}$). For the above 1400 ppm Ethoquad O12 solution, $\bar{u}$ and shear stress data for the 7 mm diameter pipe are shown in Figure 5.4

4. Using a standard curve-fit routine and u_τ, $\bar{u}$ and μ data in Equation (5.35), obtain the best fit values for, K and B. For the above 1400 ppm Ethoquad O12 solution, K = 0.0613 and B = -55.19 from the 7 mm diameter pipe.

5. Use the values of K and B obtained above and Equations (5.35) and Figure (A3.1) to predict average bulk velocity in the 154 mm diameter pipe (Figure 5.8) at a given u_τ as described in the example below:

- For the above 1400 ppm solution, we want to predict bulk velocity corresponding to τ_w = 1.045 N/m^2 in the 154 mm pipe.

From Figure A3.1, $\mu = 5.3 \times 10^{-3}$ kg/m s

-Assuming density of water, from Equation (5.35) we get $\bar{u}$ (new) = 1.46 m/s

The $\bar{u}$ obtained by Young (1996) was 1.36 m/s (Figure 5.8).

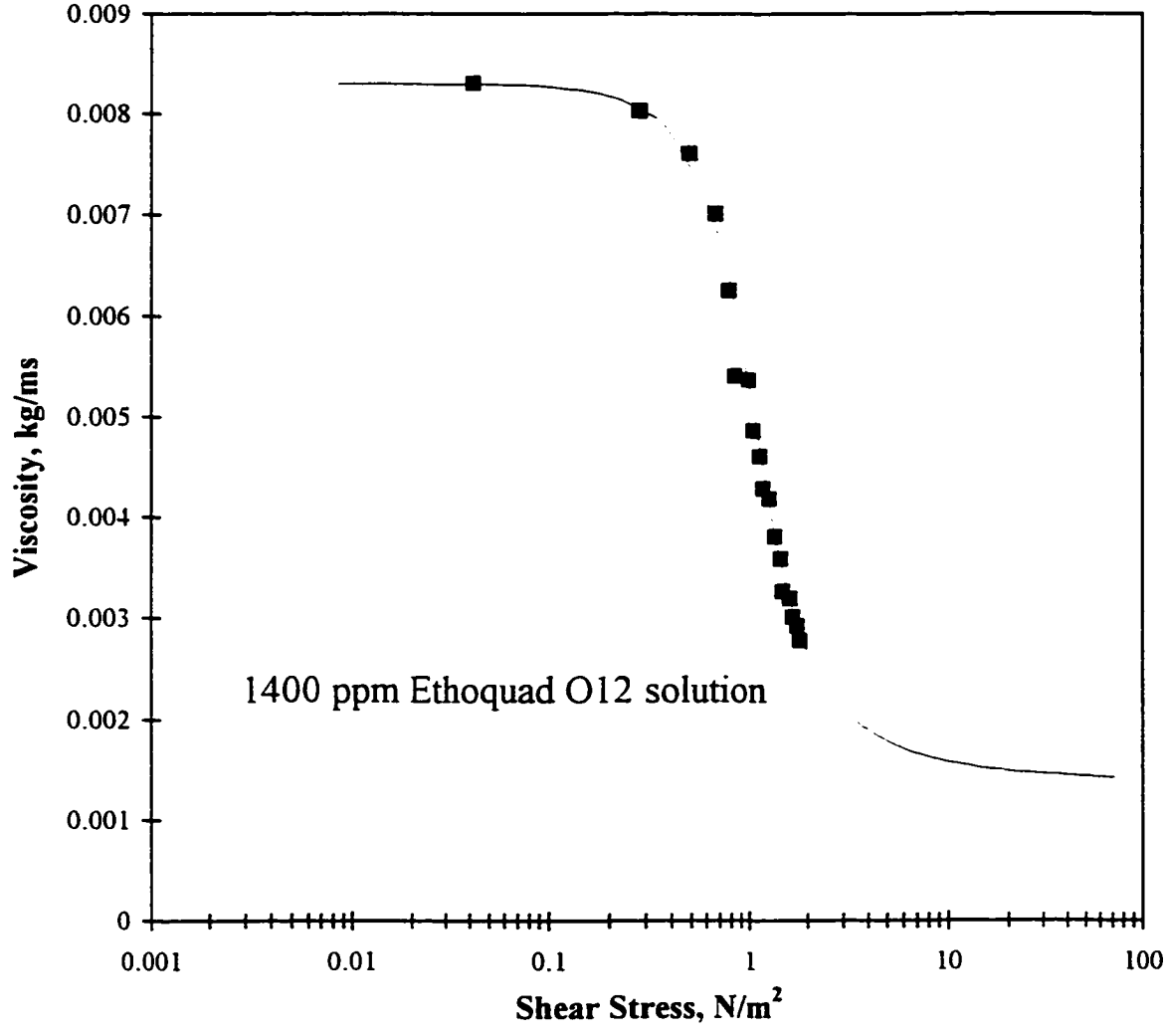

Figure A3.1 Viscosity data for 1400 ppm Ethoquad O12 solution as a function of wall shear stress (20 °C)

APPENDIX 4

Methodology for Prediction of Heat Transfer Reduction

The computations involved in predicting heat transfer reduction by the variable mixing length model are illustrated below with a specific example. The steps can be summarized as follows:

1. Measure viscosity of the given drag reducing solution as a function of shear rate. For better accuracy, the measurements should be made over the range of shear rates and temperatures to be encountered in the actual pipe. For example, the flow and heat transfer experiments using the 1400 ppm Ethoquad O12 solution were performed in our experimental set-up over the temperature range of 18-23 °C, For simplicity, viscosity measurements were conducted at 20 °C. The viscosity is correlated well by a Carreau (1972) type of equation (equation A3.1).

2. Obtain shear stress (or u_τ) and average bulk velocity $(\bar{u})$ data as discussed in Appnedix 3. For the 1400 ppm Ethoquad O12 solution, $\bar{u}$ and shear stress data for the 7 mm diameter pipe are shown in Figure 5.4

3. Using a standard curve-fit routine and equation (5.35), obtain the best fit values for, K and B. For the above 1400 ppm Ethoquad O12 solution, K = 0.0583 and B = -56.36 from the 7 mm diameter pipe. From equation (5.36), $y_{ls}^+ = 23.4$.

4. Use equation (6.17) to calculate the heat transfer coefficient for the drag reducing solution in any pipe. For example, in the 7 mm diameter pipe, for τ_w = 11.97 N/m^2, $\bar{u}$ = 4.12 m/s.

   From equation (A3.1), μ = 1.64 x 10^{-3} kg/m s

   density, ρ = 1000 kg/ m^3

   specific heat, C_p = 4180 J/ kg °C

   thermal conductivity, k = 0.59 W/ m °C

   Prandtls' mixing length constant, K = 0.0583

   thickness of laminar sublayer, y_{ls}^+ = 23.4

   substituting the above data in equation (6.17) gives the heat transfer coefficient, i.e. h = 1606 W/ m^2/ °C.

The experimental heat transfer coefficient obtained for τ_w = 11.97 N/m^2 was 1654 W/m^2/°C (Figure 6.1).

APPENDIX 5

Flow Data for Poly(acryl amide) solutions (for heat transfer calculations)

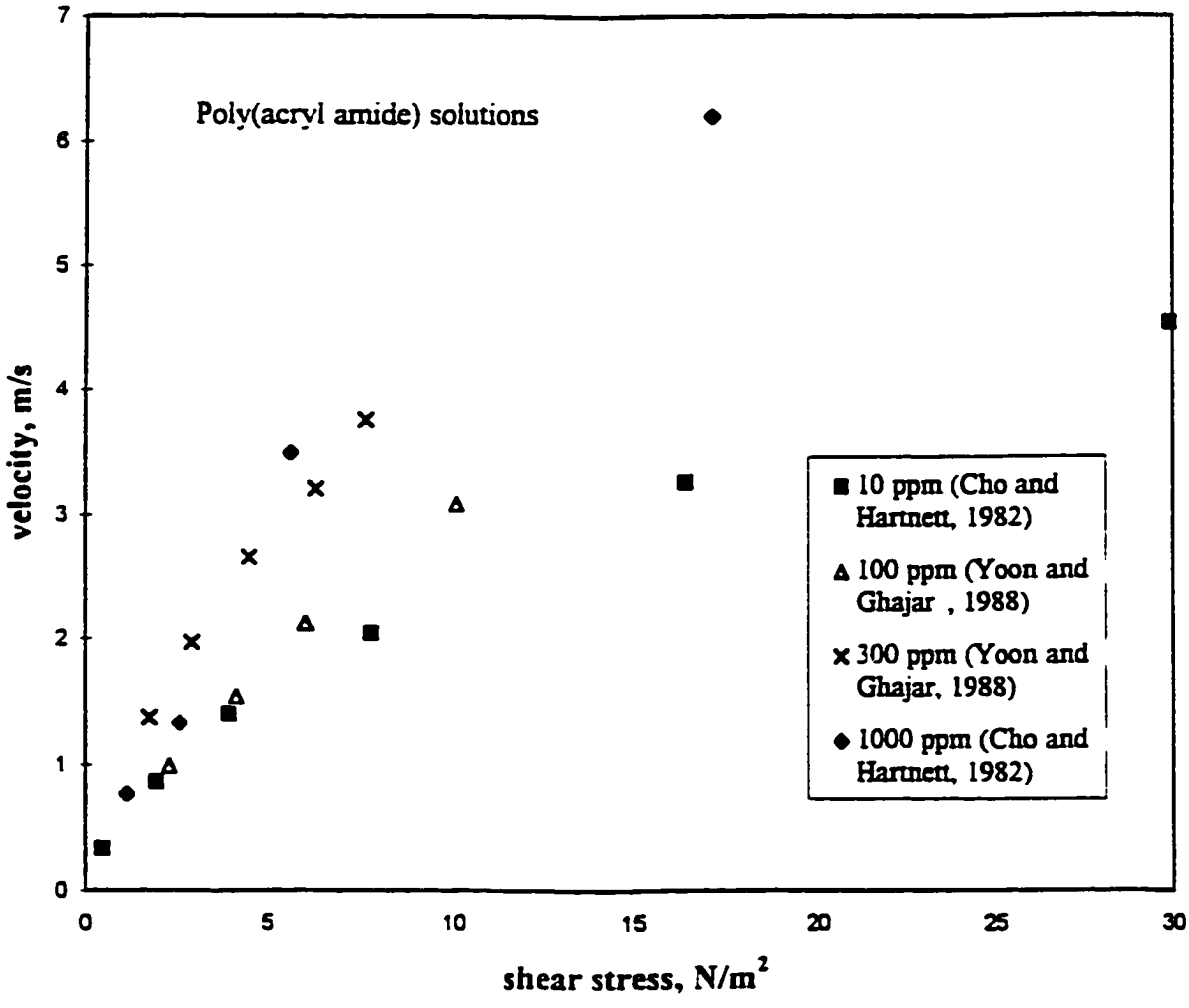

Figure A5.1 Flow Data for Poly(acryl amide) solutions (for heat transfer calculations)

IMAGE EVALUATION TEST TARGET (QA-3)

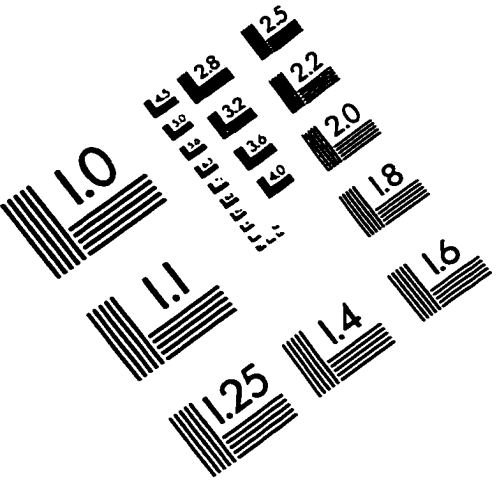

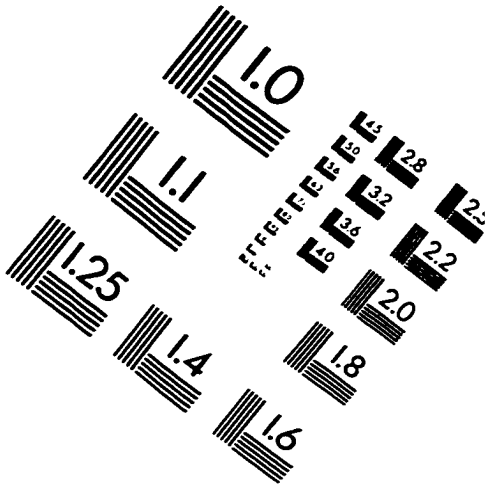

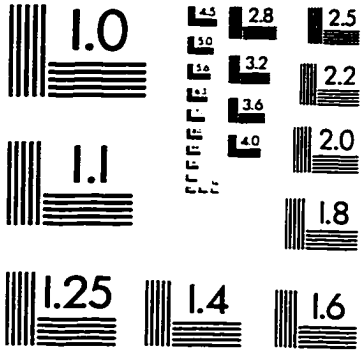

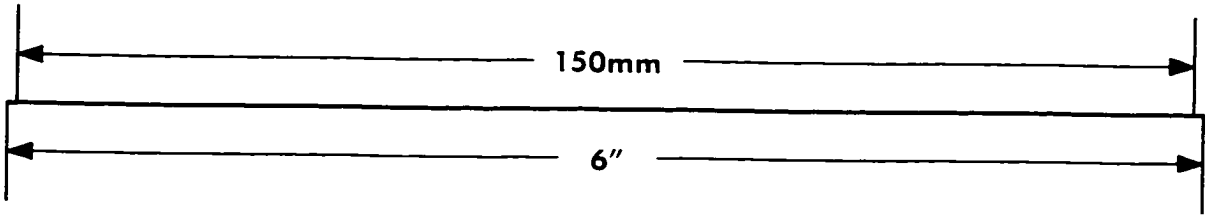

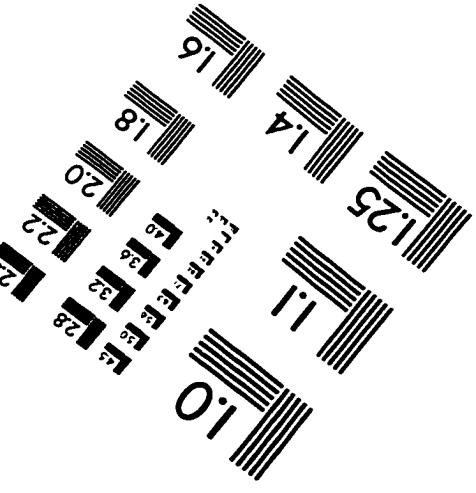

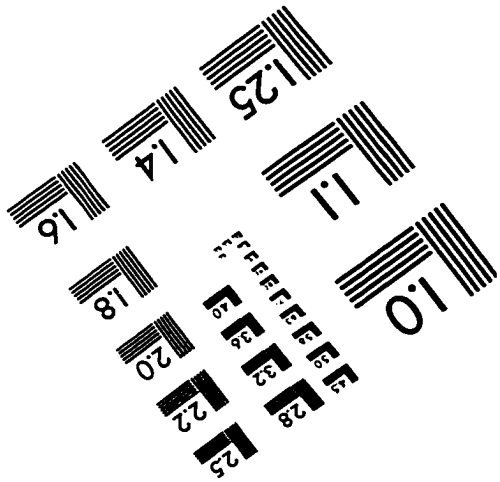

APPLIED IMAGE, Inc
1653 East Main Street
Rochester, NY 14609 USA
Phone: 716/482-0300
Fax: 716/288-5989

© 1993, Applied Image, Inc., All Rights Reserved